NASA Contractor Report 4086

One-Dimensional Wave Propagation in Rods of Variable Cross Section: A WKBJ Solution

Simeon C. U. Ochi and James H. Williams, Jr.

GRANT NAG3-328
JULY 1987

NASA

NASA Contractor Report 4086

One-Dimensional Wave Propagation in Rods of Variable Cross Section: A WKBJ Solution

Simeon C. U. Ochi and James H. Williams, Jr.
Massachusetts Institute of Technology
Cambridge, Massachusetts

Prepared for
Lewis Research Center
under Grant NAG3-328

National Aeronautics
and Space Administration

**Scientific and Technical
Information Office**

1987

ABSTRACT

As an important step in the characterization of a particular dynamic surface displacement transducer (*IQI* Model 501), this report presents one dimensional wave propagation in isotropic nonpiezoelectric and piezoelectric rods of variable cross section. With the use of the Wentzel-Kramers-Brillouin-Jeffreys (*WKBJ*) approximate solution technique, an approximate formula, which relates the ratio of the amplitudes of a propagating wave observed at any two locations along the rod to the ratio of the cross sectional radii at these respective locations, is derived. The domains of frequency for which the approximate solution is valid are discussed for piezoelectric and nonpiezoelectric materials.

INTRODUCTION

In the characterization of a transducer designed for ultrasonic and acoustic emission measurements, it is important to understand the behavior of wave propagation in all components of the transducer, especially in the piezoelement. The piezoelement is important because it is through its behavior that ultrasonic waves are introduced into and received from the materials whose properties are sought by nondestructive evaluation (NDE). A transducers is usually designed with some specific measurement capabilities, such as

(a) the type of waves (longitudinal, shear, surface, etc.) it can generate and/or detect; and

(b) the frequencies at which it can best produce its desired response.

In terms of its frequency characteristics, the transducer can often be classified as either narrow-band or broadband. The transducer whose characterization is sought in this study is a broadband type. The transducer is manufactured by Industrial Quality Incorporated (Gaithersburg, MD) and designated as IQI Model 501. The sensing elements of the transducer consist of two components: a conically shaped piezoelement fabricated from lead zirconate-titanate ($PZT - 5A$) and a backing material fabricated from brass. The transducer is designed for acoustic emission as well as ultrasonic signal generation.

The aim of this report is to investigate how the piezoelement supports one dimensional longitudinal wave propagation. One of the earliest methods of approaching this problem analytically was presented by Redwood [1]. Several other authors, including Filipczynski [2], Kazhis and Lukoshevichyus [3] and Williams and Doll [4], have subsequently dealt with the subject in various detail. However, unlike the present case where the piezoelement is conical, these authors dealt with cases where the piezoelement had a constant cross section.

The first and the second sections of this analysis deal with the derivation of

the governing wave equation in isotropic nonpiezoelectric and piezoelectric rods of variable cross section, respectively. The third section is devoted to solving the derived wave equations by using a phase-integral method known as the $WKBJ$ approximate solution technique. Through this method, an approximate formula, which relates the ratio of amplitudes of a propagating wave at any specific locations along the rod and the ratio of the cross sectional radii at these respective locations, is derived. The approximation is based on the first term of an asymptotic power series. Usually in such approximations, there is an inherent error that imposes a limit on the use of the approximate solution. These limits are also discussed in this report.

Another problem with the approximation is the existence of points of discontinuity, known also as the transition points. Heading [5] summarized attempts by several authors to improve on the approximation so as to be valid at the transition points. Gans [6], who studied the propagation of light in a stratified medium, examined the effects of the transition points in a systematic way. Since Gans, several authors have suggested ways to improve the $WKBJ$ solutions. For instance, Bailey [7] produced an improvement when considering reflections of waves in an inhomogeneous medium, replacing the $WKBJ$ solution by an approximation that is valid through a transition point. Bailey also discussed an iterative process whereby results could be further improved. Iami [8] produced a better representation of the $WKBJ$ solution through the transition point and later applied the technique to heat transfer in a laminar boundary layer. Finally, Moriguchi [9] considered a phase-shift approach to a formula developed by Hines [10].

Concerning the validity of the $WKBJ$ approximate solution, this report will not only address the conditions under which the approximation is true, but it will also establish the frequencies under which the conditions are met. Parameterized curves that relate the amplitude ratios to the frequencies of propagation are developed for

this purpose.

ONE DIMENSIONAL PLANE WAVE PROPAGATION IN NONPIEZOELECTRIC ROD OF VARIABLE CROSS SECTION

In this section the one dimensional plane longitudinal wave equation is derived for an isotropic elastic rod of variable cross section.

Consider an isotropic elastic rod of variable cross section extending from the origin $x = 0$ to $x = L$ along the x-axis as shown in Fig. 1. Assuming that a propagating plane wave becomes incident on the rod at the origin, an equation of motion which describes the propagating wave can be derived by considering a differential element dx of the rod as shown in Fig. 1.

A momentum equation of the differential element dx of the rod can be written as

$$\begin{aligned} -\sigma A(x) + \left(\sigma + \frac{\partial \sigma}{\partial x} dx\right)\left[A(x) + \frac{dA(x)}{dx} dx\right] \\ = \rho \left[A(x) + \frac{dA(x)}{dx} dx\right] \frac{\partial^2 u(x,t)}{\partial t^2} \end{aligned} \tag{1}$$

where $A(x)$ [in^2] is the cross sectional area of the rod at any location along x-axis, ρ [lb-sec^2/in^4] is the mass density, σ [lb/in^2] is the longitudinal stress, and $u(x,t)$ [in], which is a function of both space x and time t, is the displacement along the x-axis.

Neglecting the terms of the order of dx^2, eqn.(1) can be simplified to

$$\sigma \frac{dA(x)}{dx} + A(x) \frac{\partial \sigma}{\partial x} = \rho A(x) \frac{\partial^2 u(x,t)}{\partial t^2} \quad . \tag{2}$$

After rearranging the left-hand side of eqn.(2) as

$$\sigma \frac{dA(x)}{dx} + A(x) \frac{\partial \sigma}{\partial x} = \frac{\partial}{\partial x} [\sigma A(x)] \quad , \tag{3}$$

eqn.(2) can be rewritten as

$$\frac{\partial}{\partial x} [\sigma A(x)] = \rho A(x) \frac{\partial^2 u(x,t)}{\partial t^2} \quad . \tag{4}$$

The relationship between the stress σ and the displacement variable u can be written via Hookes's Law as

$$\sigma = E \frac{\partial u(x,t)}{\partial x} \quad . \tag{5}$$

where E [lb/in^2] is the modulus of elasticity of the rod.

Substituting eqn.(5) into eqn.(4) gives

$$E \frac{\partial}{\partial x} \left[A(x) \frac{\partial u(x,t)}{\partial x} \right] = \rho A(x) \frac{\partial^2 u(x,t)}{\partial t^2} \quad . \tag{6}$$

which is the one dimensional plane wave equation for an isotropic elastic rod of variable cross sectional area $A(x)$. Note that E is a constant for homogeneous isotropic elastic materials.

Eqn.(6) is a second order partial differential equation with a variable coefficient. An analytical solution can be obtained by a phase-integral method known as the *WKBJ* approximate solution technique. This technique is presented later in this report.

ONE DIMENSIONAL PLANE WAVE PROPAGATION IN PIEZOELECTRIC ROD OF VARIABLE CROSS SECTION

In this section, a one dimensional longitudinal wave equation is derived for an isotropic piezoelectric rod of variable cross section.

The momentum equation (see eqn.(1)) is unaffected by the piezoelectric effect but the Hooke's Law which requires an additional term [1] for piezoelectric materials becomes

$$\sigma = E\,\frac{\partial u(x,t)}{\partial x} - hD_x \quad . \tag{7}$$

Eqn.(7) shows that the presence of an electric flux D_x in the x-direction produces a "piezoelectric stress" D_x, where D_x [coul/in^2] is the electric flux density in the x-direction, and h [lb/coul] is the piezoelectric constant of the material measured with D_x held constant.

Substituting eqn.(7) into eqn.(4) and simplifying give

$$E\frac{\partial}{\partial x}\left[A(x)\frac{\partial u(x,t)}{\partial x}\right] - h\frac{\partial D_x}{\partial x} = \rho A(x)\frac{\partial^2 u(x,t)}{\partial x} \quad . \tag{8}$$

Even though the electric field is not uniformly distributed in the rod along the x-axis as shown in Fig. 2, there is no free charge inside the piezoelectric rod. Therefore, Gauss's Law, which is given by [1]

$$\nabla \cdot \mathbf{D} = 0 \quad , \tag{9}$$

where the vector $\mathbf{D}$ is the resultant electric flux density, remains valid.

Eqn.(9) can also be written as

$$\frac{\partial D_x}{\partial x} + \frac{\partial D_y}{\partial y} + \frac{\partial D_z}{\partial z} = 0 \quad , \tag{10}$$

where D_x, D_y and D_z repesent the x, y and z components of the electric flux density, respectively.

Since plane wave propagation is assumed, differentials with respect to y and z are zero. In particular,

$$\frac{\partial D_y}{\partial y} + \frac{\partial D_z}{\partial z} = 0 \quad . \tag{11}$$

Therefore, from eqn.(10)

$$\frac{\partial D_x}{\partial x} = 0 \quad . \tag{12}$$

Considering eqn.(12), eqn.(8) reduces to

$$E\frac{\partial}{\partial x}\left[A(x)\frac{\partial u(x,t)}{\partial x}\right] = \rho A(x)\frac{\partial^2 u(x,t)}{\partial t^2} \quad , \tag{13}$$

which is the one dimensional plane wave equation for a piezoelectric rod of variable cross section.

Note that eqn.(13) is identical to eqn.(6) which holds for a nonpiezoelectric rod. Consequently, eqn.(13) can also be solved by the $WKBJ$ approximate solution technique which is presented in the next section.

WKBJ APPROXIMATE SOLUTION TO A SECOND-ORDER PARTIAL DIFFERENTIAL EQUATION WITH A VARIABLE COEFFICIENT

The Method

The method derives its name from the physicists Wentzel, Kramers, Brillouin and Jeffreys, who were the first to develop and apply the technique to solve wave propagation equations for slowly-varying stratified media; hence, the name "*WKBJ*" method.

Stratified media are not relevant in the present case; however, the method will be applied to the wave equations derived for an isotropic rod of variable cross section.

Application of the Method

Recall the wave equation derived earlier for isotropic piezoelectric and non-piezoelectric rods of variable cross section:

$$E\frac{\partial}{\partial x}\left[A(x)\frac{\partial u(x,t)}{\partial x}\right] = \rho A(x)\frac{\partial^2 u(x,t)}{\partial t^2} \quad . \tag{14}$$

The *WKBJ* approximation technique presupposes a gradual variation of the cross section $A(x)$ and assumes a solution of the form

$$u(x,t) = a(x)e^{i\theta(x,t)} \quad , \tag{15}$$

where $a(x)$ is the amplitude of the propagating wave, $i = \sqrt{-1}$, and θ is the phase which can be defined as

$$\theta(x,t) = \int_{x_0}^{x} k(x)dx - \omega t \quad , \tag{16}$$

where $k(x)$ is the wave number of the propagating wave, ω is the circular frequency, and t is the time variable.

Eqn.(15) can de differentiated as

$$\begin{aligned}\frac{\partial u(x,t)}{\partial x} &= \frac{\partial}{\partial x}\left[a(x)e^{i\theta}\right] \\ \frac{\partial u(x,t)}{\partial x} &= e^{i\theta}\frac{\partial}{\partial x}\left[a(x)\right] + a(x)\frac{\partial}{\partial x}\left[e^{i\theta}\right] \quad .\end{aligned} \tag{17}$$

But $a(x)$ is a function of x only. Therefore,

$$\frac{\partial}{\partial x}\left[a(x)\right] = \frac{d}{dx}\left[a(x)\right] \quad . \tag{18}$$

Considering eqn.(18), eqn.(17) can be expressed as

$$\frac{\partial u(x,t)}{\partial x} = e^{i\theta}\left(\frac{d}{dx} + ik(x)\right)a(x) \quad . \tag{19}$$

Also,

$$\begin{aligned}\frac{\partial^2 u(x,t)}{\partial x^2} &= \frac{\partial}{\partial x}\left[e^{i\theta}\left(\frac{\partial}{\partial x} + ik(x)\right)a(x)\right] \\ \frac{\partial^2 u(x,t)}{\partial x^2} &= ik(x)e^{i\theta}\left(\frac{d}{dx} + ik(x)\right)a(x) + e^{i\theta}\frac{\partial}{\partial x}\left[\frac{d}{dx} + ik(x)\right]a(x) \\ \frac{\partial^2 u(x,t)}{\partial x^2} &= e^{i\theta}\left[ik(x)\left(\frac{d}{dx} + ik(x)\right)a(x)\right] + e^{i\theta}\frac{\partial}{\partial x}\left[\frac{d}{dx} + ik(x)\right]a(x) \\ \frac{\partial^2 u(x,t)}{\partial x^2} &= e^{i\theta}\left[\left(\frac{d}{dx} + ik(x)\right)\left(\frac{d}{dx} + ik(x)\right)a(x)\right] \quad .\end{aligned} \tag{20}$$

Similarly,

$$\frac{\partial^2 u(x,t)}{\partial t^2} = -\rho A(x)\omega^2 a(x)e^{i\theta} \quad . \tag{21}$$

Substituting eqns.(20) and (21) into eqn.(14) and dividing through by $e^{i\theta}$ give

$$\left[\frac{d}{dx} + ik(x)\right]\left[EA(x)\left(\frac{d}{dx} + ik(x)\right)a(x)\right] = -\rho A(x)\omega^2 a(x) \quad . \tag{22}$$

Solution of eqn.(22) can be obtained by introducing a dimensionless variable, ξ, which can be defined as

$$\xi = \frac{x}{L} \quad , \tag{23}$$

where x is the independent variable along the direction of wave propagation and L is the scale length, which can be defined as the distance from the point of incidence of the propagating wave to the location of the output measurement.

Differentiating eqn.(23) gives

$$\frac{d}{dx} = \frac{1}{L}\frac{d}{d\xi} \quad . \tag{24}$$

Assuming that the wave number k_0 of the incident wave is large or simply that the frequency of the incident wave is high, the amplitude $a(\xi)$ can be asymptotically expanded in powers of a dimensionless constant $k_0 L$ by using Poincare's definition [11]

$$a(\xi) = a_0(\xi) + \frac{1}{k_0 L}a_1(\xi) + \cdots + \frac{1}{(k_0 L)^n}a_n(\xi) + \cdots \quad , \tag{25}$$

where $a_0(\xi), a_1(\xi), \ldots, a_n(\xi), \ldots$ represent the amplitude terms of the asymptotic power series.

Substituting eqn.(25) into eqn.(22) and rearranging give

$$\begin{aligned}
&\frac{E}{L^2}\frac{d}{d\xi}\left[A(\xi)\left(\frac{da_0(\xi)}{d\xi} + \frac{1}{k_0 L}\frac{da_1(\xi)}{d\xi} + \cdots\right)\right] \\
&\quad + \frac{iE}{L}\left\{A(\xi)k(\xi)\left(\frac{da_0(\xi)}{d\xi} + \frac{1}{k_0 L}\frac{da_1(\xi)}{d\xi} + \cdots\right)\right. \\
&\qquad \left. + \frac{d}{d\xi}\left[EA(\xi)k(\xi)\left(a_0(\xi) + \frac{a_1(\xi)}{k_0 L} + \cdots\right)\right]\right\} \\
&\quad + \left[\rho A(\xi)\omega^2 - EA(\xi)k^2(\xi)\right]\left[a_0(\xi) + \frac{a_1(\xi)}{k_0 L} + \cdots\right] \\
&= 0 \quad .
\end{aligned} \tag{26}$$

Multiplying the first, second, and third terms of eqn.(26) by $(k_0/k_0)^2$, $(k_0/k_0)^1$, and $(k_0/k_0)^0$, respectively, results in

$$\begin{aligned}
&\left(\frac{1}{k_0 L}\right)^2 Ek_0{}^2\frac{d}{d\xi}\left[A(\xi)\left(\frac{da_0(\xi)}{d\xi} + \frac{1}{k_0 L}\frac{da_1(\xi)}{d\xi} + \cdots\right)\right] \\
&\quad + \left(\frac{1}{k_0 L}\right)^1 ik_0 E\left\{A(\xi)k(\xi)\left[\frac{da_0(\xi)}{d\xi} + \frac{1}{k_0 L}\frac{da_1(\xi)}{d\xi} + \cdots\right]\right. \\
&\qquad \left. + \frac{d}{d\xi}\left[EA(\xi)k(\xi)\left(a_0(\xi) + \frac{a_1(\xi)}{k_0 L} + \cdots\right)\right]\right\} \\
&\quad + \left[\rho A(\xi)\omega^2 - EA(\xi)k^2(\xi)\right]\left[a_0(\xi) + \frac{a_1(\xi)}{k_0 L} + \cdots\right] \\
&= 0 \quad .
\end{aligned} \tag{27}$$

Separating eqn.(27) by powers of $1/k_0L$ gives

$$\begin{aligned}
\left(\frac{1}{k_0L}\right)^0 &: \quad \left[\rho A(\xi)\omega^2 - EA(\xi)k^2(\xi)\right] a_0(\xi) = 0 \quad , \\
\left(\frac{1}{k_0L}\right)^1 &: \quad ik_0 \left\{ EA(\xi)k(\xi)\frac{da_0(\xi)}{d\xi} + \frac{d}{d\xi}\left[EA(\xi)k(\xi)a_0(\xi)\right] \right\} \\
&\qquad + \left[\rho A(\xi)\omega^2 - EA(\xi)k^2(\xi)\right] a_1(\xi) = 0 \quad , \\
\left(\frac{1}{k_0L}\right)^2 &: \quad {k_0}^2 \frac{d}{d\xi}\left[EA(\xi)\frac{da_0(\xi)}{d\xi}\right] \\
&\qquad + ik_0 \left\{ EA(\xi)k(\xi)\frac{da_1(\xi)}{d\xi} + \frac{d}{d\xi}\left[EA(\xi)k(\xi)a_1(\xi)\right] \right\} \\
&\qquad + \left[\rho A(\xi)\omega^2 - EA(\xi)k^2(\xi)\right] a_2(\xi) = 0 \quad .
\end{aligned} \tag{28}$$

The first expression of eqn.(28) gives the dispersion relation for the plane propagating wave, that is,

$$\rho A(\xi)\omega^2 - EA(\xi)k^2(\xi) = 0 \tag{29}$$

or

$$k^2(\xi) = \frac{\omega^2}{E/\rho} \quad . \tag{30}$$

But the phase velocity c of the propagating wave is defined as

$$c = \sqrt{\frac{E}{\rho}} \quad , \tag{31}$$

and so, considering eqn.(31), eqn.(30) becomes

$$k(\xi) = \frac{\omega}{c} \quad . \tag{32}$$

Since the circular frequency ω and the phase velocity c are constants, the wave number $k(\xi)$ is also constant and hence independent of ξ. Denoting this constant as k yields

$$k = \frac{\omega}{c} \quad . \tag{33}$$

If the dispersion relation as expressed in eqn.(29) is true, then the last terms of the second and the third expressions of eqn.(28) vanish. So, the second expression of eqn.(28) can be expanded as

$$2EA(\xi)k(\xi)\frac{da_0(\xi)}{d\xi} + a_0(\xi)\frac{d}{d\xi}\left[EA(\xi)k(\xi)\right] = 0 \tag{34}$$

and rearranged as

$$\frac{1}{a_0(\xi)}\frac{d}{d\xi}\left[EA(\xi)k{a_0}^2(\xi)\right]=0 \quad . \tag{35}$$

or

$$EA(\xi)k{a_0}^2(\xi)=constant \quad . \tag{36}$$

For any segment L of the rod between the $x=x_1$ and $x=x_2$, it can be deduced from eqn.(36) that

$$\left[\frac{a(x_2)}{a(x_1)}\right]^2=\frac{A(x_1)}{A(x_2)} \quad . \tag{37}$$

where $a(x_1)$ and $a(x_2)$ represent the amplitudes of the propagating wave at the locations $x=x_1$ and $x=x_2$, respectively, and $A(x_1)$ and $A(x_2)$ are the corresponding cross sectional areas.

Eqn.(37), which relates the variation of the amplitudes of the traveling wave to the cross sectional areas of the rod, was also derived by Green [12] and Liouville [13] who were the early investigators of this type of problem. Green [12] arrived at this solution by an energy conservation argument.

Eqn.(37) can be simplified to

$$\frac{a(x_2)}{a(x_1)}=\frac{r(x_1)}{r(x_2)} \quad , \tag{38}$$

where $r(x_1)$ and $r(x_2)$ are the radii of the rod at the locations $x=x_1$ and $x=x_2$, respectively.

Eqn.(38) is useful for quick practical approximations but it lacks information about the frequencies at which this approximation is true. In order to incorporate the information on the frequency into the approximation, it is necessary to investigate the order of magnitude of the second term, $a_1(\xi)$, of the asymptotic power series such that the approximate solution is true only when the first term $a_0(\xi)$ is retained.

The order of magnitude for $a_1(\xi)$ can be obtained from the third term of eqn.(28) which can be reproduced as

$$k_0{}^2 \frac{d}{d\xi}\left[EA(\xi)\frac{da_0(\xi)}{d\xi}\right] + ik_0\left\{EA(\xi)k\frac{da_1(\xi)}{d\xi} + \frac{d}{d\xi}\left[EA(\xi)a_1(\xi)k\right]\right\} = 0 \quad . \quad (39)$$

The second term of eqn.(39) can be expanded as

$$\begin{aligned} ik_0\left\{EA(\xi)k\frac{da_1(\xi)}{d\xi} + \frac{d}{d\xi}\left[EA(\xi)a_1(\xi)\right]\right\} \\ = 2EA(\xi)k\frac{da_1(\xi)}{d\xi} + a_1(\xi)\frac{d}{d\xi}\left[EA(\xi)k\right] \quad . \end{aligned} \quad (40)$$

Therefore, eqn.(39) becomes

$$k_0{}^2 \frac{d}{d\xi}\left[EA\frac{da_0}{d\xi}\right] + ik_0\left\{2EAk\frac{da_1}{d\xi} + \frac{d}{d\xi}\left[EAk\right]\right\} = 0 \quad , \quad (41)$$

where the argument ξ is dropped for convenience.

But from eqn.(34)

$$\frac{d}{d\xi}\left[EAk\right] = -\left(\frac{2EAk}{a_0}\right)\frac{da_0}{d\xi} \quad . \quad (42)$$

Substituting eqn.(42) into eqn.(41) and rearranging give

$$k_0\frac{d}{d\xi}\left[EA\frac{da_0}{d\xi}\right] + 2iEAk\left(\frac{da_1}{d\xi} - \frac{a_1}{a_0}\frac{da_0}{d\xi}\right) = 0 \quad . \quad (43)$$

The expressions in the second set of parantheses in eqn.(43) can be rearranged as

$$\frac{da_1}{d\xi} - \frac{a_1}{a_0}\frac{da_0}{d\xi} = -a_0\frac{d}{d\xi}\left[\frac{a_1}{a_0}\right] \quad . \quad (44)$$

Substituting eqn.(44) into eqn.(43) and rearranging give

$$\frac{d}{d\xi}\left[\frac{a_1}{a_0}\right] = \frac{i}{2}\left(\frac{k_0}{k}\right)\left(\frac{1}{EAa_0}\right)\frac{d}{d\xi}\left[EA\frac{da_0}{d\xi}\right] \quad . \quad (45)$$

Since it is desired to have the results in terms of L, dividing both sides of eqn.(45) by k_0L gives

$$\frac{1}{k_0L}\frac{d}{d\xi}\left[\frac{a_1}{a_0}\right] = \frac{i}{2kL}\left(\frac{1}{EAa_0}\right)\frac{d}{d\xi}\left[EA\frac{da_0}{d\xi}\right] \quad , \quad (46)$$

or

$$\frac{d}{d\xi}\left[\frac{a_1/k_0L}{a_0}\right] = \frac{i}{2kL}\left(\frac{1}{EAa_0}\right)\frac{d}{d\xi}\left[EA\frac{da_0}{d\xi}\right] \quad . \tag{47}$$

Also since the only purpose here is to estimate how large a_1/k_0L is with respect to a_0 , from eqn.(47) one can write

$$\frac{d}{d\xi}\left[\frac{a_1/k_0L}{a_0}\right] = O\left(\frac{1}{kL}\right) \quad . \tag{48}$$

where "O" represents "order of".

Note that since both sides of eqn.(47) have the same scale length, the term

$$\frac{1}{EAa_0}\frac{d}{d\xi}\left[EA\frac{da_0}{d\xi}\right] \quad , \tag{49}$$

can be estimated to be order of unity.

Integrating eqn.(48) results in

$$\frac{a_1/k_0L}{a_0} = O\left(\frac{\xi}{kL}\right) \quad . \tag{50}$$

Substituting for ξ from eqn.(23) into eqn.(50) and rearranging result in

$$\frac{a_1}{k_0L} = O\left(\frac{x/L}{kL}\right)a_0 \quad . \tag{51}$$

Eqn.(51) gives the order of magnitude of the second term a_1 of the asymptotic power series as a function of the first term a_0.

Substituting for a_1 into eqn.(25) yields

$$a(\xi) = a_0(\xi) + O\left(\frac{x/L}{kL}\right)a_0(\xi) + \cdots + \frac{1}{(k_0L)^n}a_n(\xi) + \cdots \tag{52}$$

The concern here is to determine, analytically, the condition under which the higher order terms of the asymptotic power series, including the second term a_1 , can be neglected in applying the *WKBJ* approximation. The condition can be derived from eqn.(52) as follows. Since a_1 is of "order" $(x/L)/kL$ and also since k_0 was assumed to be large, then if

$$\frac{x/L}{kL} << 1 \quad , \tag{53}$$

the first and other higher terms of the power series can be neglected. Therefore, the $WKBJ$ solution expressed in eqn.(38) would be true if the condition stated in eqn.(53) is satisfied.

The physical signficance of the condition expressed in eqn.(53) can be obtained by expanding the equation as

$$\frac{x}{L^2} << k \quad , \tag{54}$$

or

$$\frac{x}{L^2} << \frac{2\pi}{\lambda} \quad , \tag{55}$$

where λ is the wavelength of the propagating wave.

Consider a situation where the rod has a finite length L and where an observer is located at the end of the rod. In other words, the variable x is equal in magnitude to the scale length. In that case, eqn.(55) becomes

$$\frac{1}{L} << \frac{2\pi}{\lambda} \quad , \tag{56}$$

or

$$\lambda << 2\pi L \quad . \tag{57}$$

The inequality eqn.(57) is satisfied only by very short wavelengths or simply when the frequency of the propagating wave is high. Also, the inequality statement implies that the error associated with the $WKBJ$ approximation is negligible at high frequencies. In short, according to Heading [5], the error associated with use of the $WKBJ$ solution is expressed as $O(1/kL)$ times the approximation (eqn.(38)). Hence,

$$E = O\left(\frac{1}{kL}\right)\frac{r(x_1)}{r(x_2)} \quad . \tag{58}$$

Eqn.(58) can also be derived from eqn.(52). Finally, the solution can be summarized as

$$A = R\left[1 + O\left(\frac{1}{kL}\right)\right]$$

$$if$$

$$\frac{x}{L} << kL \quad , \tag{59}$$

where A replaces the ratio $a(x_2)/a(x_1)$, and R equals the ratio $r(x_1)/r(x_2)$.

The expressions of eqn.(59) represent the complete $WKBJ$ solutions, after Wentzel [14], Kramers [15], Brillouin [16], and Jeffreys [17], for this problem.

The conditional statement in the second expression of eqn.(59) indicates that the use of the formula is limited to cases when the frequency of the incident wave is high. How high the frequency must be is one of the issues of investigation in this report. The results are presented for some well-defined geometric parameters of the rod and are presented in the next section.

RESULTS AND DISCUSSIONS

It is clear from the preceeding section that the validity of the $WKBJ$ solution rests on two important parameters, namely, the scale length, which in practice represents the length of the rod, and the frequency of the propagating wave. The $WKBJ$ solution was derived under the assumption that the frequency of the propagating wave was high. How high the frequency must be in order to satisfy the solution is therefore an important question.

In this section, investigation of the lower bound frequency at which the $WKBJ$ solution is valid is pursued for both piezoelectric and nonpiezoelectric materials. One part of the investigation focuses on four piezoelectric materials and the other focuses on two nonpiezoelectric materials.

The piezoelectric materials selected are lead mentaniobate ($PbNb_2O_6$), lead zirconate-titanate ($PZT-5A$), quartz (SiO_2), and lithium niobate ($LiNiO_3$) with longitudinal wave speeds of [18] 131 $\times$ 10^3 in/sec (3,323 m/sec), 172 $\times$ 10^3 in/sec (4,350 m/sec), 226 $\times$ 10^3 in/sec (5,740 m/sec), and 291 $\times$ 10^3 in/sec (7,400 m/sec), respectively. These four materials represent the most widely used piezoelectric materials in ultrasonic and acoustic emission transducers.

For this report, a range of values from 0.025 in (0.635 mm) to 0.25 in (6.35 mm), which represents the usual thickness range of piezoelements of ultrasonic and acoustic emission transducers, was assigned to the length of the rod of each piezoelectric material. Six values, namely, 0.125, 0.250, 0.375, 0.500, 0.625, and 0.750, were selected as values of the ratio of the cross sectional radii.

Based on the $WKBJ$ solution

$$A = R\left(1 + \frac{1}{kL}\right) \quad , \quad \frac{x}{L} << kL \quad , \tag{60}$$

where "O" is omitted for computational convenience, six plots (one for each value of R) were generated for each piezoelectric material. These plots are shown in

Figs. 3 through 6. Each plot represents a family of ten curves that relate the amplitude ratio A to the different frequencies of the propagating wave. Each curve was generated for one value of L.

Before discussing the results of these plots, it is necessary to state that the $WKBJ$ solution is satisfied when A is approximately equal to R, that is,

$$A \approx R \quad . \tag{61}$$

Although the frequencies at which the solution is satisfied can be deduced from Figs. 3 through 6, it is probably not the easiest way to do so. For this reason, it is necessary to recall that the error associated with the solution (eqn.(60)) is given by

$$E = R\left(\frac{1}{kL}\right) \quad , \tag{62}$$

which in percentage terms may be written as

$$E[\%] = 100R\left(\frac{1}{kL}\right) \quad . \tag{63}$$

With this in mind, it becomes a matter of selecting an acceptable error and thereafter establishing the minimum frequency that satisfies the solution. In this report, an arbitrarily acceptable error of 1.4% is selected. The frequency at which the error is approximately 1.4% is termed the lower- bound frequency and is denoted by F_T. So, from eqn.(63), F_T can be defined as

$$F_T \approx 16\frac{c}{L}\frac{R}{E_a} \quad , \tag{64}$$

where c is the wave speed in the material, R is the ratio of the cross sectional radii, and L is the length of the rod.

Eqn.(64) shows that F_T increases proportionally as R and decreases proportionally as L. Because R and L are variables, eqn.(64) is most easily understood if either R or L is a constant.

By fixing the value of L at 0.25 in and Ea at 1.4%, plots of F_T versus R are generated for the four piezoelectric materials and shown in Figs. 7 through 10. The linear relationship between F_T and R can be observed from these plots. Similar plots can be generated for other values of L.

In order to show the relationship between E and L, eqn.(64) can be reexpressed as

$$E(\%) \approx 16R\frac{c}{F_T} \quad . \tag{65}$$

But the wavelenght λ_T at the lower bound frequency can be expresssed as

$$\lambda_T = \frac{c}{F_T} \quad . \tag{66}$$

Combining eqns.(65) and (66) gives

$$E(\%) \approx 16R\frac{\lambda_T}{L} \tag{67}$$

So, based on eqn.(67) the relationship between E and L in parametrized form were generated and shown in Figs. 11 through 14. For each piezoelectric material, the plots are generated for only 3 values of R because the relationship between E and R can easily be deduced from other values of R. It can be observed from Figs. 11 through 14 that when the value of L is 0.25in, the value of E is equal to the acceptable error E_a which was fixed to about 1.4%. A list of the estimated values of the lower bound frequencies and the corresponding acceptable errors are shown in Table 1.

Another aspect of this report is directed towards establishing similar parameters in nonpiezoelectric materials. Aluminum and brass with longitudinal wave speeds of 250 $\times$ 10^3 in/sec (6,350 m/sec) and 175 $\times$ 10^3 in/sec (4,430 m/sec), respectively, were selected for the investigation. These two materials were selected primarily in preparation for experimental studies of wave propagation in isotropic elastic rods of variable cross section, which are presented in sbsequent report. Also,

brass was selected because its acoustic properties are very close to those of $PZT-5A$ from which the piezoelement of the IQI transducer was fabricated. For instance, the longitudinal wave speed in $PZT-5A$ is only 1.7% lower than that of brass. Aluminum was selected because it is widely used in nondestructive testing (NDT) of materials and also for reference purposes.

A range of values varying from 0.25 in to 2.5 in, which represents the usual thickness range encountered in UT of materials, was assigned to L. The same set of values of R was also selected in this case.

With these parameters and using eqn.(60), parametrized curves that relate the amplitude ratio to the frequencies of the propagating wave are generated and shown in Figs. 15 and 16 for aluminum and brass, respectively. The interpretations of the results from these plots are quite similar to those presented above for the piezoelectric materials.

Similarly, plots of F_T versus R are generated for aluminum and brass by using

$$E_a = 1.4\% \tag{68}$$

in eqn.(64) but by assigning the value of 2.5 in to L. These plots are shown in Figs. 17 and 18. Also, plots of E versus λ_T/L are generated and shown in Figs. 19 and 20 for aluminum and brass, respectively. The estimated lower bound frequencies and the corresponding acceptable errors are shown in Table 2. Note that the lower bound frequencies are lower because the values of L for the nonpiezoelectric materials are ten the values of L for the piezoelectric materials.

It can be observed that, in general, the lower bound frequency not only varies with respect to the geometric parameters of the rod, such as R and L, but also it varies with respect to the acoustic properties of the rod, such as wave speeds. This observation is important when applying the $WKBJ$ approximate solution technique to solving wave equations for materials whose properties not only vary in cross

section but also in acoustic properties in the direction of the wave propagation, such as stratified media.

CONCLUSIONS AND RECOMMENDATIONS

In this report, a formula that relates the ratio $a(x_2)/a(x_1)$ of the amplitudes of a longitudinal propagating wave to the ratio $r(x_1)/r(x_2)$ of the cross sectional radii was derived by using the $WKBJ$ approximate solution technique. Furthermore, the $WKBJ$ solution was shown to hold only when the frequency of the propagating wave was high, that is, $x/L << kL$.

How high the frequency should be was investigated for four piezoelectric materials and two nonpiezoelectric materials. The minimum frequency, at which the approximate solution is valid is within 1.4% error, was defined as the lower bound frequency. At the lower bound frequency, the error associated with the approximation was fixed at approximately 1.4% for all the materials discussed here. For instance, it was found that F_T was attained in all the piezoelectric materials when the ratio λ_T/L was $1.4, 2.8, \ldots, 8.4$ for the corresponding values $0.125, 0.250, \ldots, 0.750$ for R. So, for the piezoelement of the transducer with $L = 0.100$ in and $R = 0.250$, the lower bound frequency can be deduced to be approximately equal to 4600 kHz.

In conclusion, one can say that the one dimensional wave propagation analysis presented here not only enhances understanding of wave propagation in rods of variable cross section, but also forms a step in the characterization of conical transducers in general and, in particular, in the characterization of transducer IQI model 501.

Note, however, that the analysis neglects the effects of attenuation (energy loss) of the propagating wave in the materials and hence on the $WKBJ$ solution. For this reason, it is recommended that the $WKBJ$ solution presented here be verified experimentally.

REFERENCES

[1] M. Redwood, "Transient Performance of a piezoelectric Transducer", Journal of the Acoustical Society of America, Vol. 33 , 1961 , pp 527 – 536 .

[2] L. Filipczynski, "Transients and the Equivalent Electriacl Circuit of the piezoelectric Transducer", Acoustica, Vol. 10 , 1960 , pp 149 – 154 .

[3] R. I. Kazhis and A. I. Lukoshevichyus, "Wideband piezoelectric Transducers with an Inhomogeneous Electric Field", Soviet Physical Acoustics, Vol. 22 , 1976 , pp 167 – 168 .

[4] J. H. Williams, Jr. and B. Doll, "A Simple Wave Propagation Analysis of piezoelectric Ultrasonic Transducer Response", Materials Evaluation, Vol. 40 , No. 13 , 1982 , pp 1374 – 1381 .

[5] J. H. Heading, An Introduction to Phase Integral Methods, Matheun & Co., London, 1982 .

[6] R. Gans, "Annales de Physique", Vol. 47 , No. 4 , 1915 , pp 709 – 736 .

[7] V. A. Bailey, "Physics Review", Vol. 96 , 1954 , pp 865 – 868 .

[8] I. Iami, "Quarterly Journal of Applied Mathematics", Vol. 16 , 1958 , pp 35 – 45 .

[9] H. Moriguchi, "Progress in Theoretical Physics", Vol. 23 , 1960 , pp 750 – 752 .

[10] C. O. Hines,"Quarterly Applied Mathematics", No. 11, 1953, pp 9 – 31 .

[11] H. Jeffreys and B. Jeffreys, Methods of Mathematical Physics, Cambridge University Press, 1956 .

[12] G. Green, "Cambridge Philosophical Transactions", Vol. 2 , 1837 , pp 457–462 .

[13] J. Liouville, "Journal of Pure Applied Mathematics", Vol.2 , 1837 , pp 16 – 35 .

[14] G. Wentzel, "Zeitschrift fuer Philologie", Vol. 38 , 1926 , pp 518 .

[15] H. A. Kramers , "Zeitschrift fuer Philologie", Vol. 38 , 1926 , pp 828 – 840 .

[16] L. Brillouin, "Computes Rendus Acadamie des Sciences.", Vol. 183 , 1926 , pp 24 – 26 .

[17] H. Jeffreys, "Proceedings of London Mathematical Science", Vol. 23 , 1923 , pp 428 – 436 .

[18] V. M. Ristic, Principles of Acoustic Devices, John Wiley & Sons, New York, 1983 .

Table 1

Lower Bound Frequencies for Four Piezoelectric Materials

Material	Ratio R	Lower bound frequency F_T(kHz)	$\frac{\lambda_T}{L}$	Error at F_T [%]
Lead metaniobate	0.125	750	1.431	1.400
	0.250	1500	2.862	1.400
	0.375	2250	4.294	1.400
	0.500	3000	5.925	1.400
	0.625	3750	7.156	1.400
	0.750	4500	8.588	1.400
Lead zirconate-titanate (PZT - 5A)	0.125	1000	1.453	1.400
	0.250	2000	2.906	1.400
	0.375	3000	4.359	1.400
	0.500	4000	5.812	1.400
	0.625	5000	7.265	1.400
	0.750	6000	8.718	1.400
Quartz	0.125	1300	1.438	1.400
	0.250	2600	2.876	1.400
	0.375	3900	4.314	1.400
	0.500	5200	5.752	1.400
	0.625	6500	7.190	1.400
	0.750	7800	8.626	1.400
Lithium niobate	0.125	1600	1.372	1.400
	0.250	3200	2.744	1.400
	0.375	4800	4.116	1.400
	0.500	6400	5.488	1.400
	0.625	8000	6.868	1.400
	0.750	9600	8.232	1.400

Table 2

Lower Bound Frequencies for Two Nonpiezoelectric Materials

Material	Ratio R	Lower bound frequency F_T(kHz)	$\frac{\lambda_T}{L}$	Error at F_T (%)
Brass	0.125	100	1.389	1.400
	0.250	200	2.778	1.400
	0.375	300	4.167	1.400
	0.500	400	5.556	1.400
	0.625	500	6.945	1.400
	0.750	600	8.330	1.400
Aluminum	0.125	143	1.500	1.400
	0.250	286	3.000	1.400
	0.375	429	4.500	1.400
	0.500	572	6.000	1.400
	0.625	715	7.500	1.400
	0.750	858	9.000	1.400

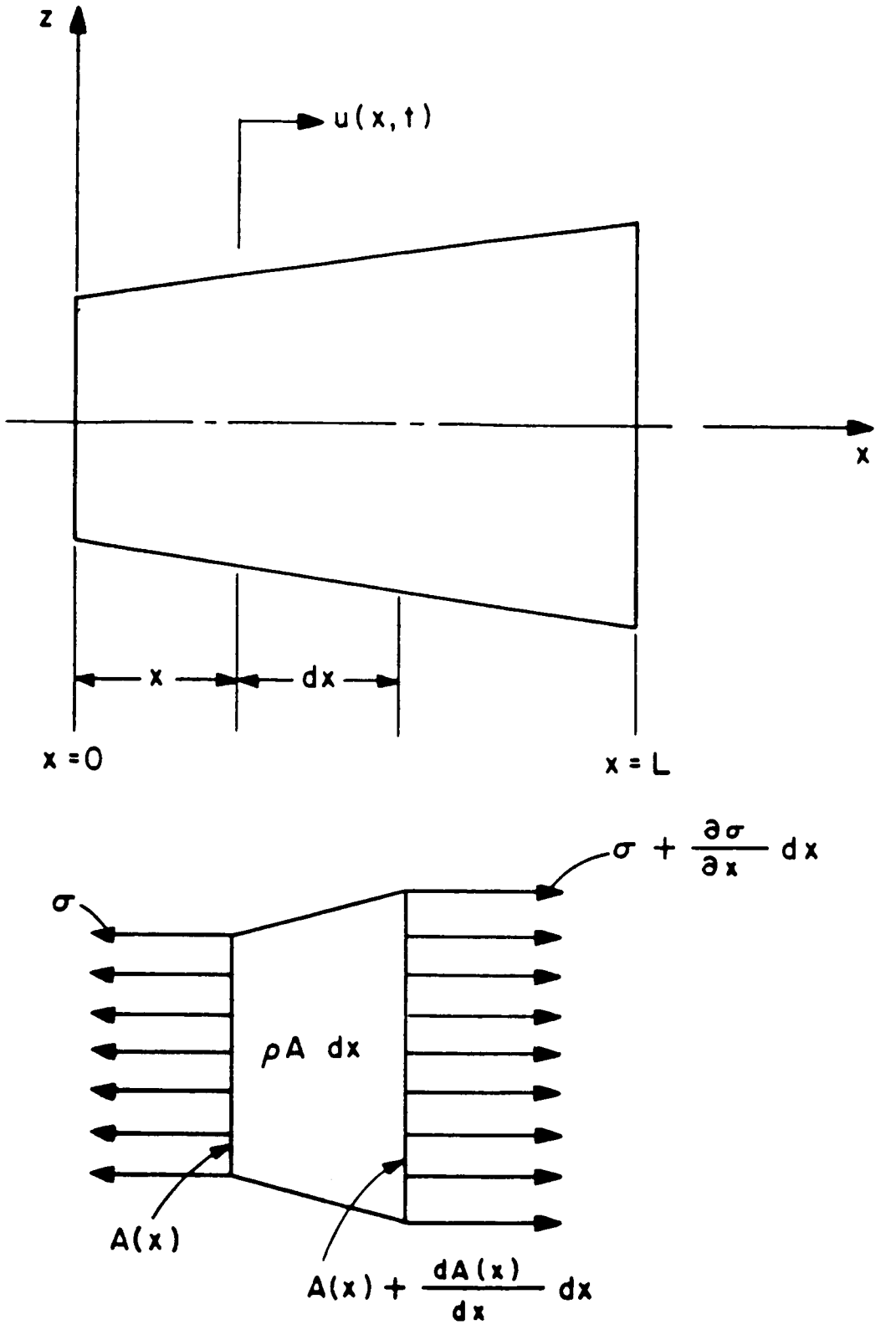

Fig. 1 Elastic rod (nonpiezoelectric material) of variable cross-section conducting longitudinal wave propagation in x-direction.

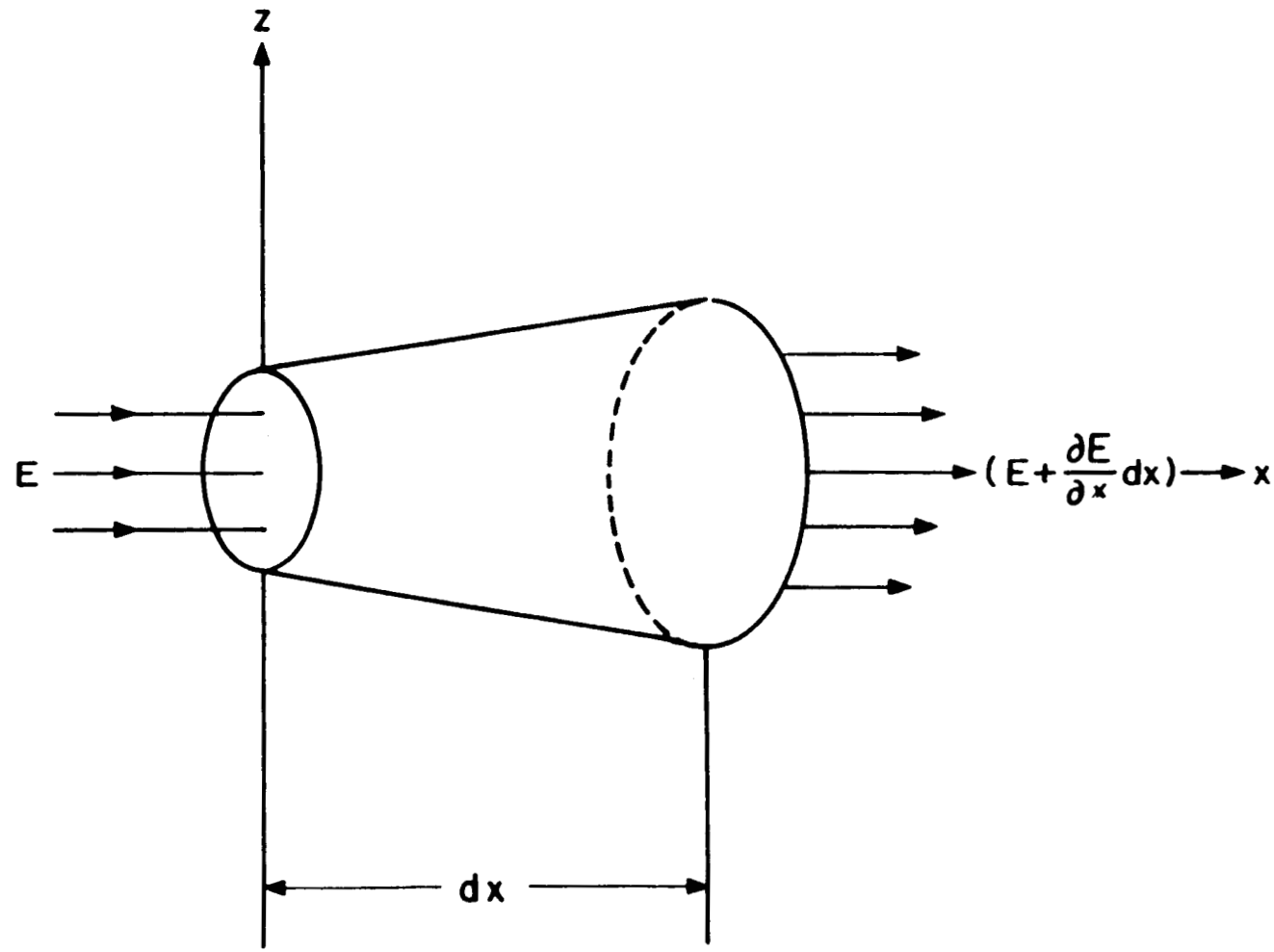

Fig.2 Schematic of electric field distribution in differential element of piezoelectric truncated cone.

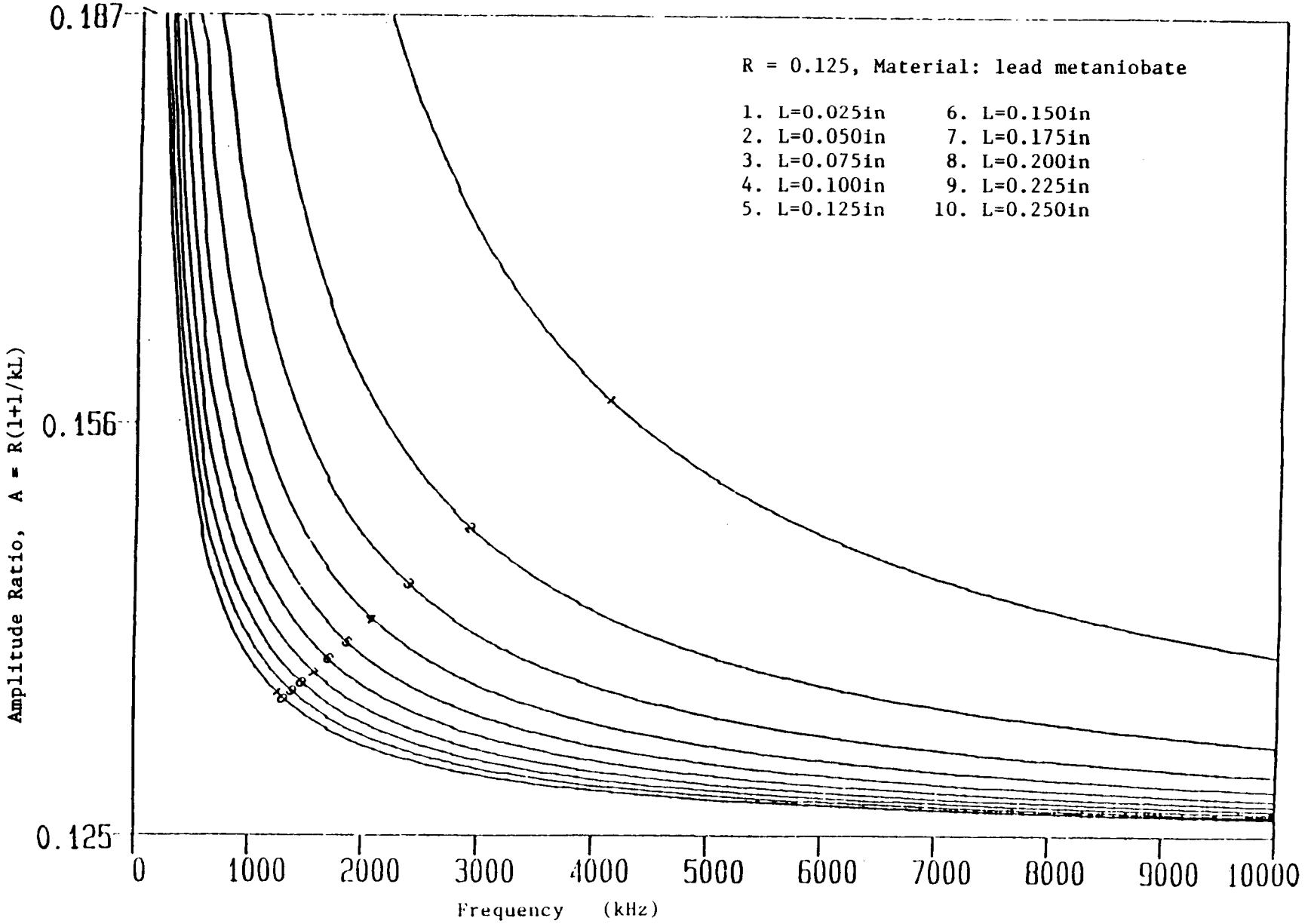

Fig. 3a Amplitude ratio versus frequency for lead metaniobate rod with R = 0.125

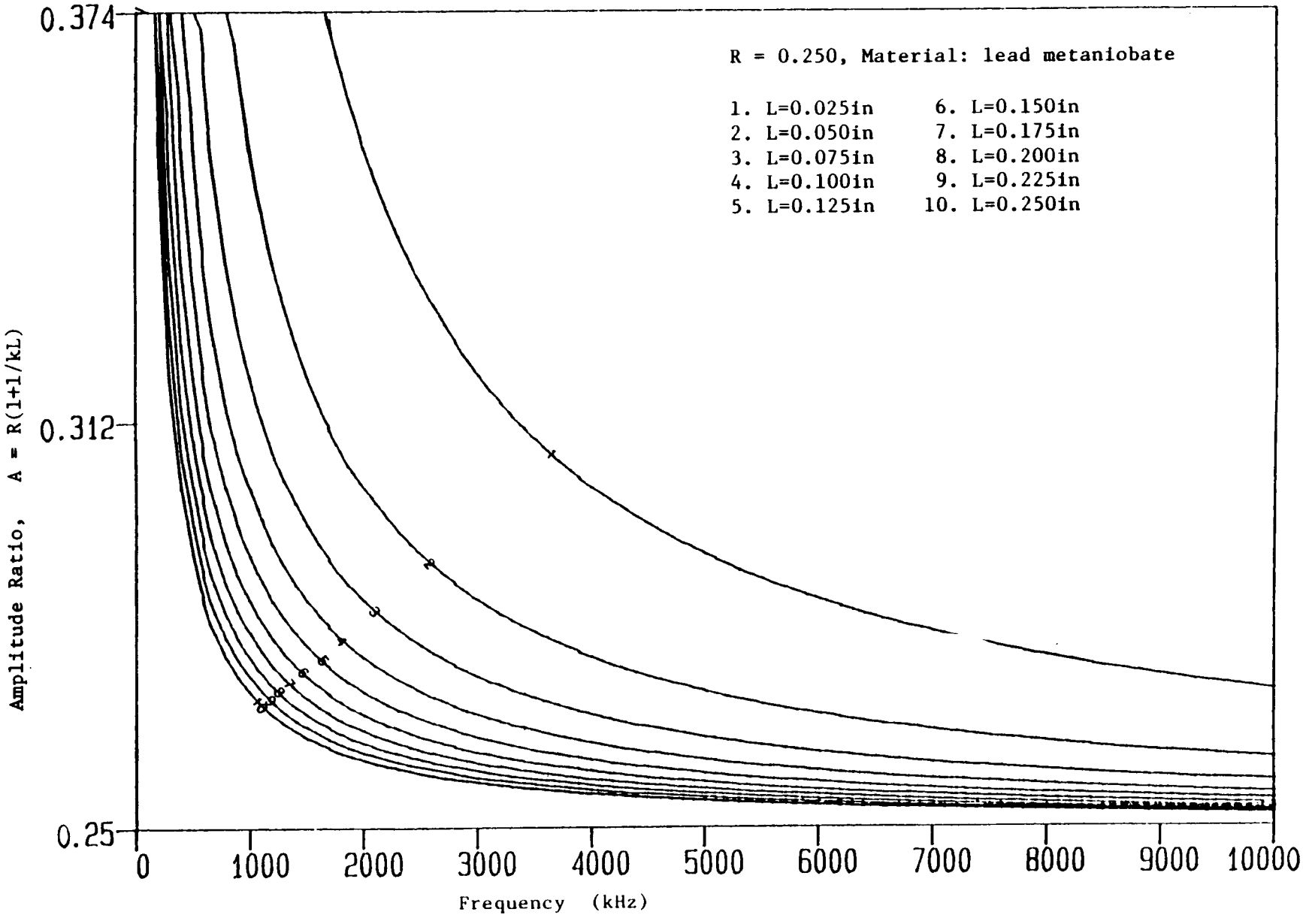

Fig. 3b Amplitude ratio versus frequency for lead metaniobate rod with R = 0.250

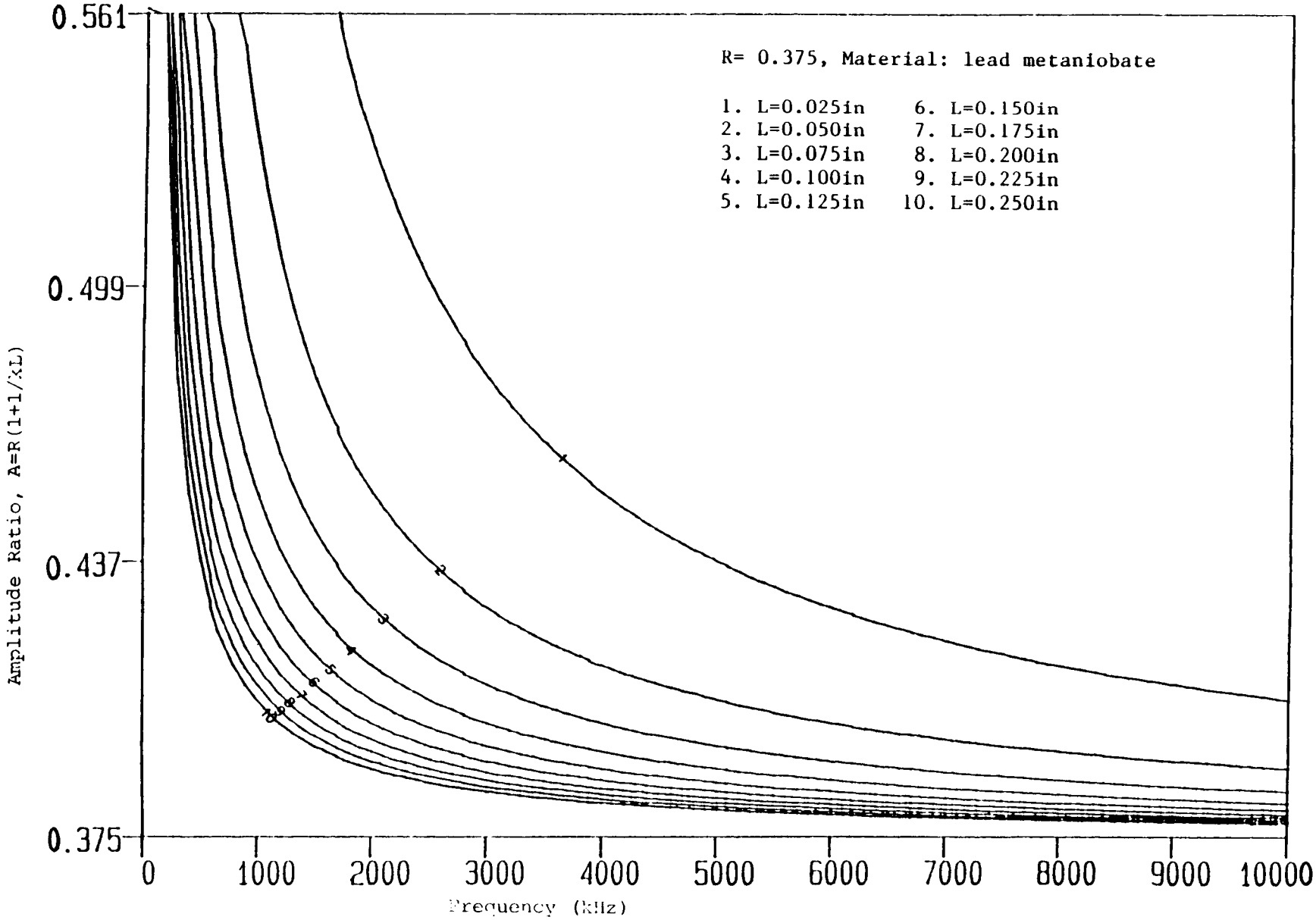

Fig. 3c Amplitude ratio versus frequency for lead metaniobate rod with R = 0.375.

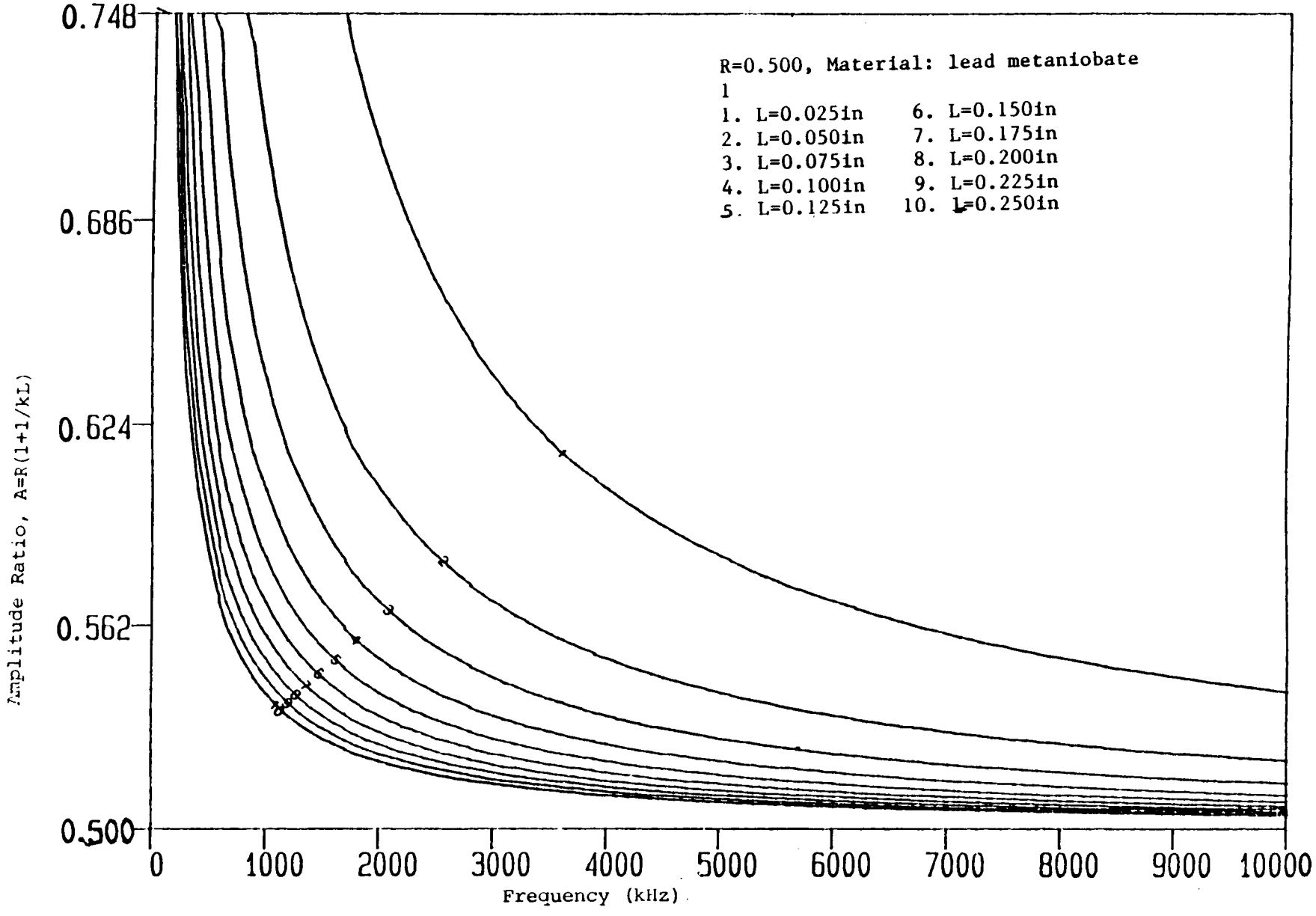

Fig. 3d Amplitude ratio versus frequency for lead metaniobate rod with R = 0.500.

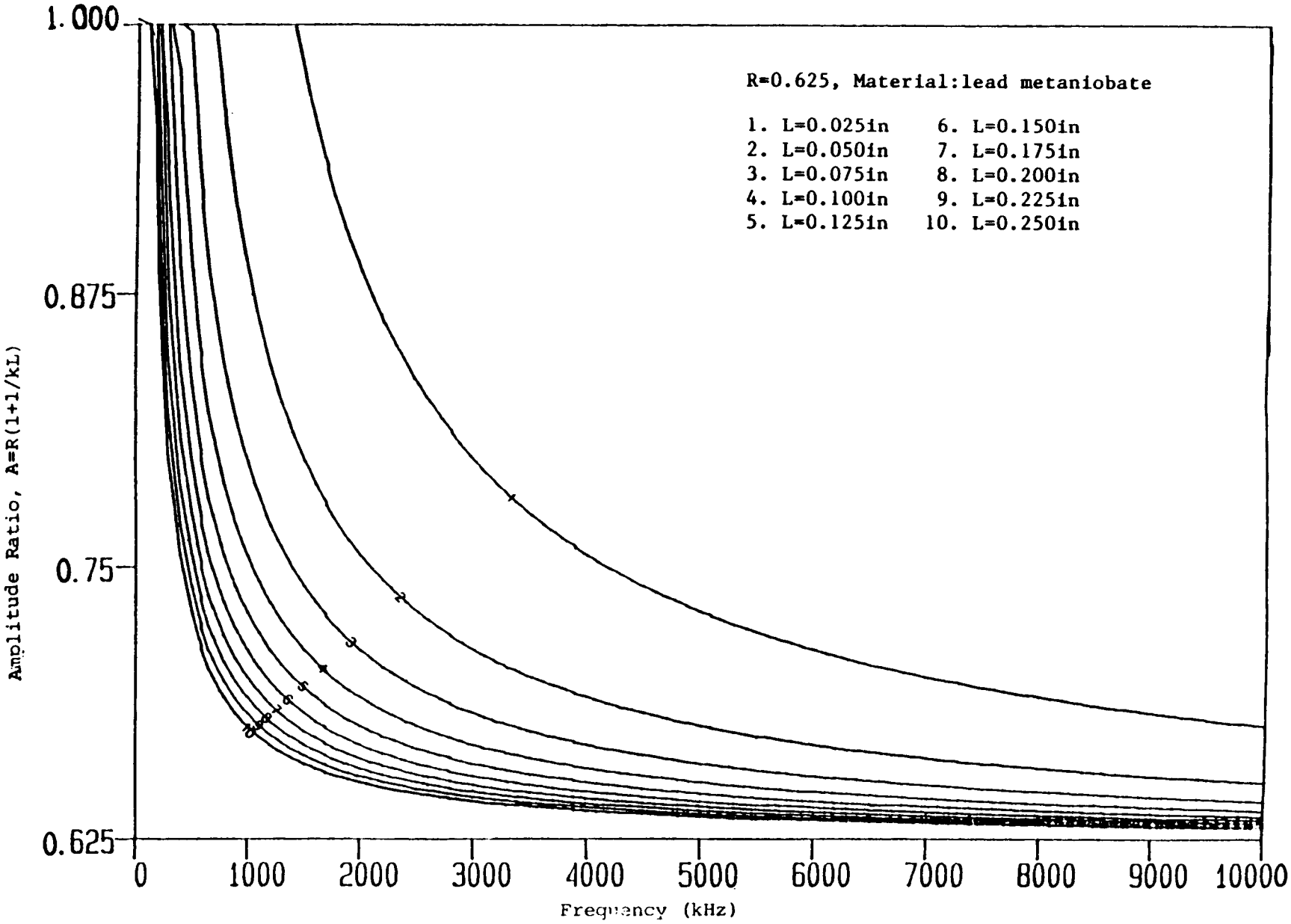

Fig. 3e Amplitude ratio versus frequency for lead metaniobate rod with R = 0.625.

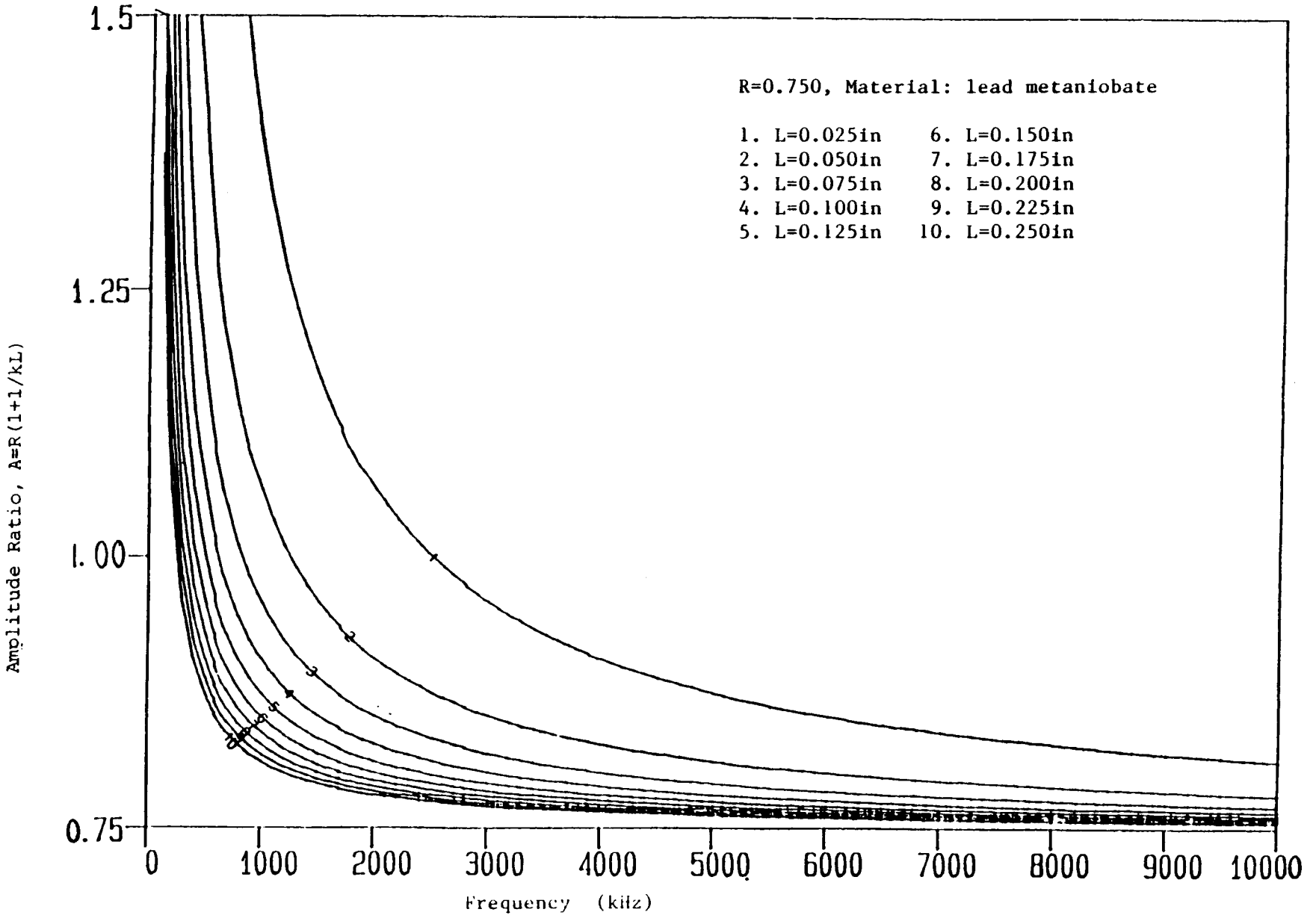

Fig. 3f Amplitude ratio versus frequency for lead metaniobate rod with R = 0.625.

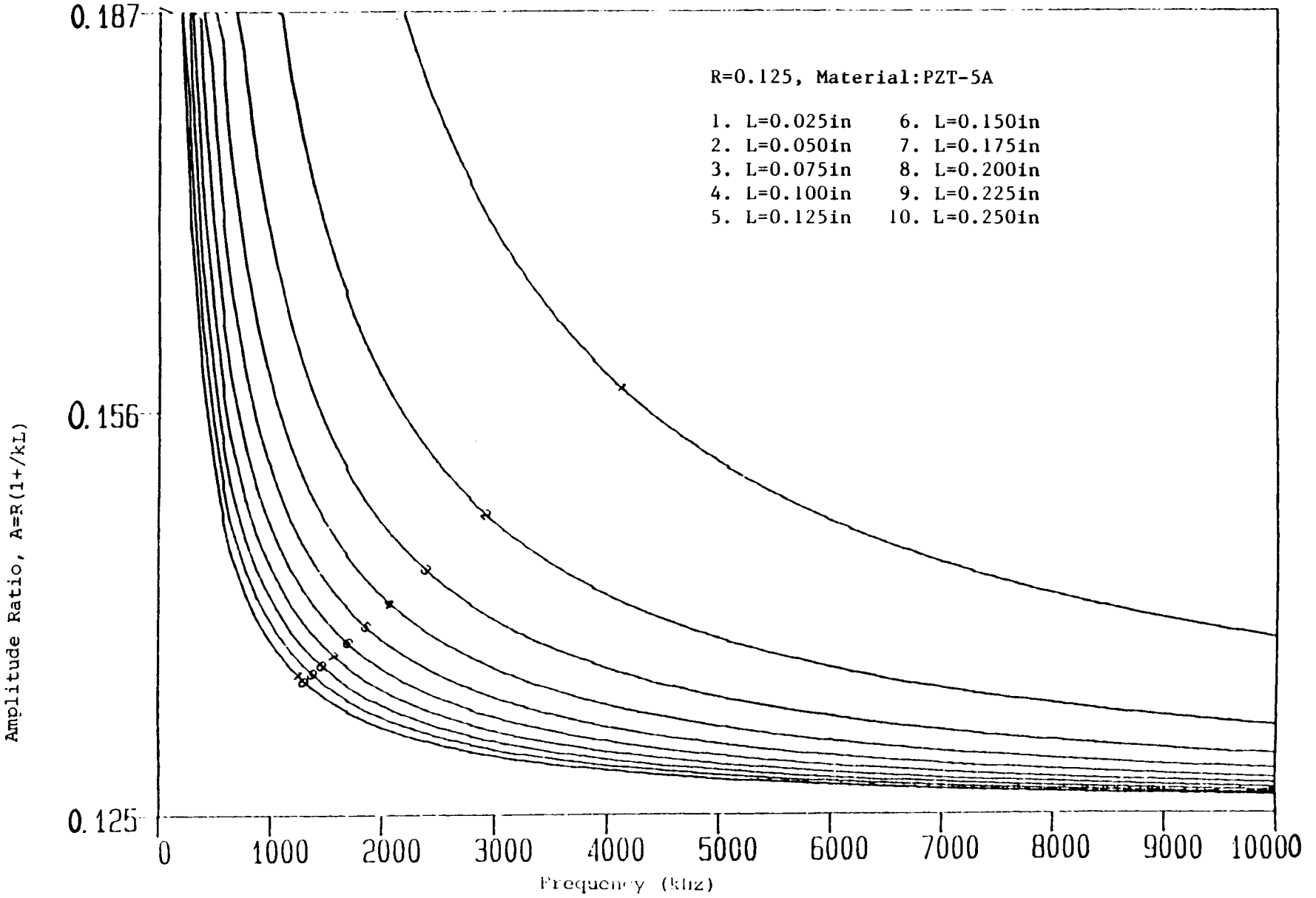

Fig. 4a Amplitude ratio versus frequency for PZT-5A rod with R = 0.125.

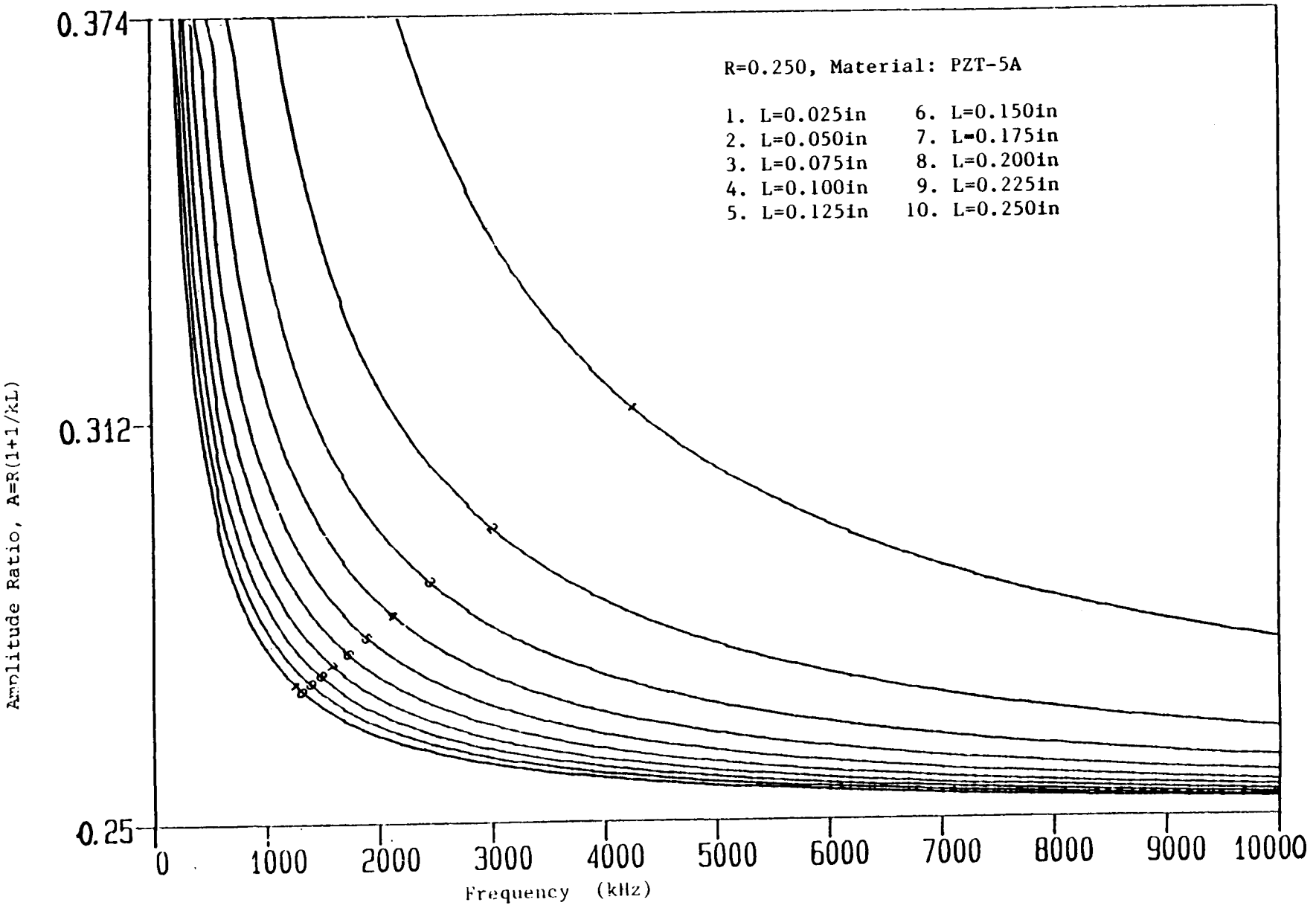

Fig. 4b Amplitude ratio versus frequency for PZT-5A rod with R = 0.250.

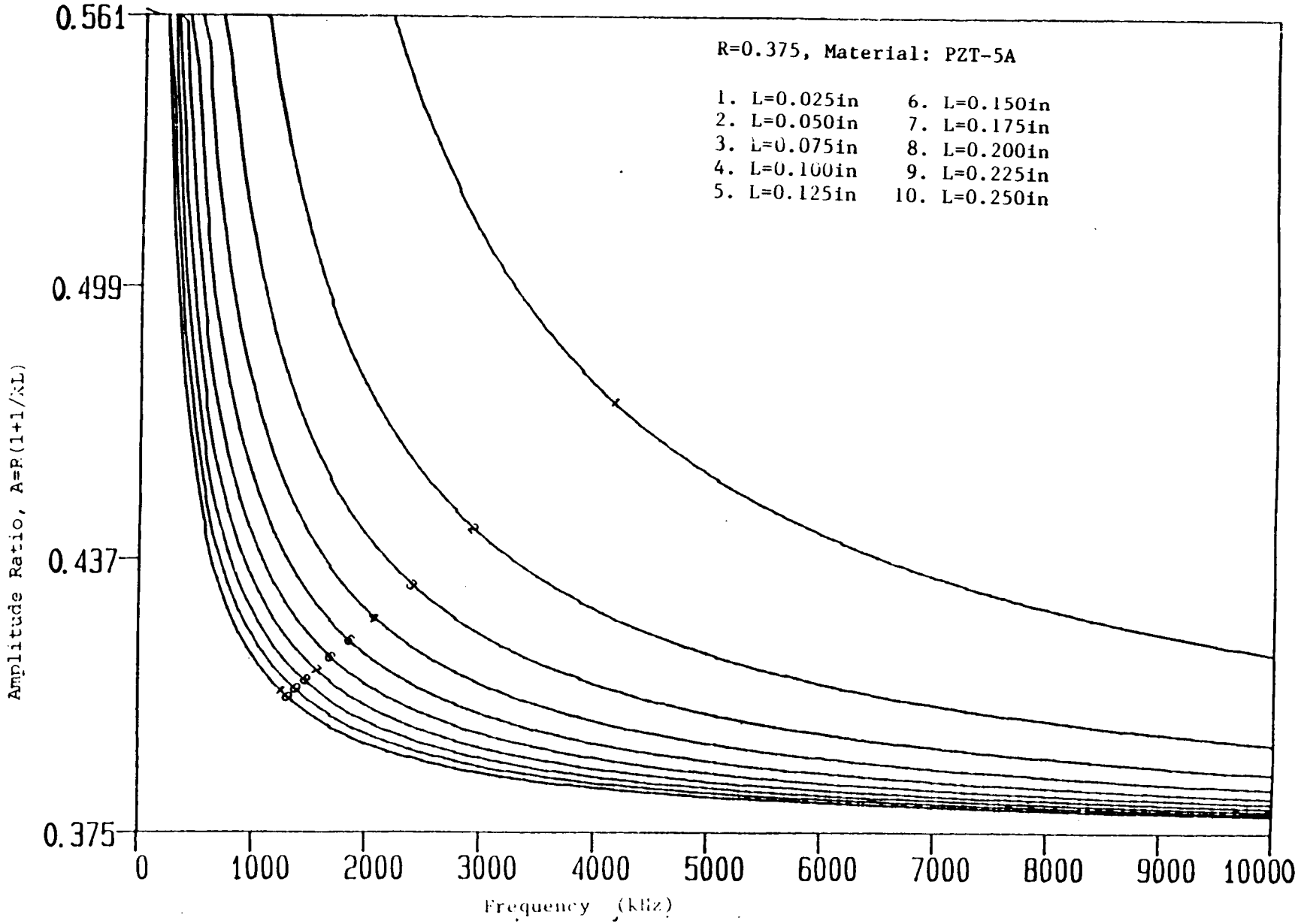

Fig. 4c Amplitude ratio versus frequency for PZT-5A rod with R = 0.375.

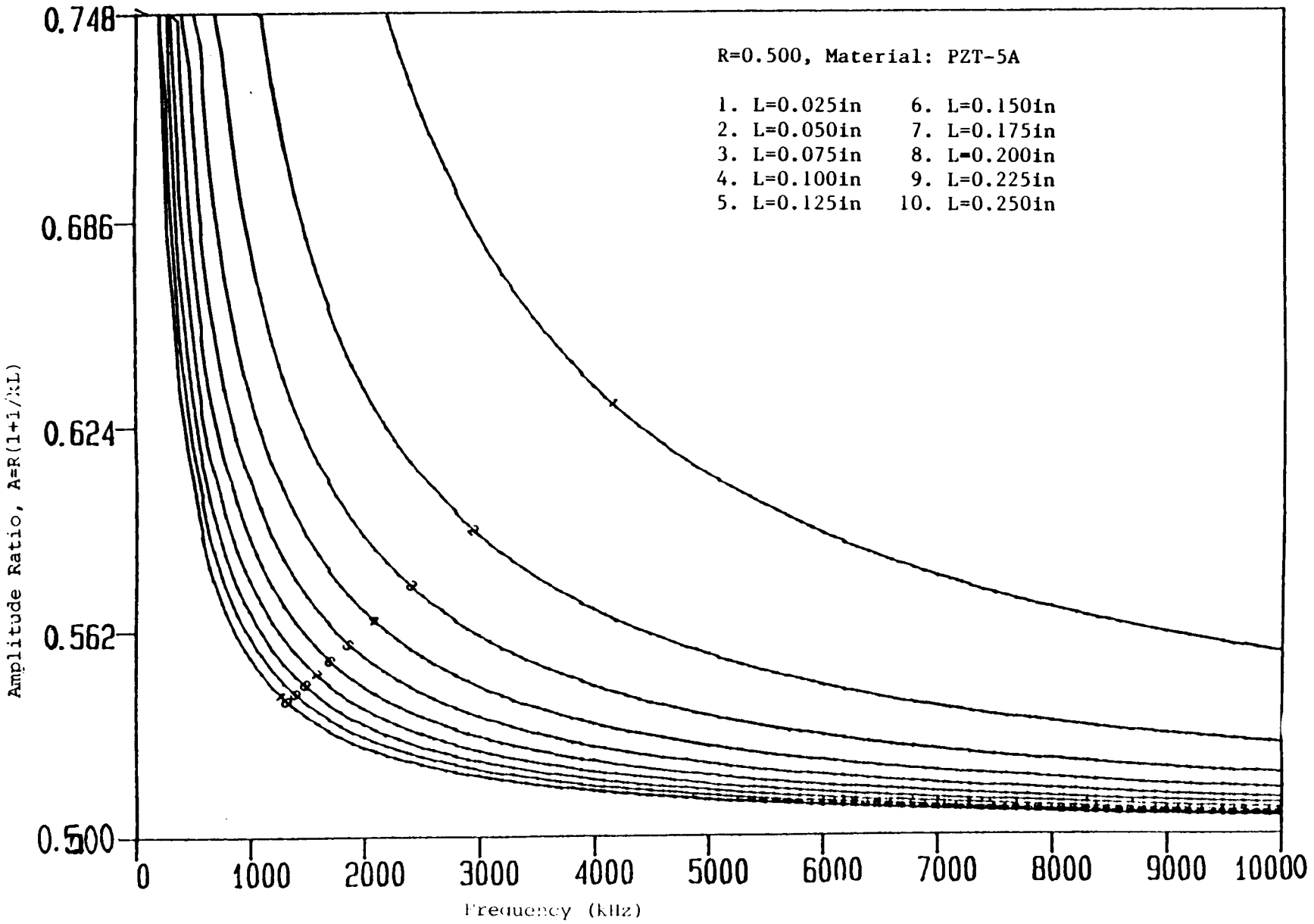

Fig. 4d Amplitude ratio versus frequency for PZT-5A rod with R = 0.500.

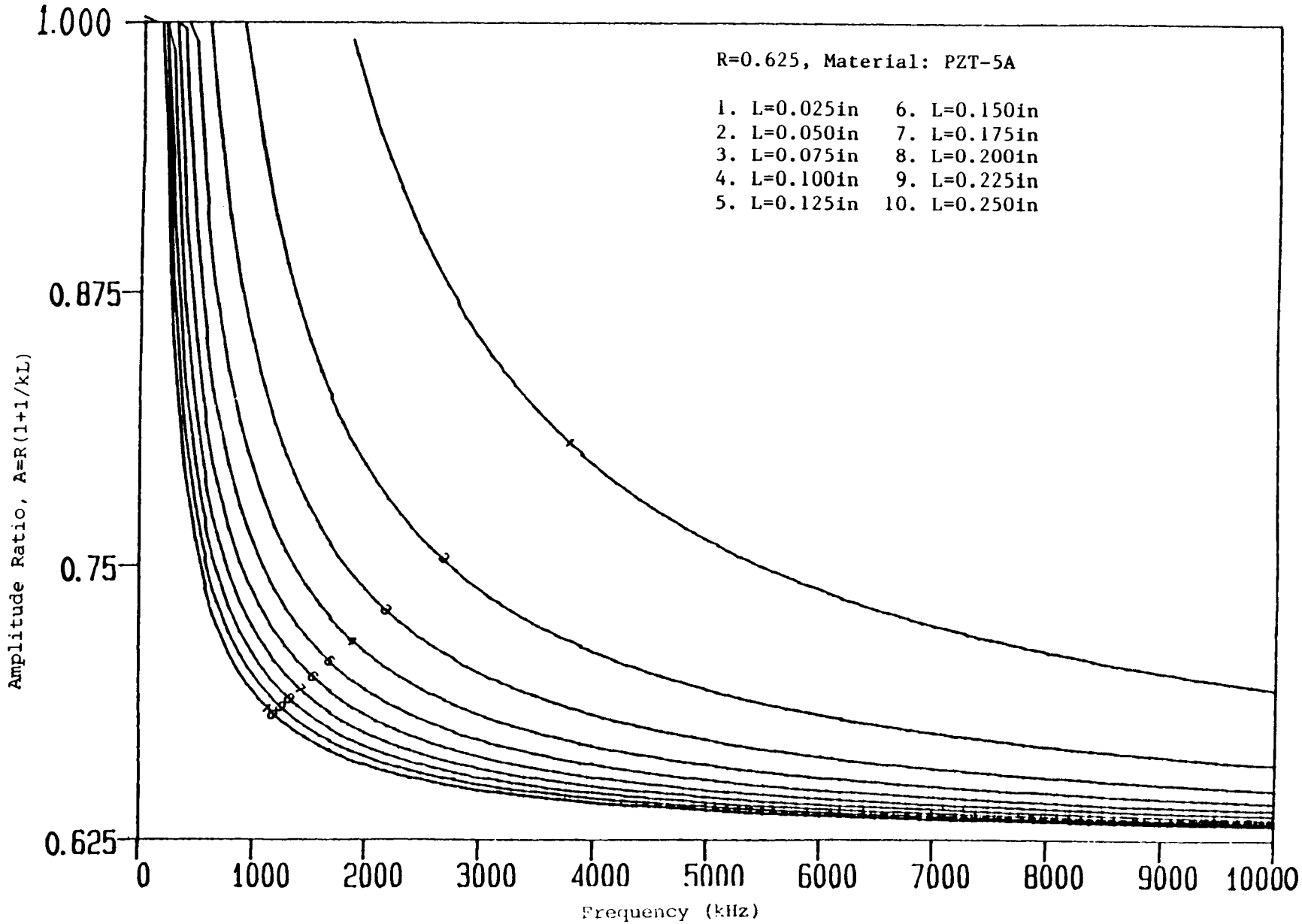

Fig. 4e Amplitude ratio versus frequency for PZT-5A rod with R = 0.625.

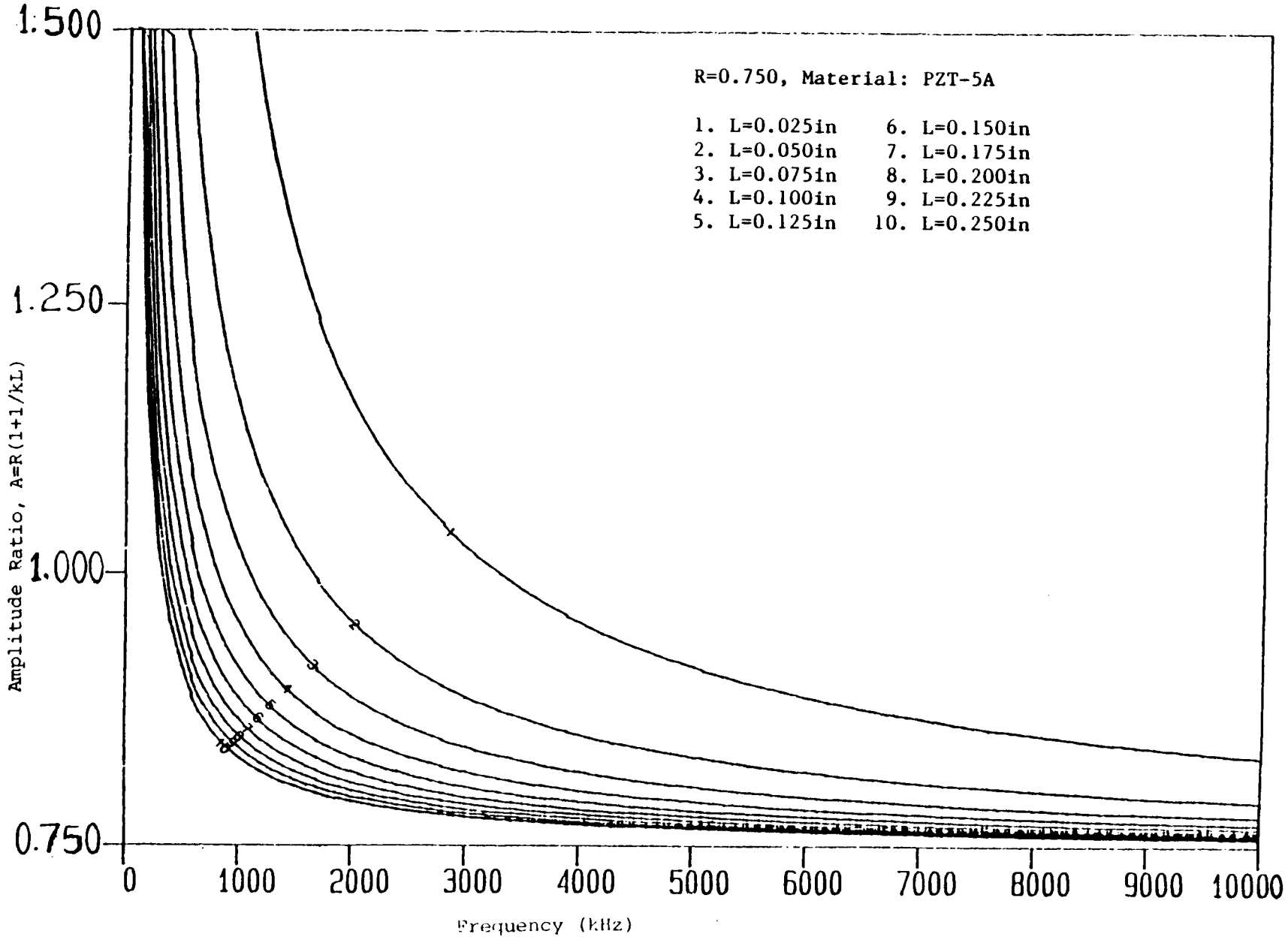

Fig. 4f Amplitude ratio versus frequency for PZT-5A rod with R = 0.750.

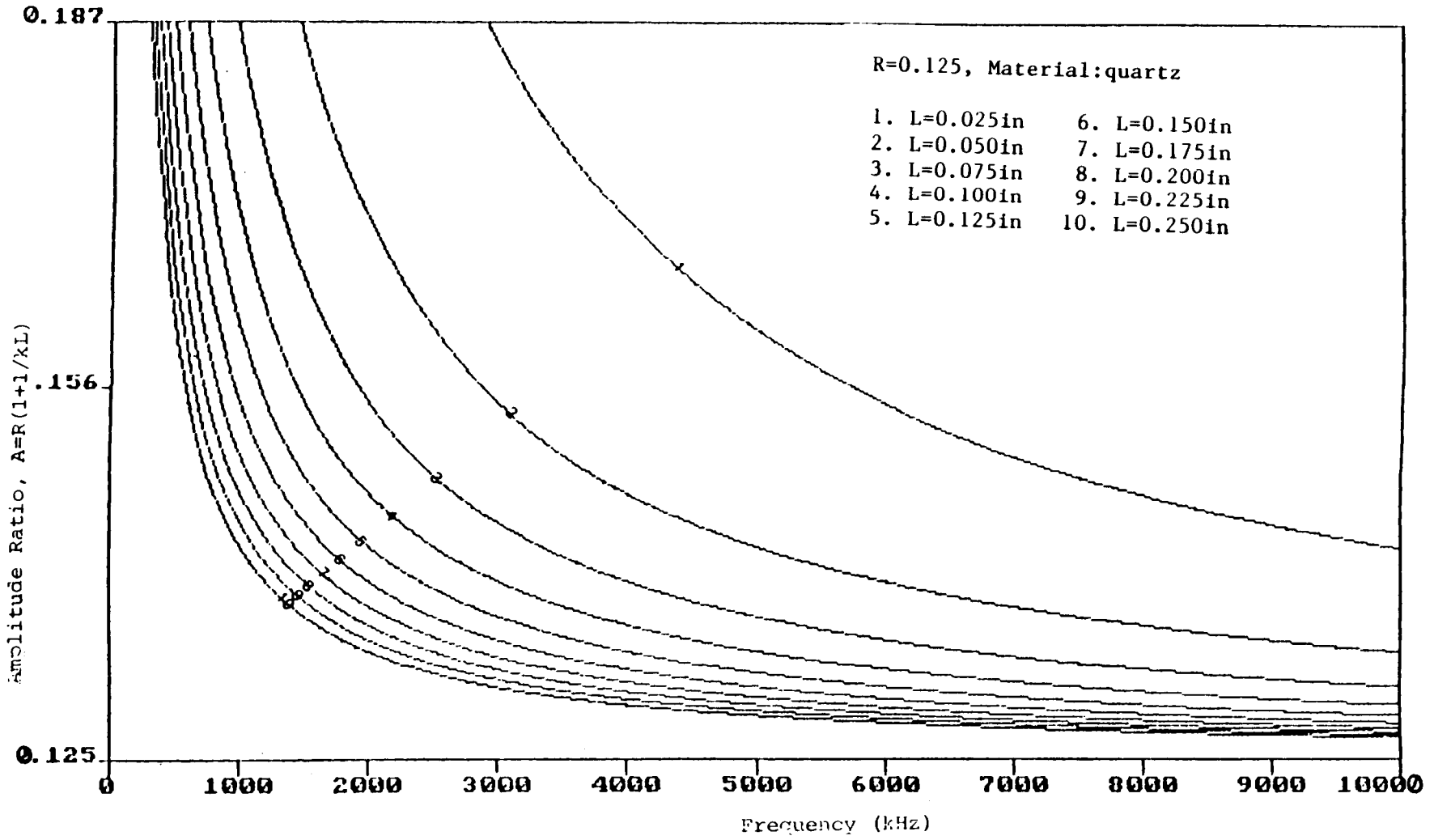

Fig. 5a Amplitude ratio versus frequency for quartz rod with R = 0.125.

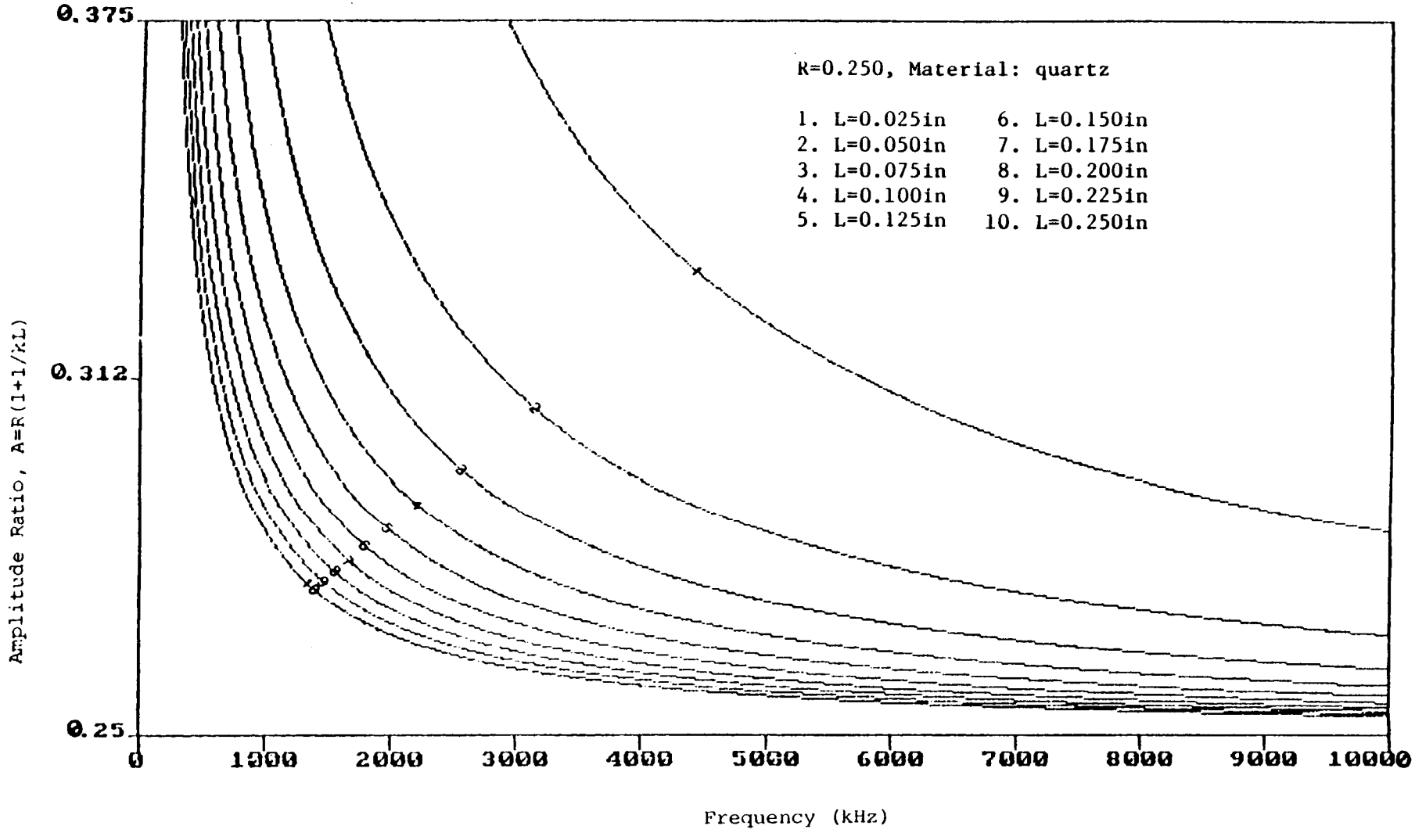

Fig. 5b Amplitude ratio versus frequency for quartz rod with R = 0.250.

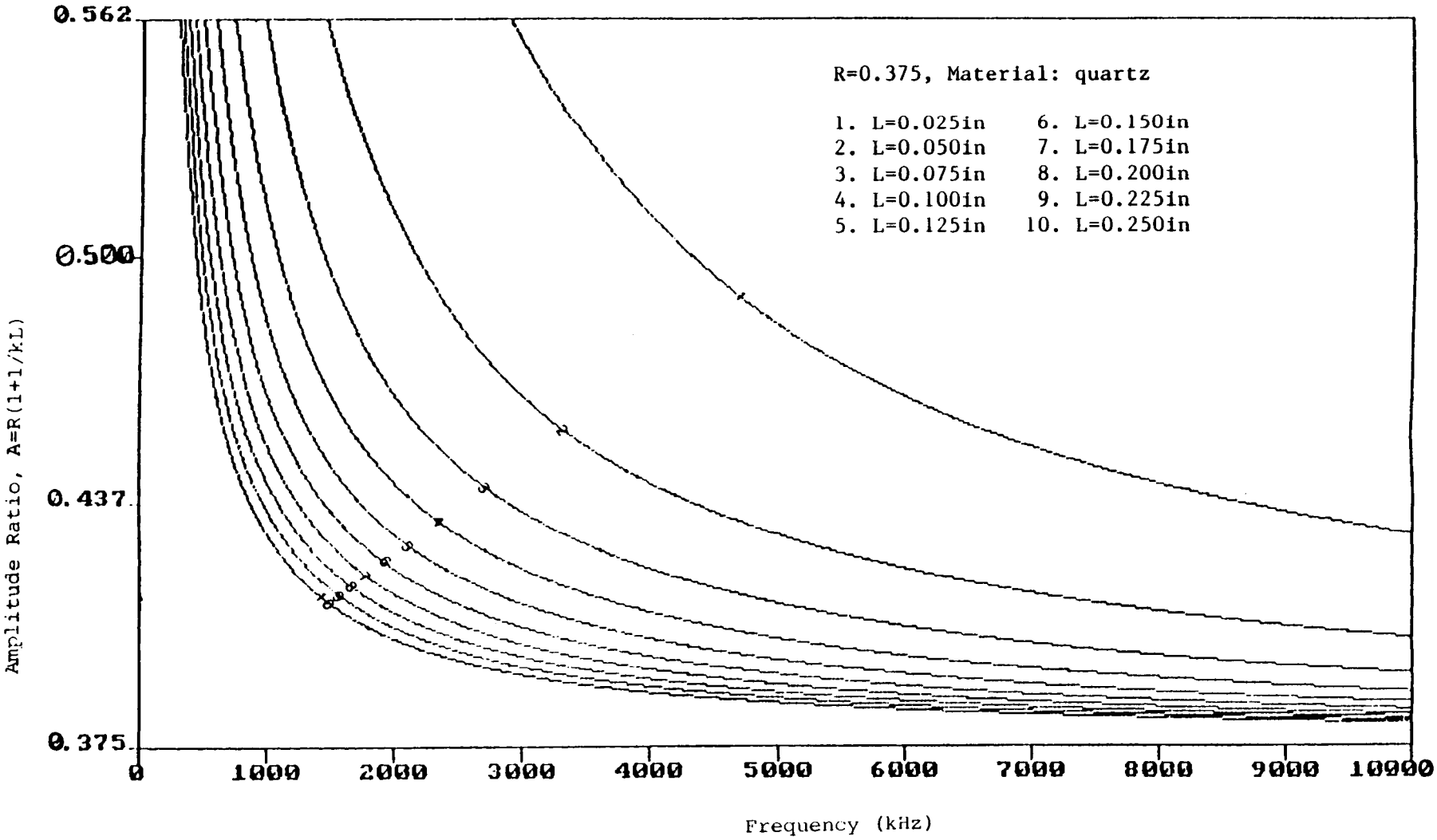

Fig. 5c Amplitude ratio versus frequency for quartz rod with R = 0.375.

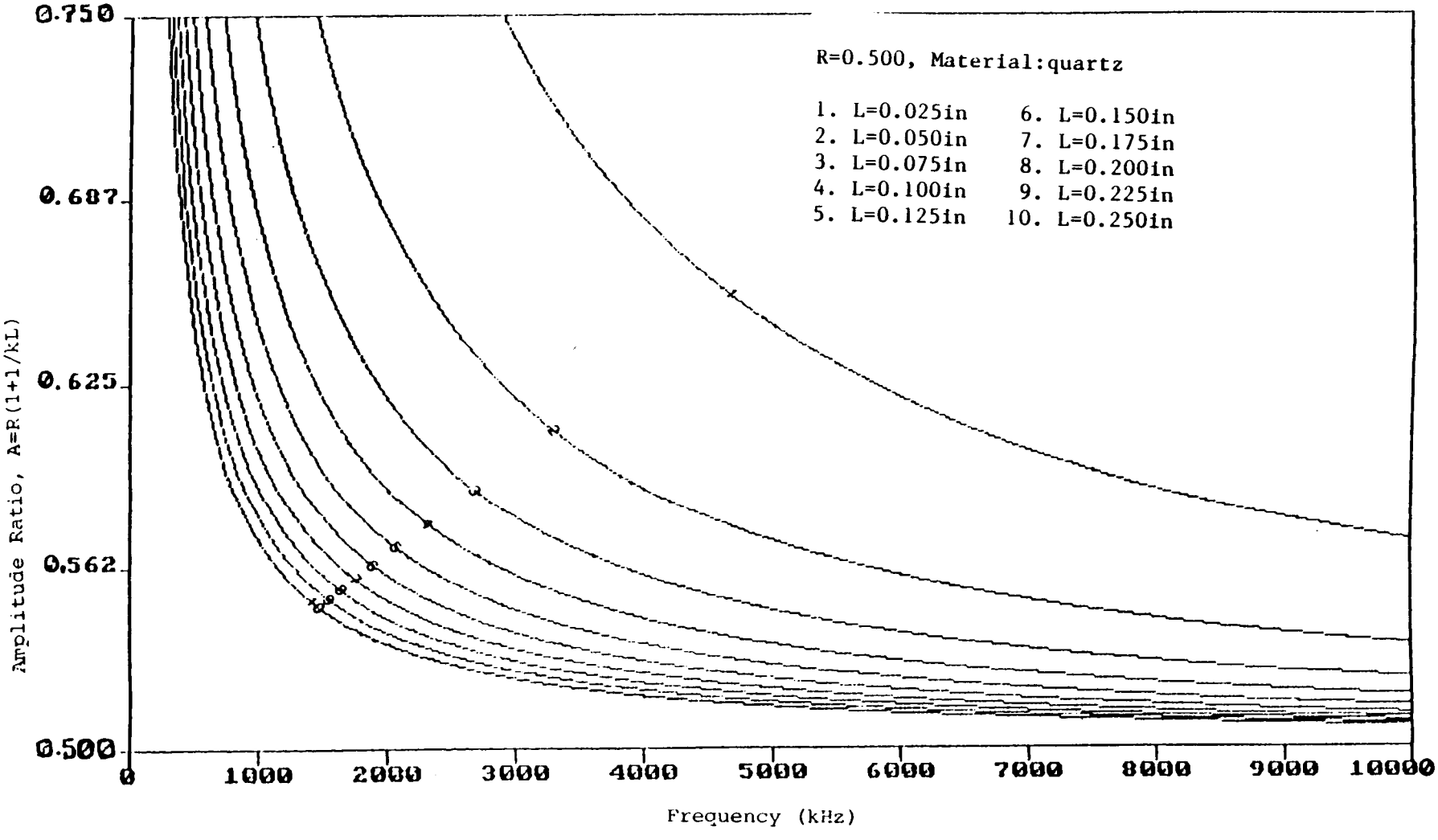

Fig. 5d Amplitude ratio versus frequency for quartz rod with R = 0.500.

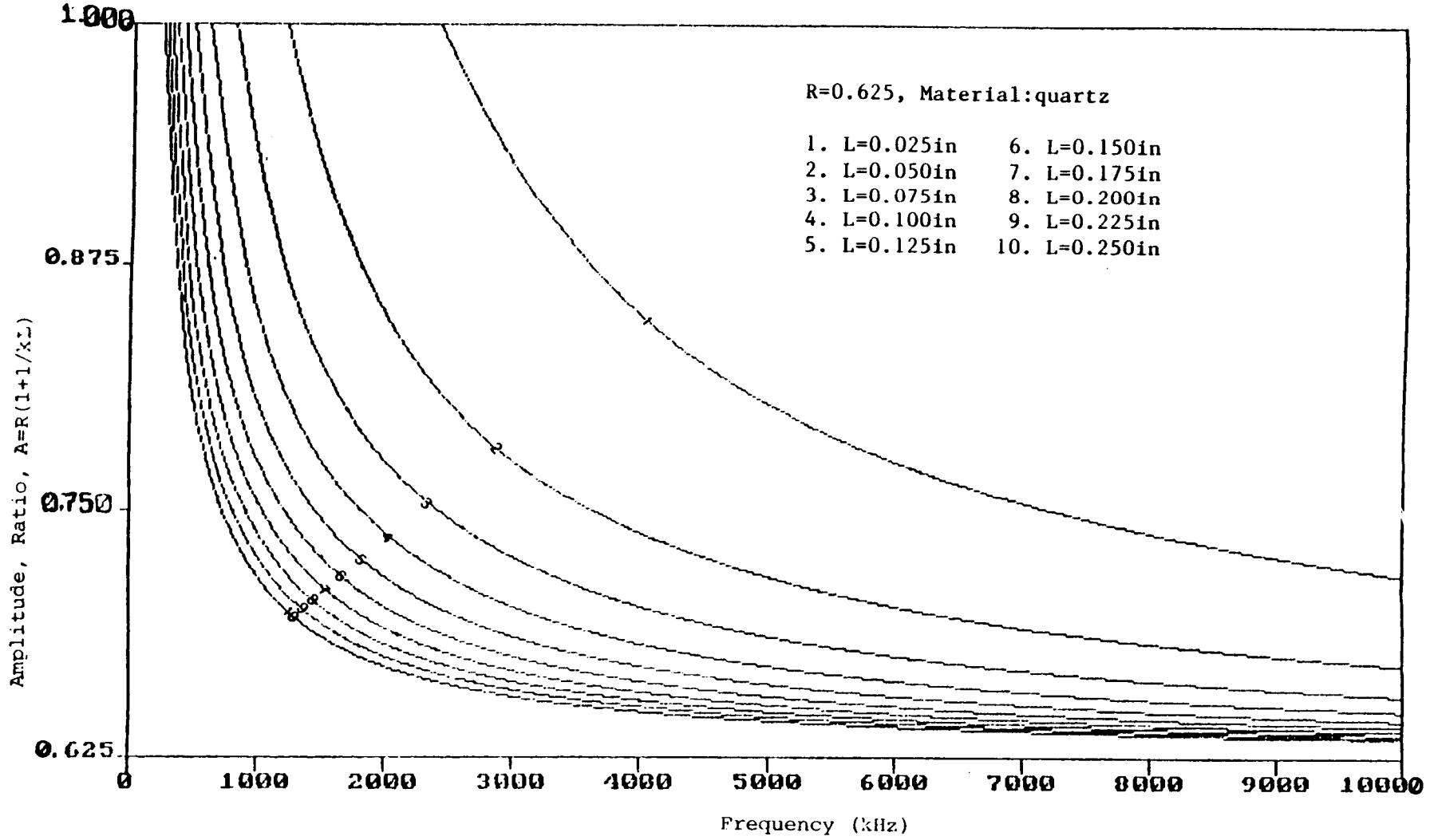

Fig. 5e Amplitude ratio versus frequency for quartz rod with R = 0.625.

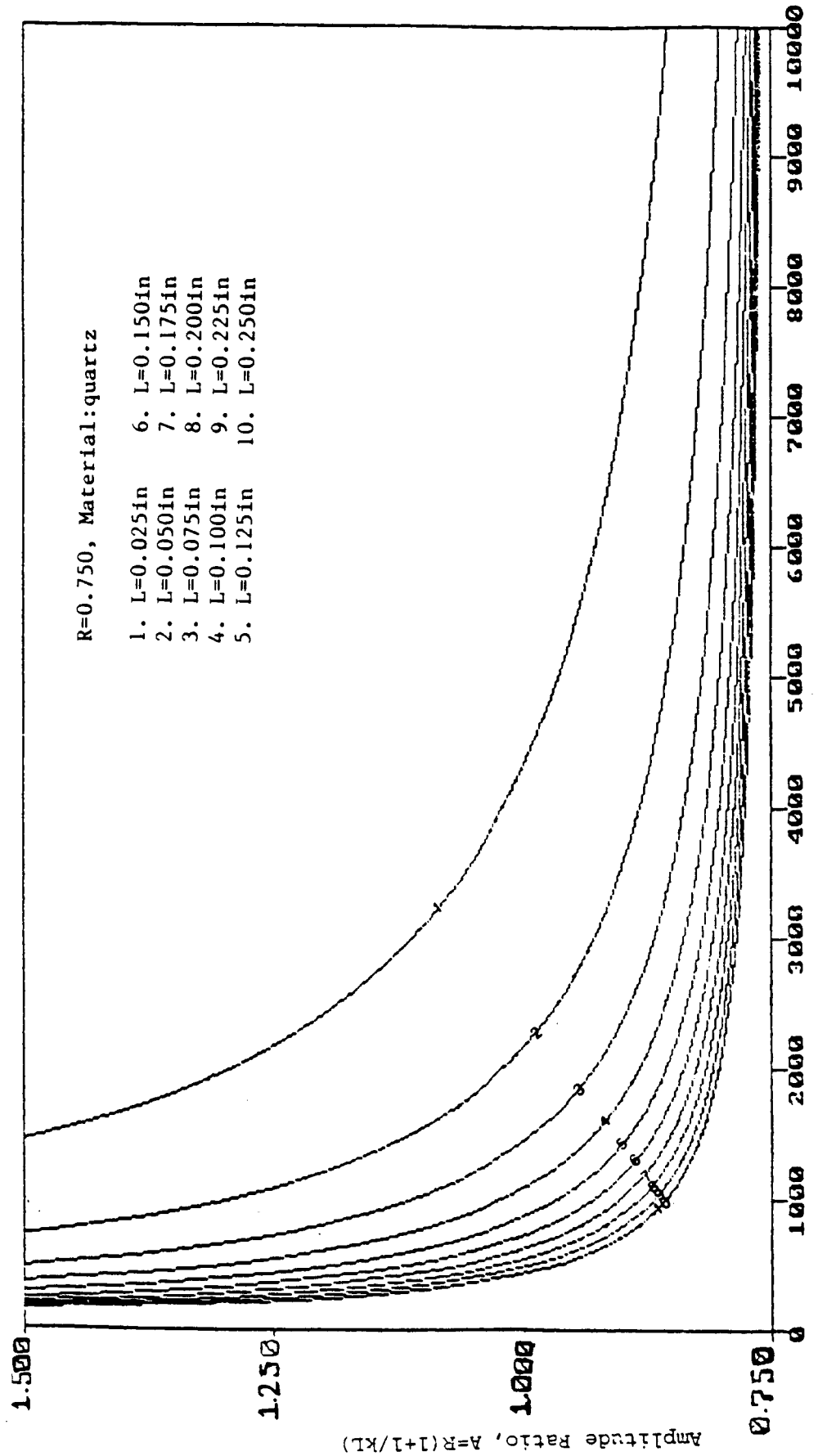

Fig. 5f Amplitude ratio versus frequency for quartz rod with R = 0.750.

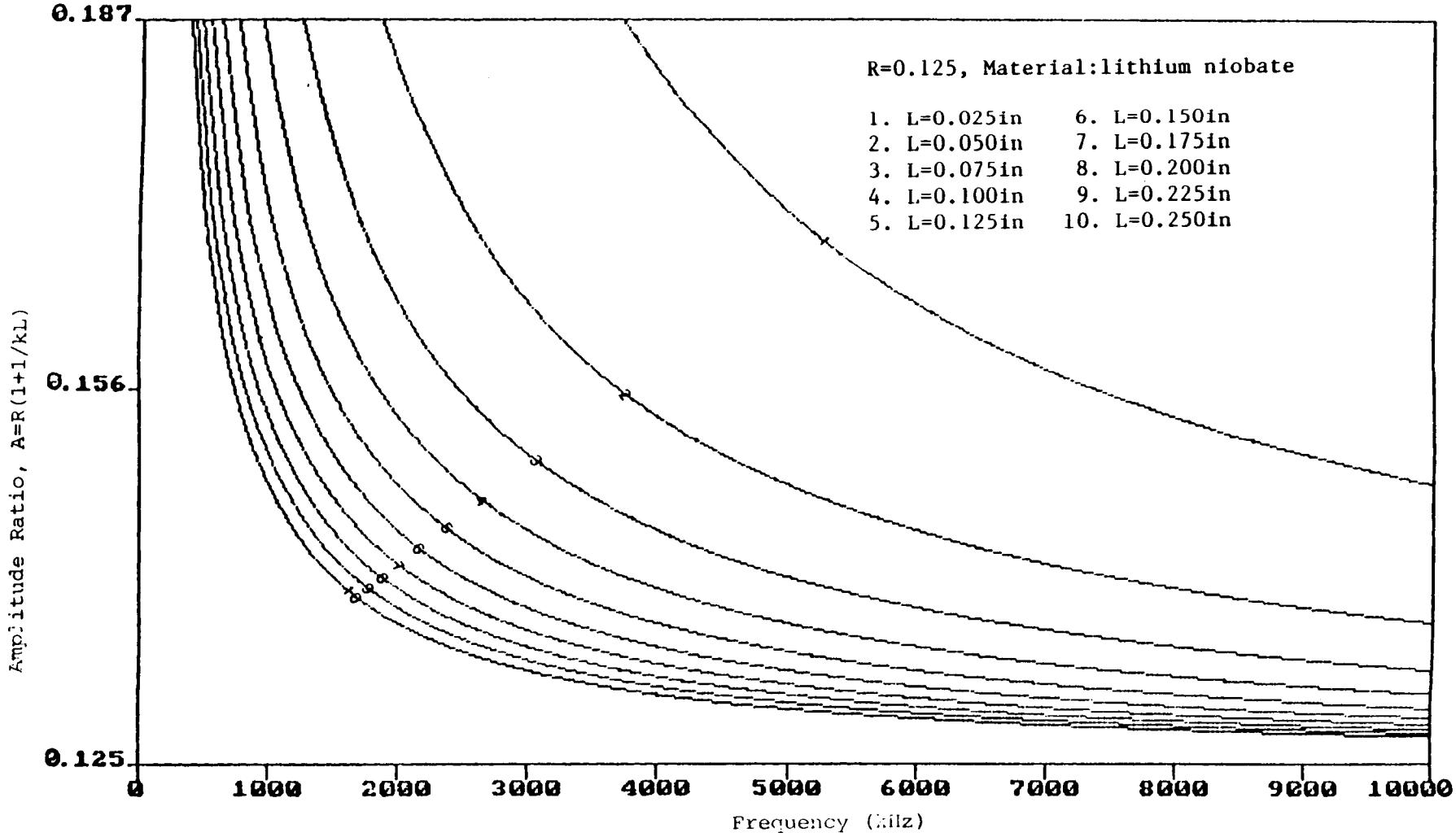

Fig. 6a Amplitude ratio versus frequency for lithium niobate rod with R = 0.125.

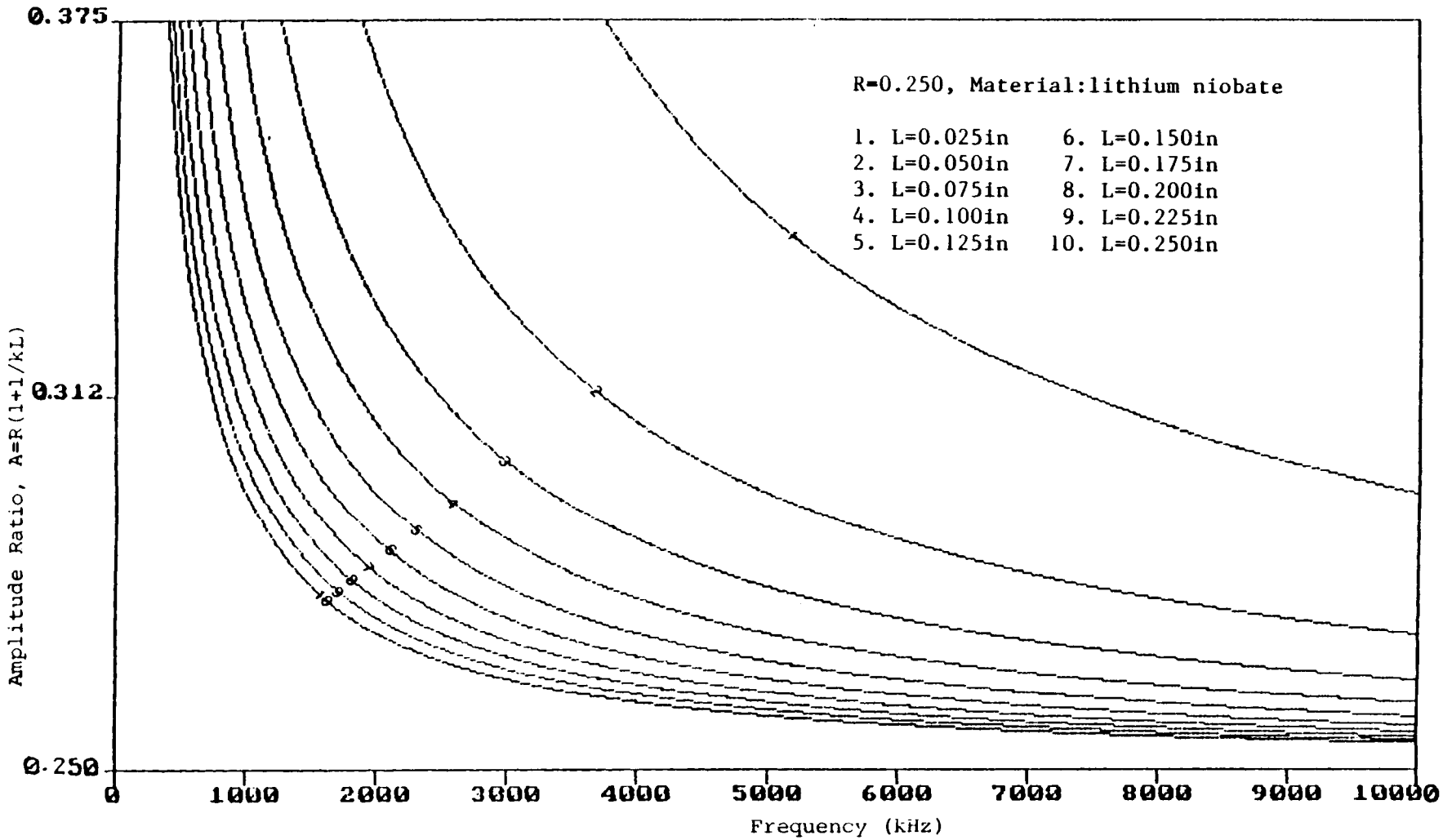

Fig. 6b Amplitude ratio versus frequency for lithium niobate rod with R = 0.250.

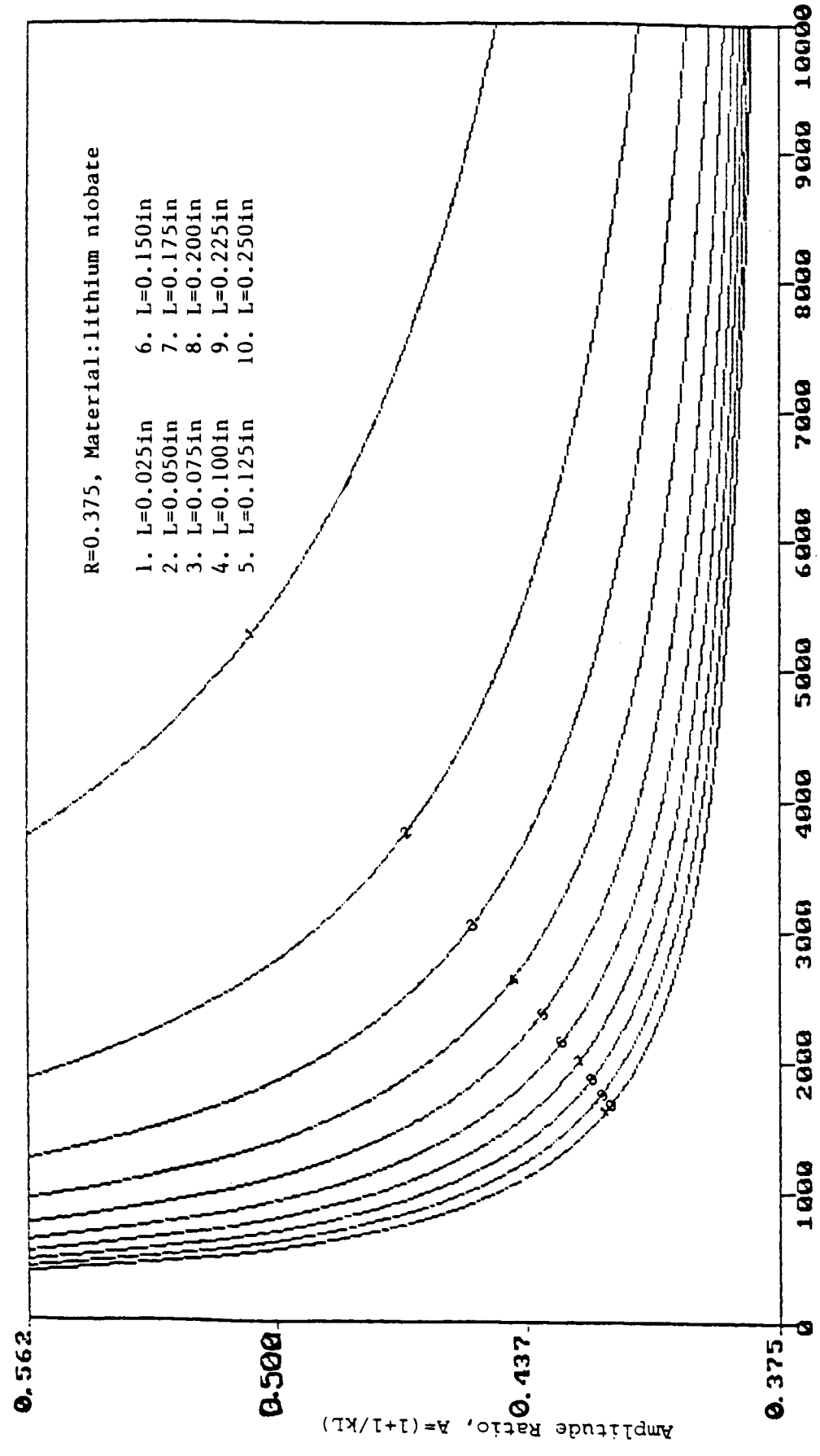

Fig. 6c Ampliture ratio versus frequency for lithium niobate rod with R = 0.375.

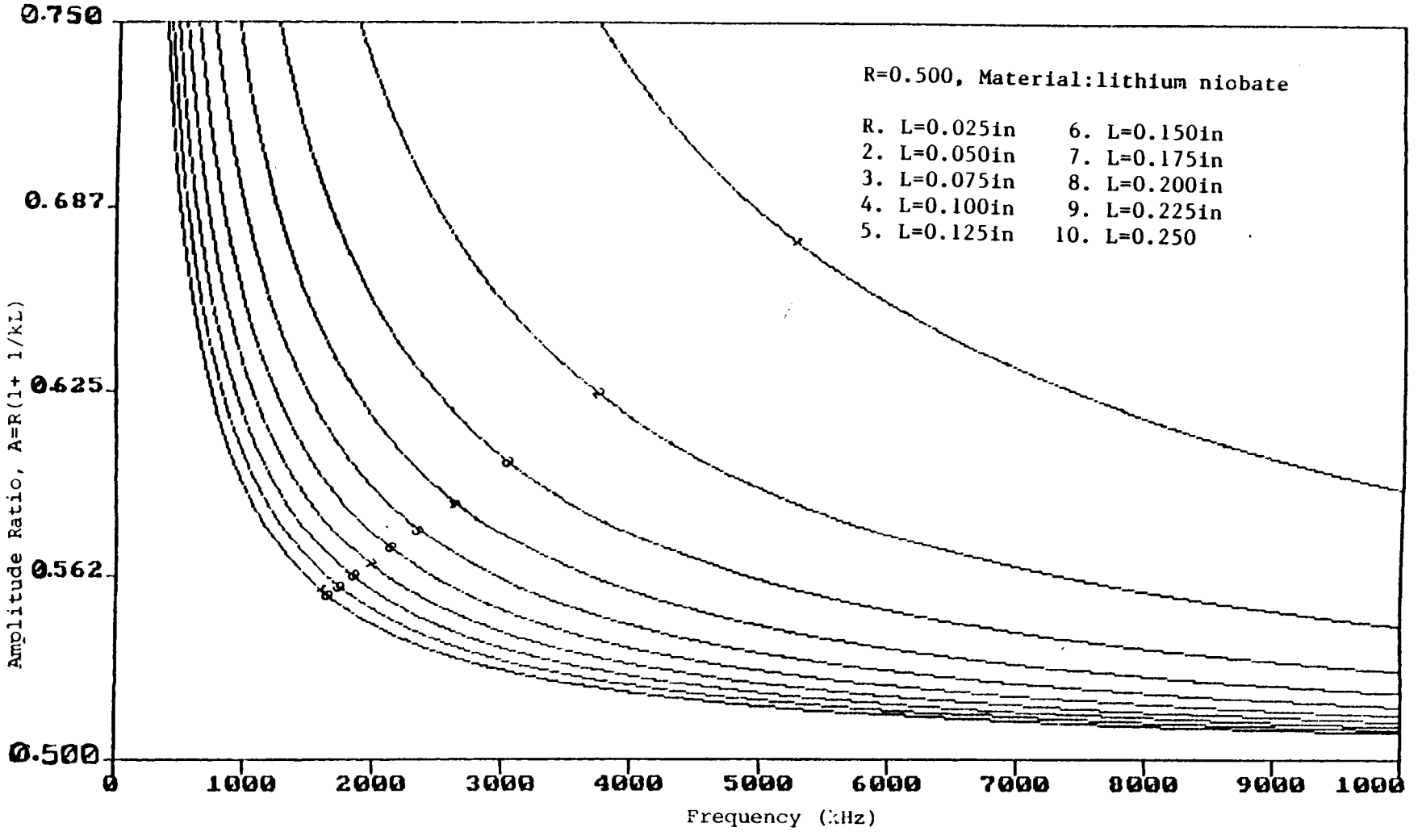

Fig. 6d Amplitude ratio versus frequency for lithium niobate rod with R = 0.500

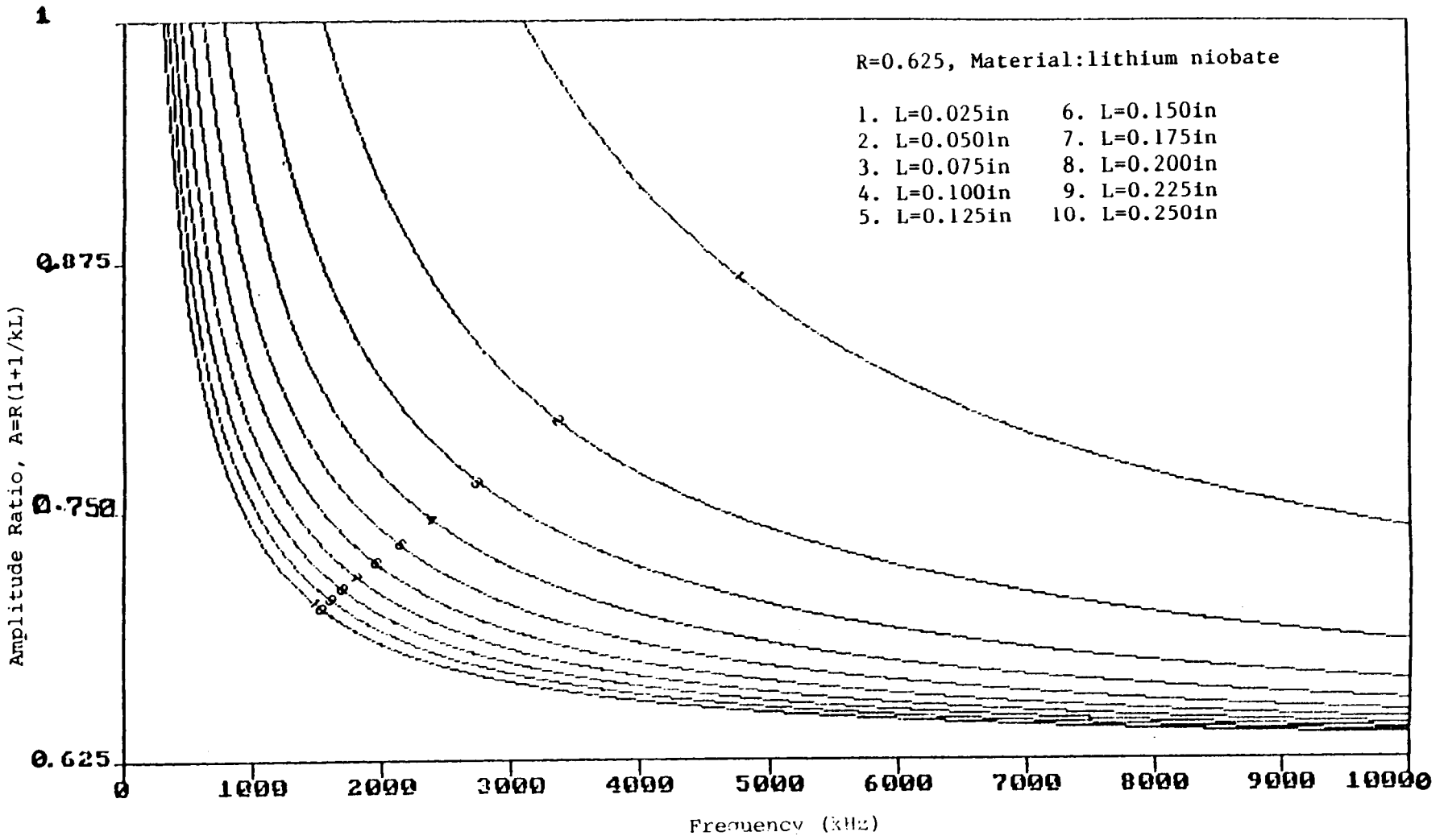

Fig. 6e Amplitude ratio versus frequency for lithium niobate rod with R = 0.625.

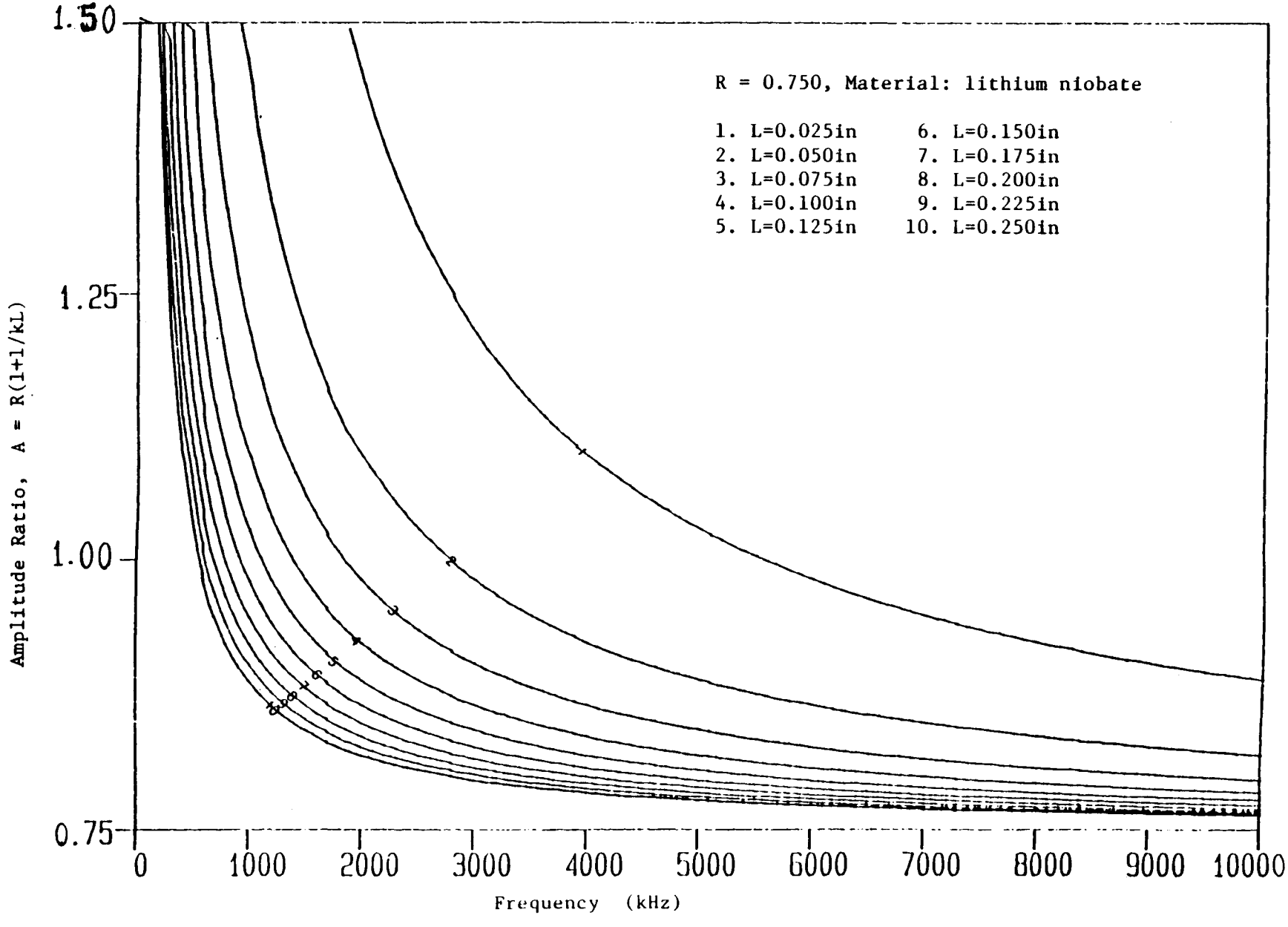

Fig. 61 Amplitude ratio versus frequency for lithium niobate rod with R = 0.750.

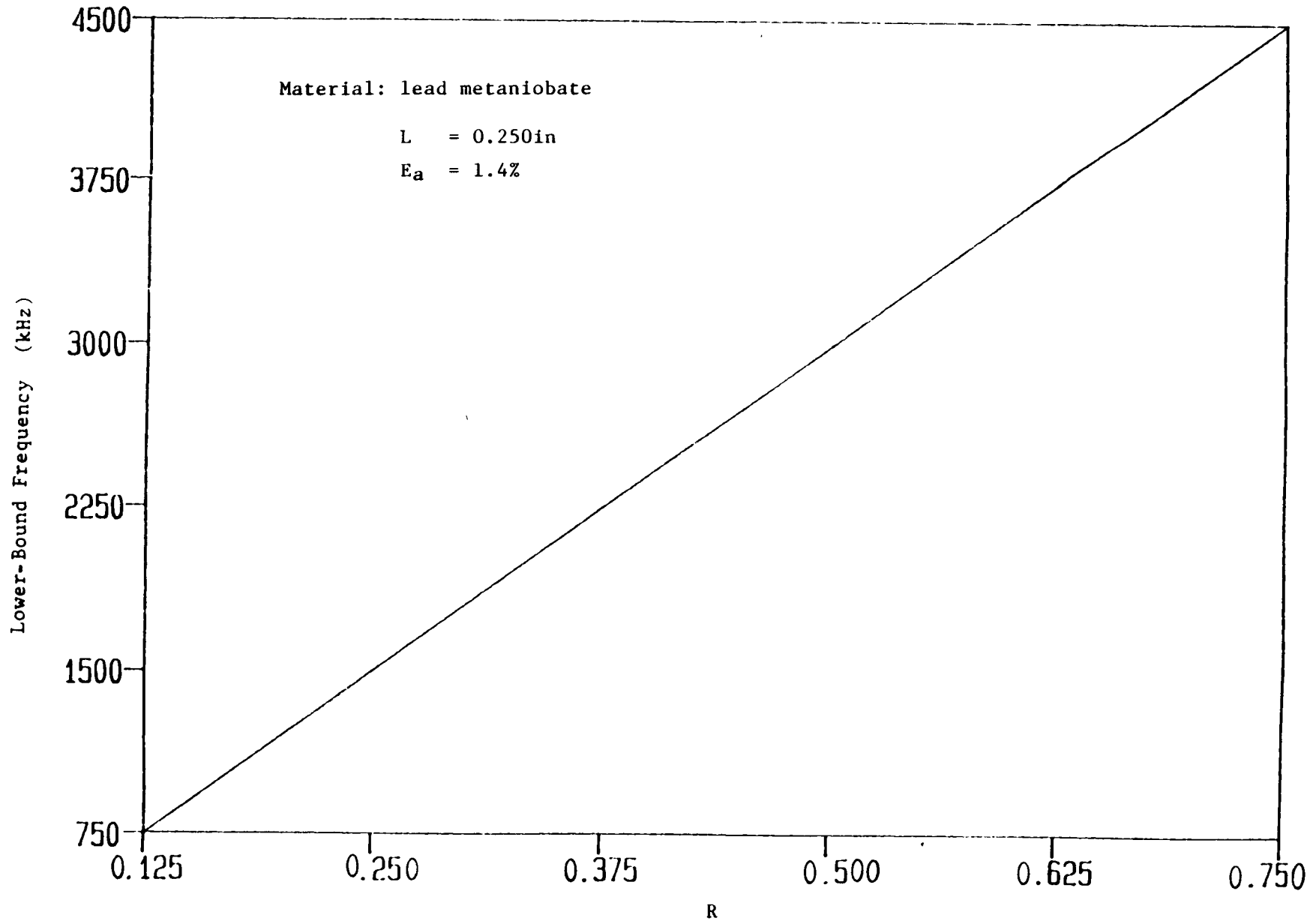

Fig. 7 Lower bound frequency versus R for lead metaniobate.

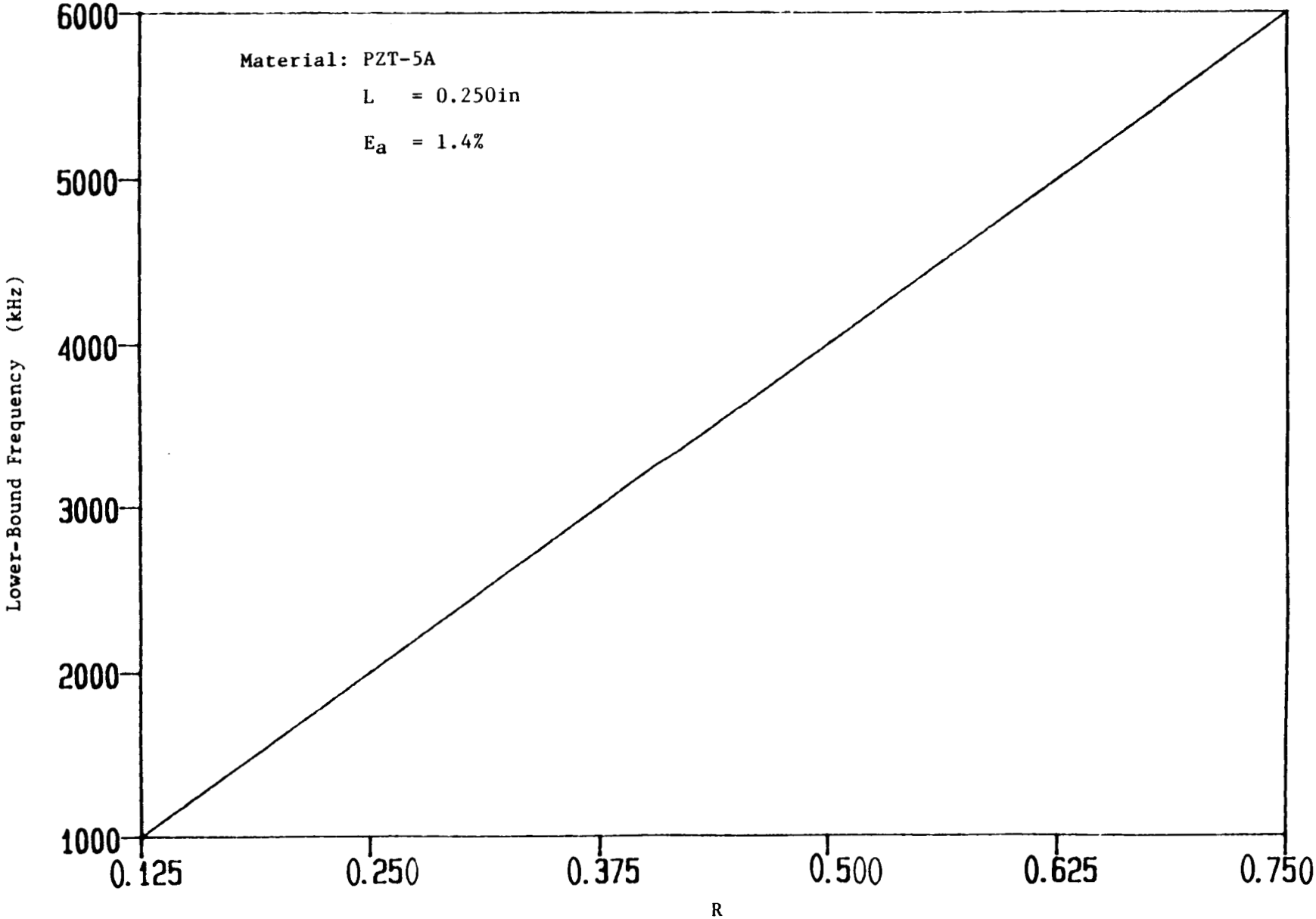

Fig. 8 Lower bound frequency versus R for PZT-5A.

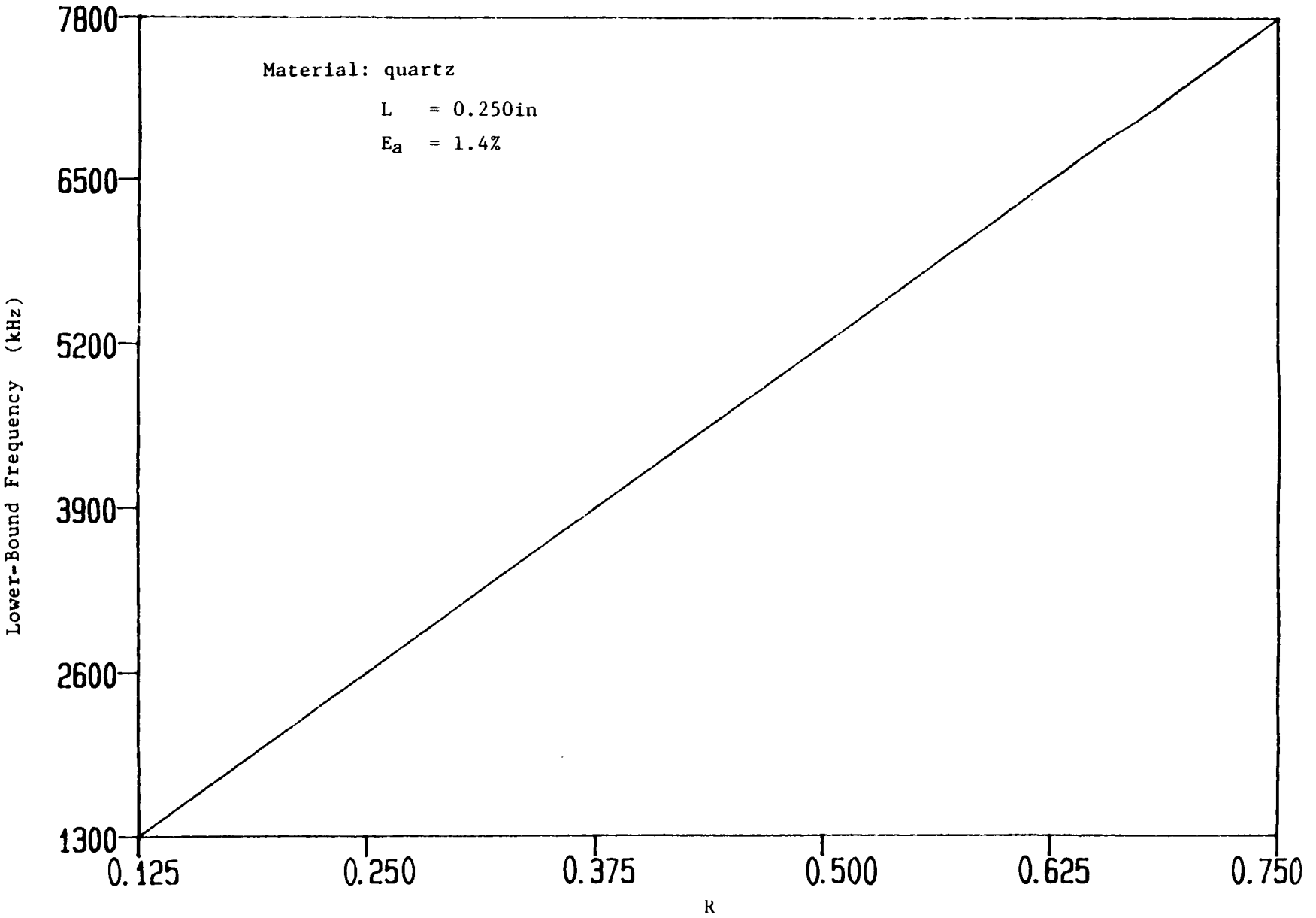

Fig. 9 Lower bound frequency versus R for quartz

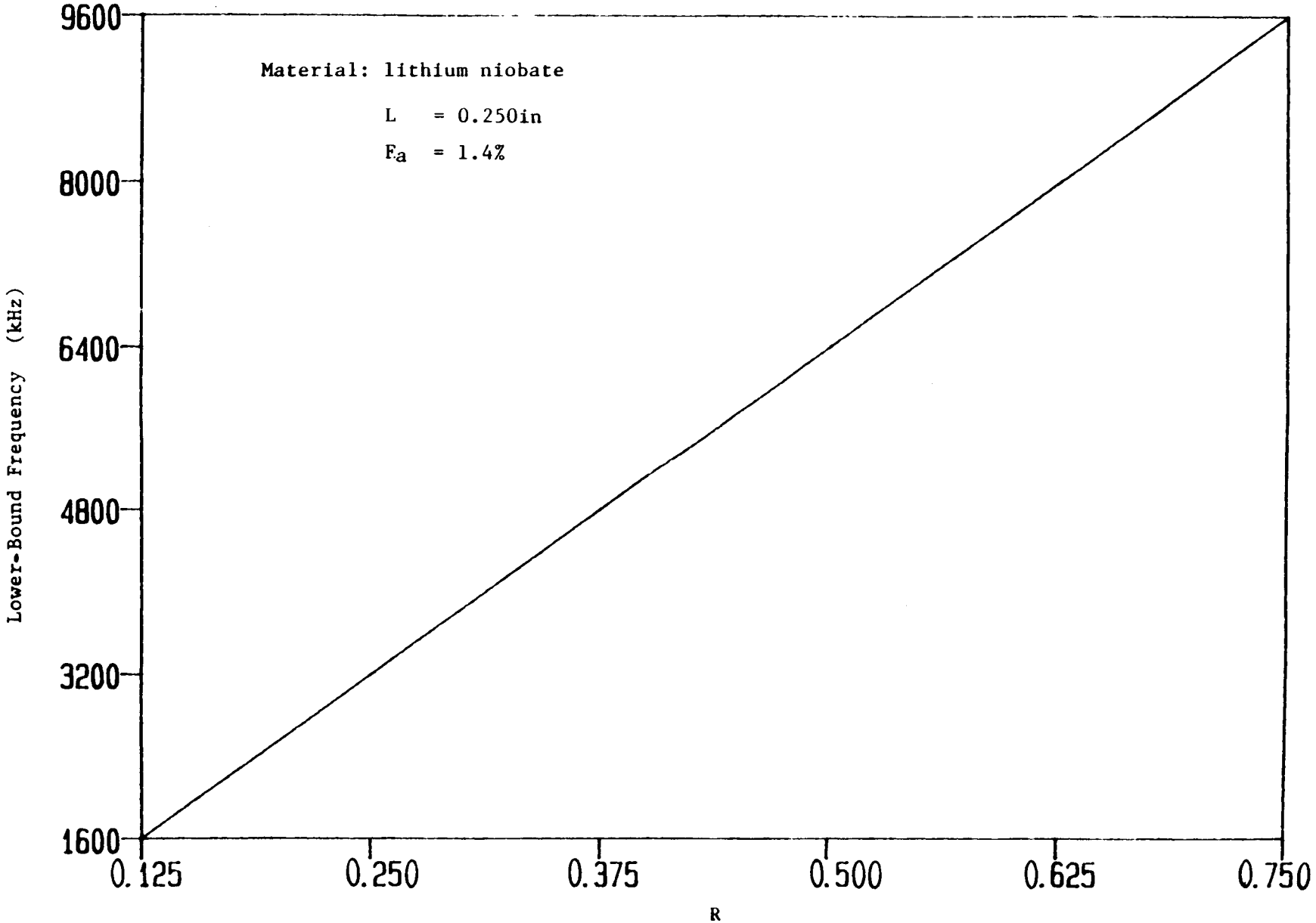

Fig. 10 Lower bound frequency versus R for lithium niobate

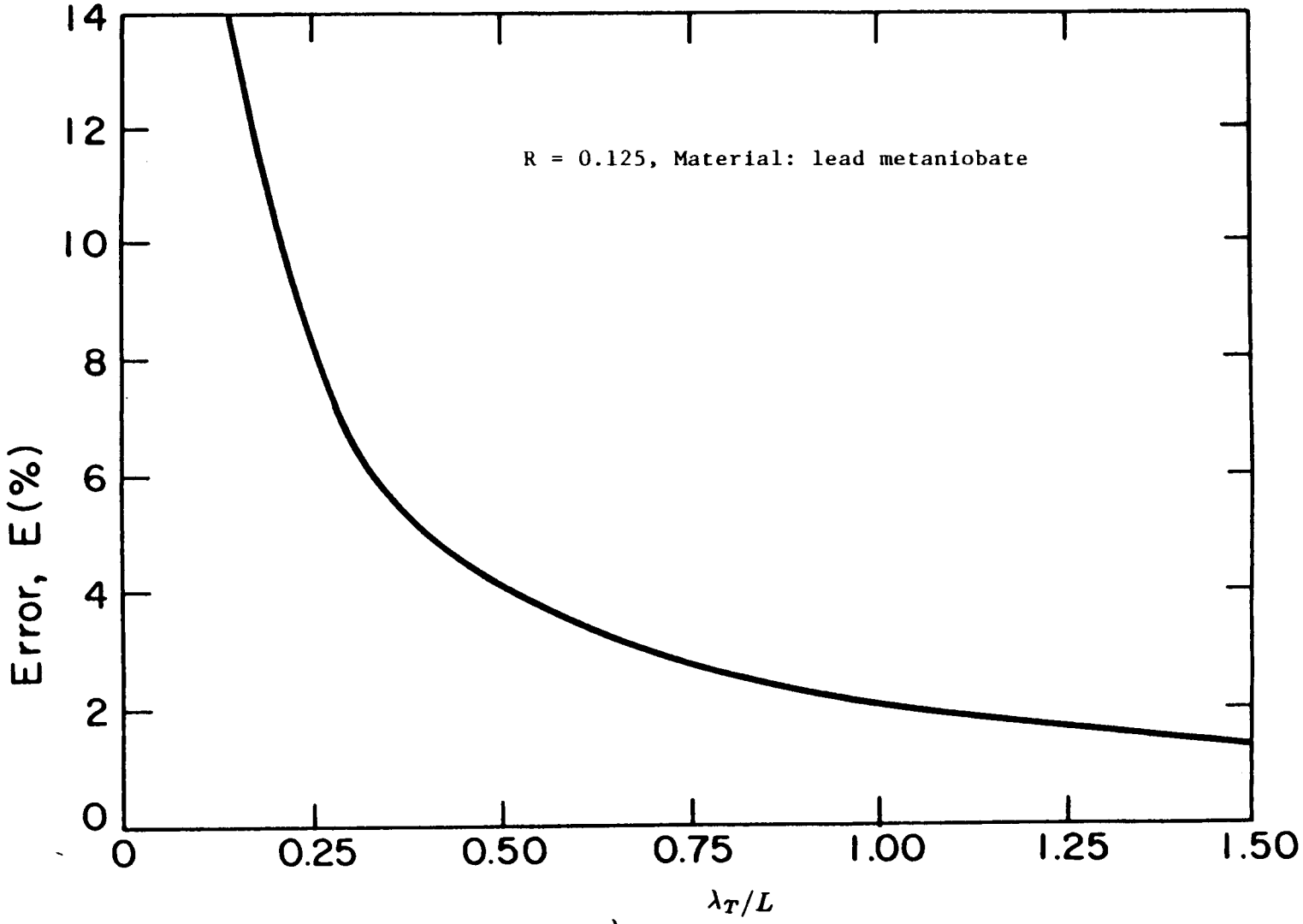

Fig. 11a Error versus $\frac{\lambda_T}{L}$ for lead metaniobate rod with R = 0.125.

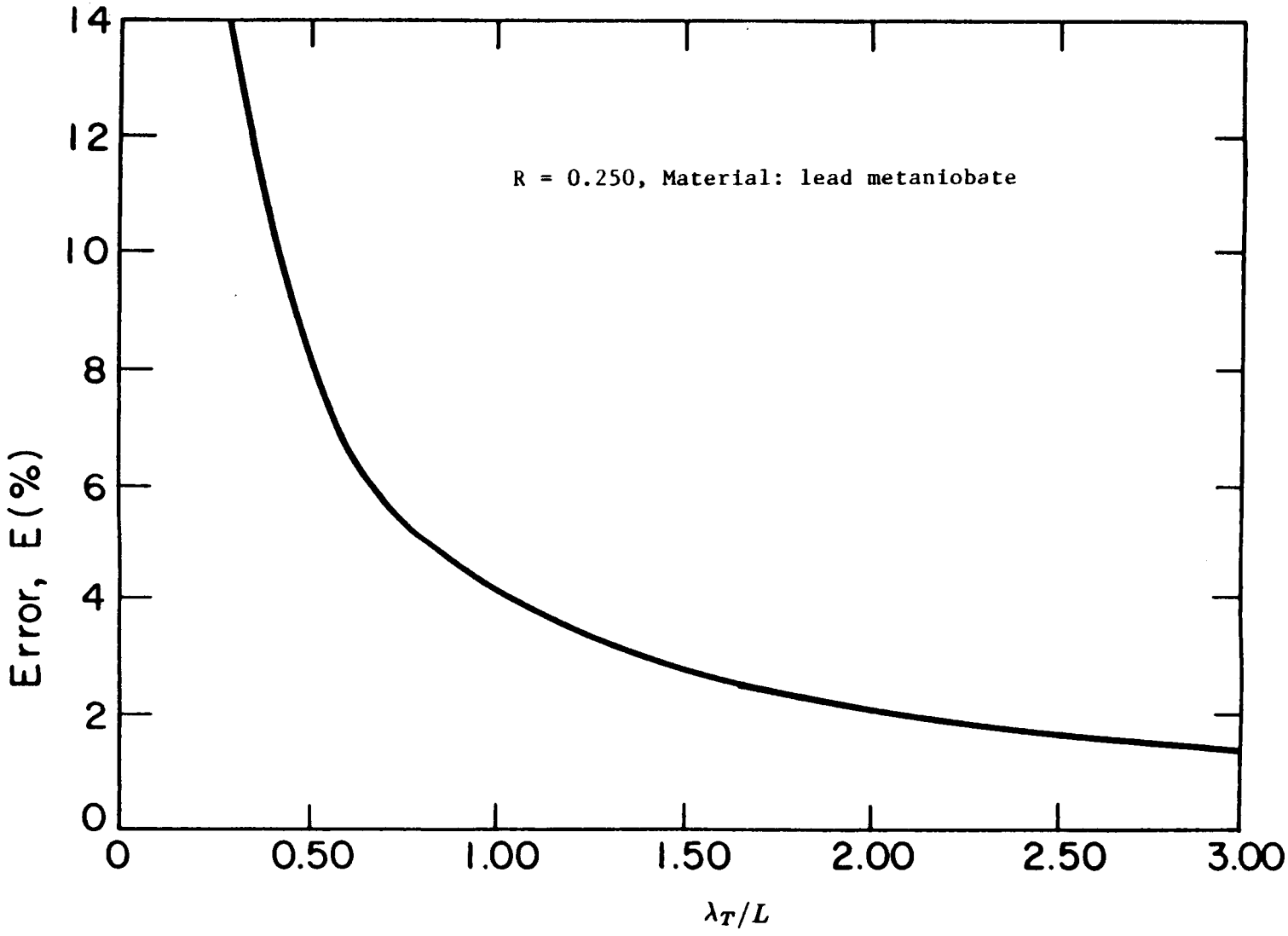

Fig. 11b Error versus $\frac{\lambda_T}{L}$ for lead metaniobate rod with R = 0.250.

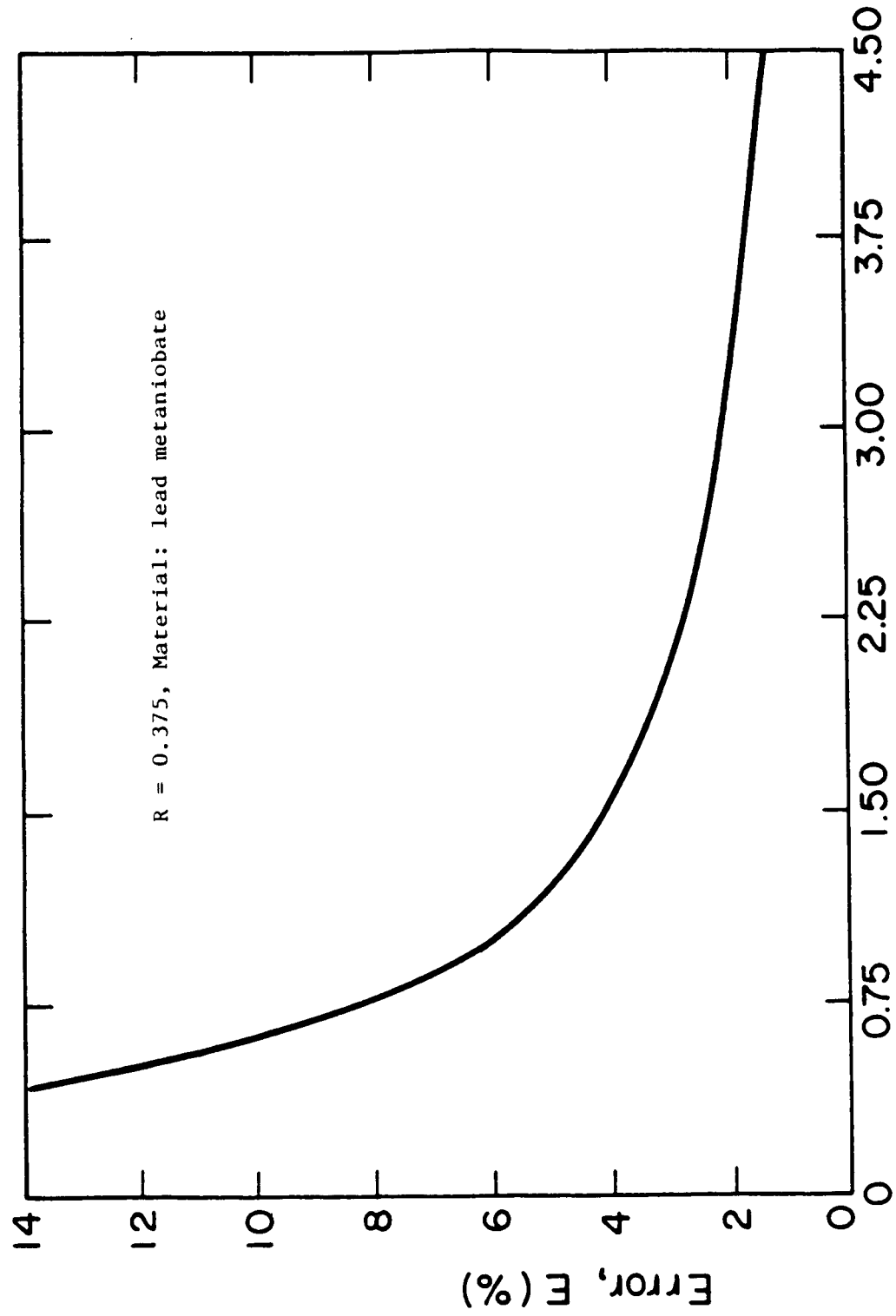

Fig. 11c Error versus $\frac{\lambda_T}{L}$ for lead metaniobate rod with R = 0.375.

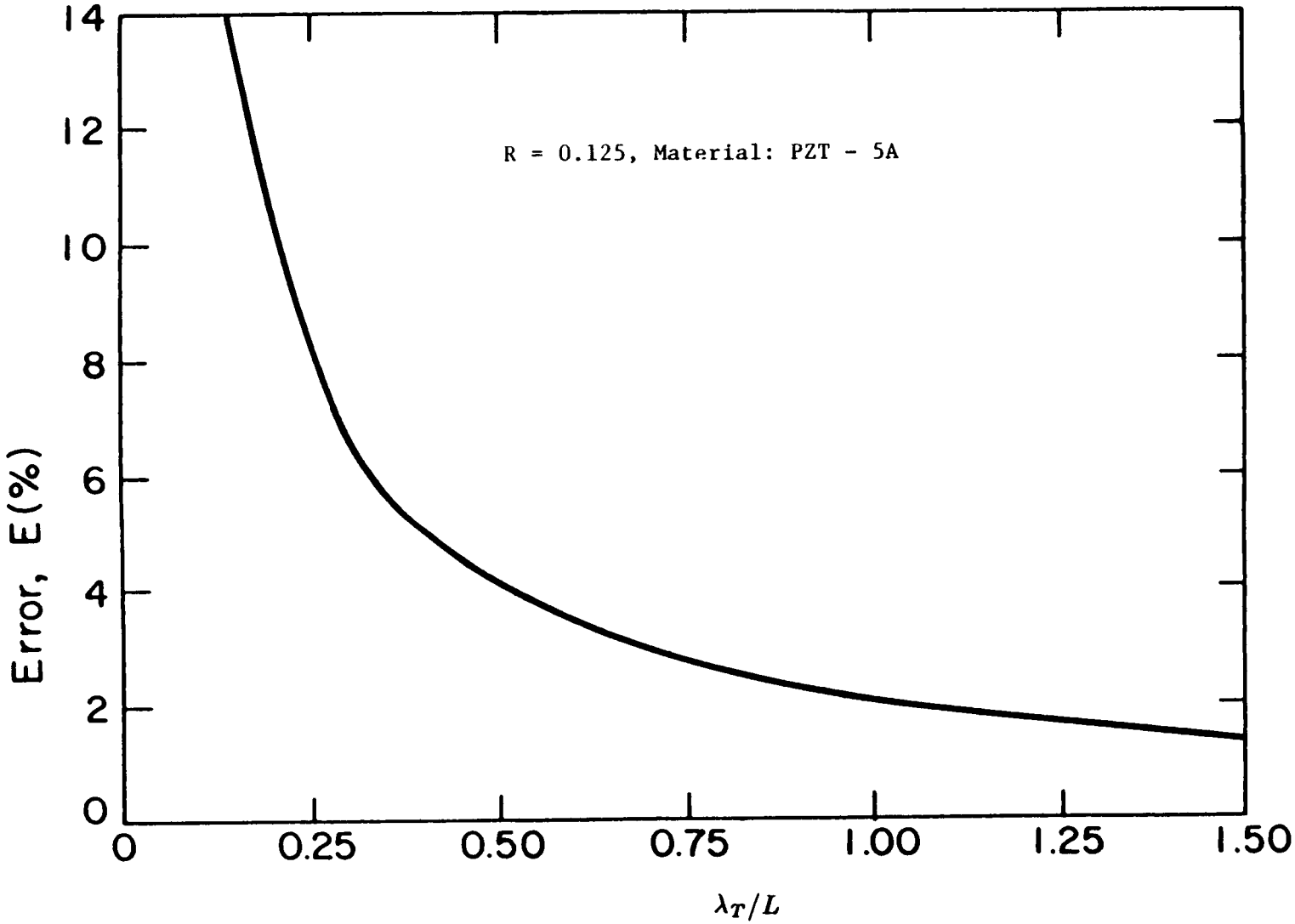

Fig. 12a Error versus $\frac{\lambda_T}{L}$ for a PZT - 5A's rod with R = 0.125.

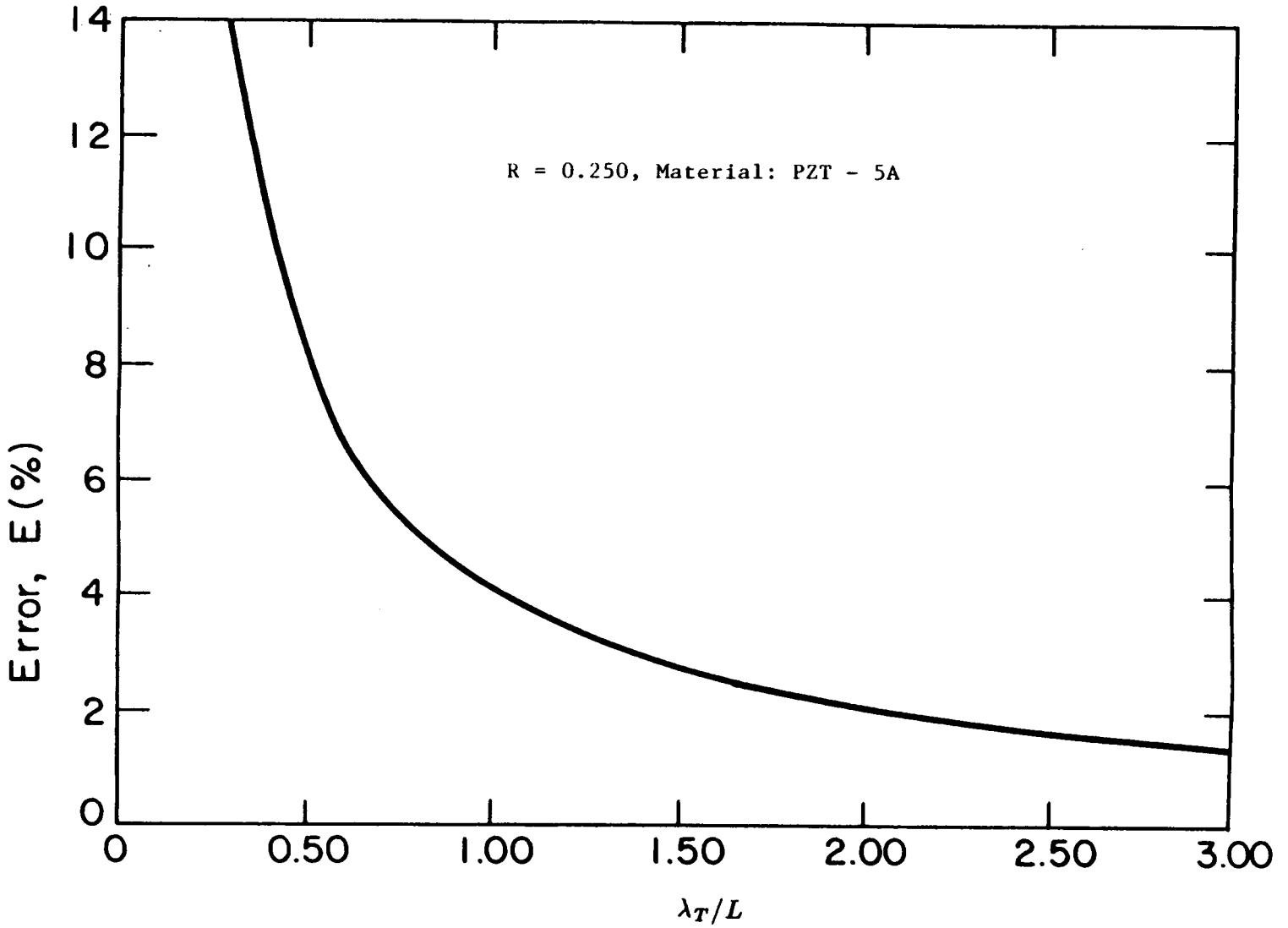

Fig. 12b Error versus $\frac{\lambda_T}{L}$ for PZT - 5A rod with R = 0.250.

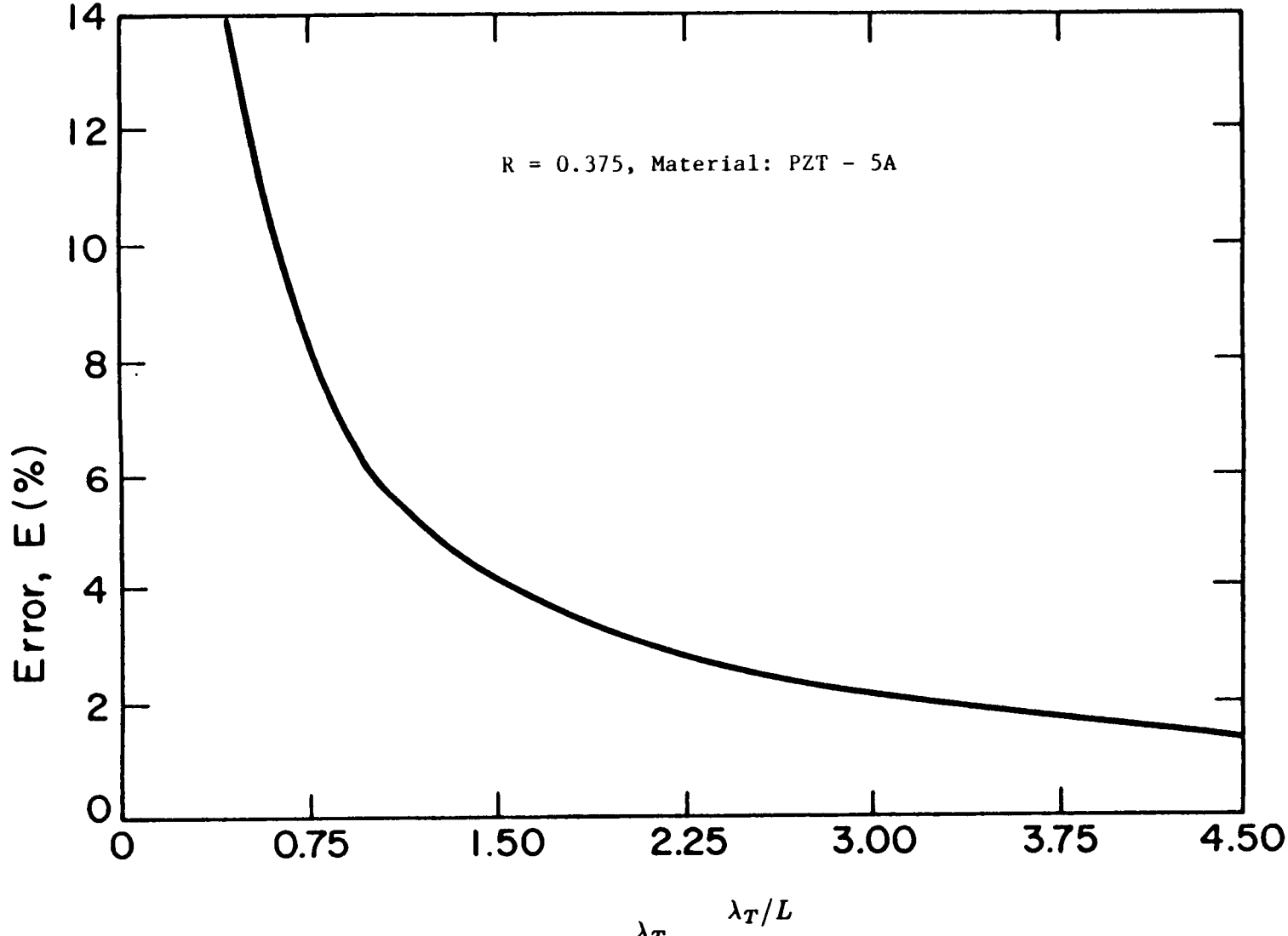

Fig. 12c Error versus $\frac{\lambda_T}{L}$ for PZT - 5A rod with R = 0.375.

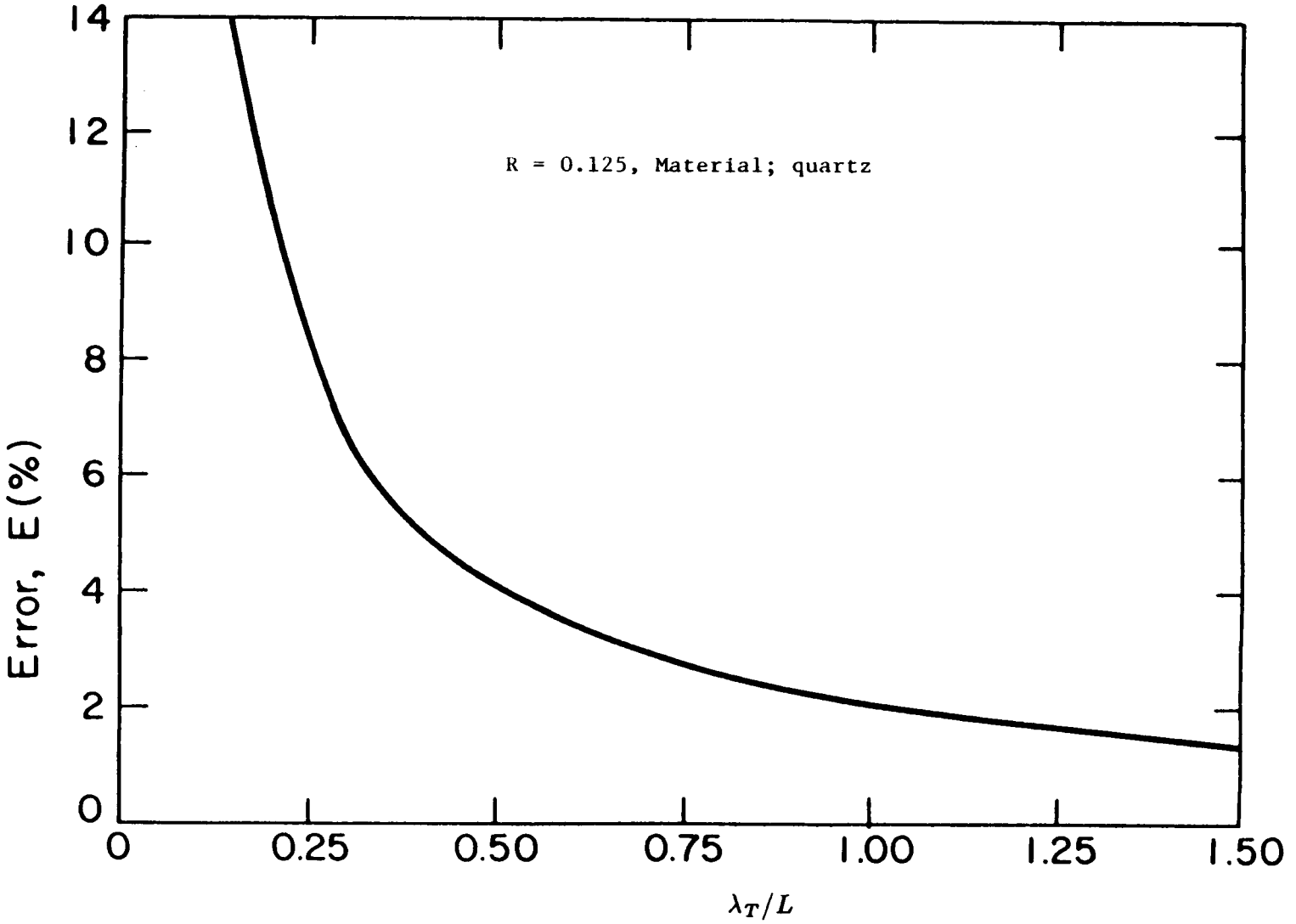

Fig. 13a Error versus $\frac{\lambda_T}{L}$ for quartz rod with R = 0.125.

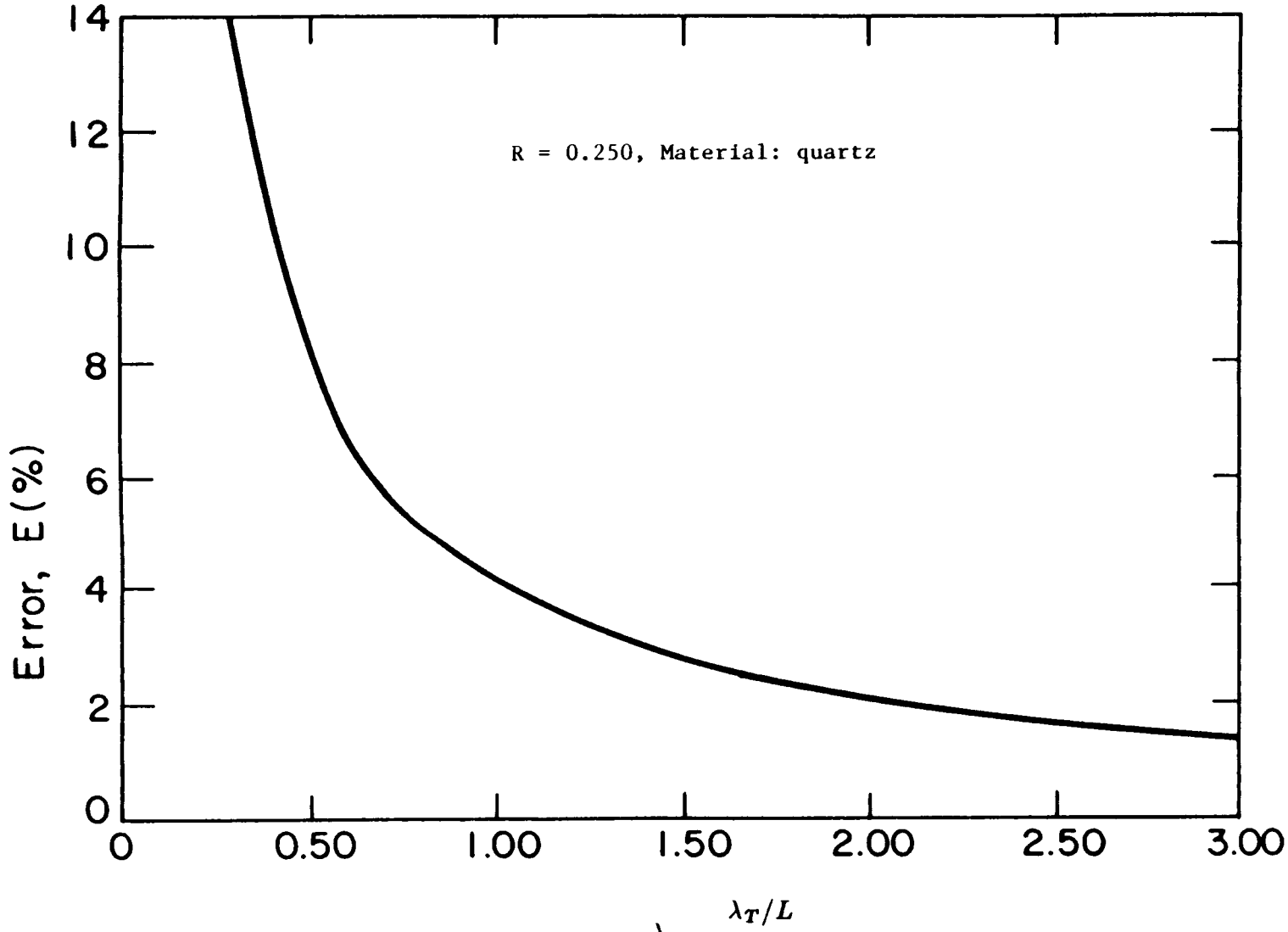

Fig. 13b Error versus $\frac{\lambda_T}{L}$ for quartz rod with R = 0.250.

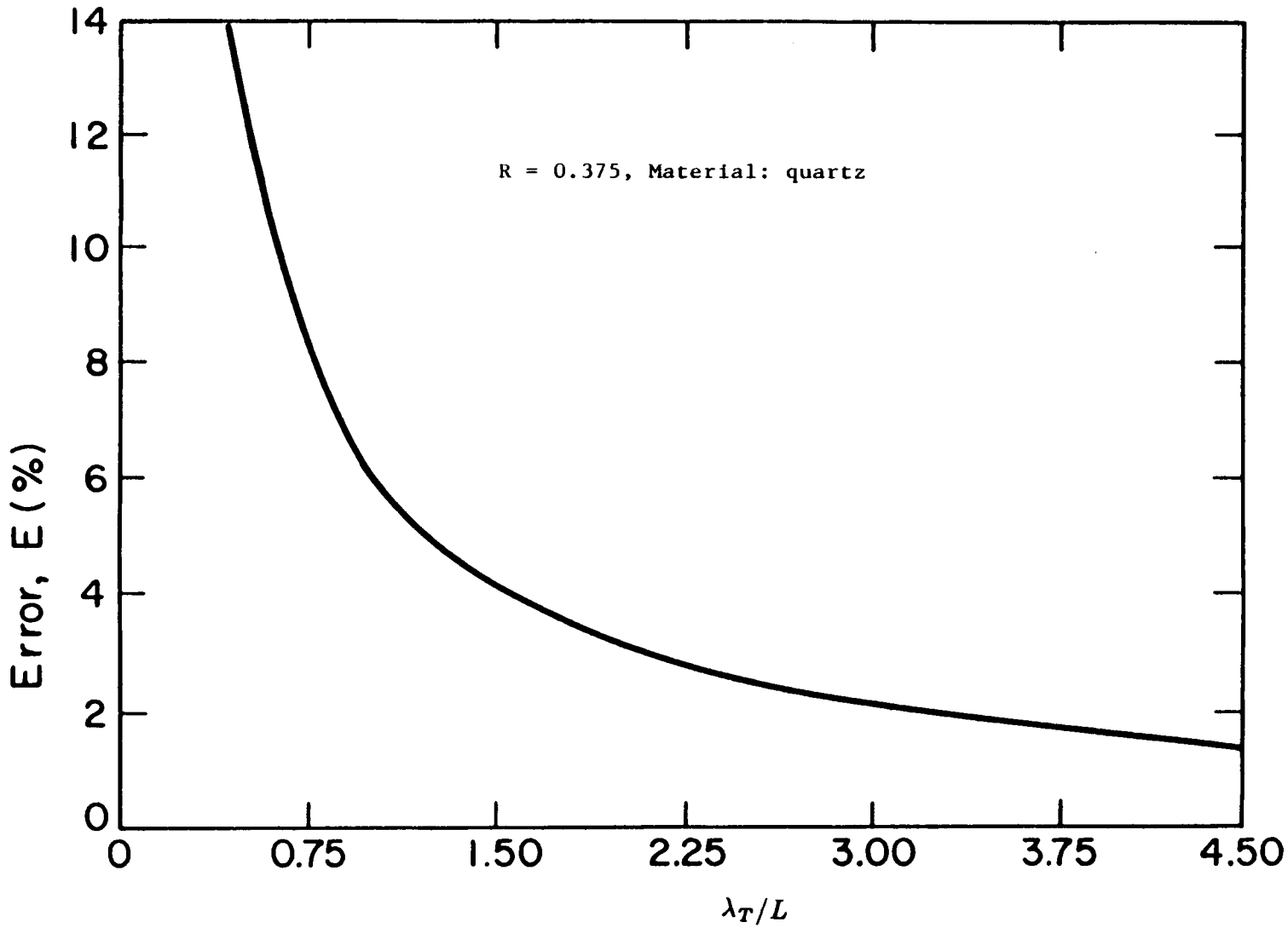

Fig. 13c Error versus $\frac{\lambda_T}{L}$ for quartz rod with R = 0.375.

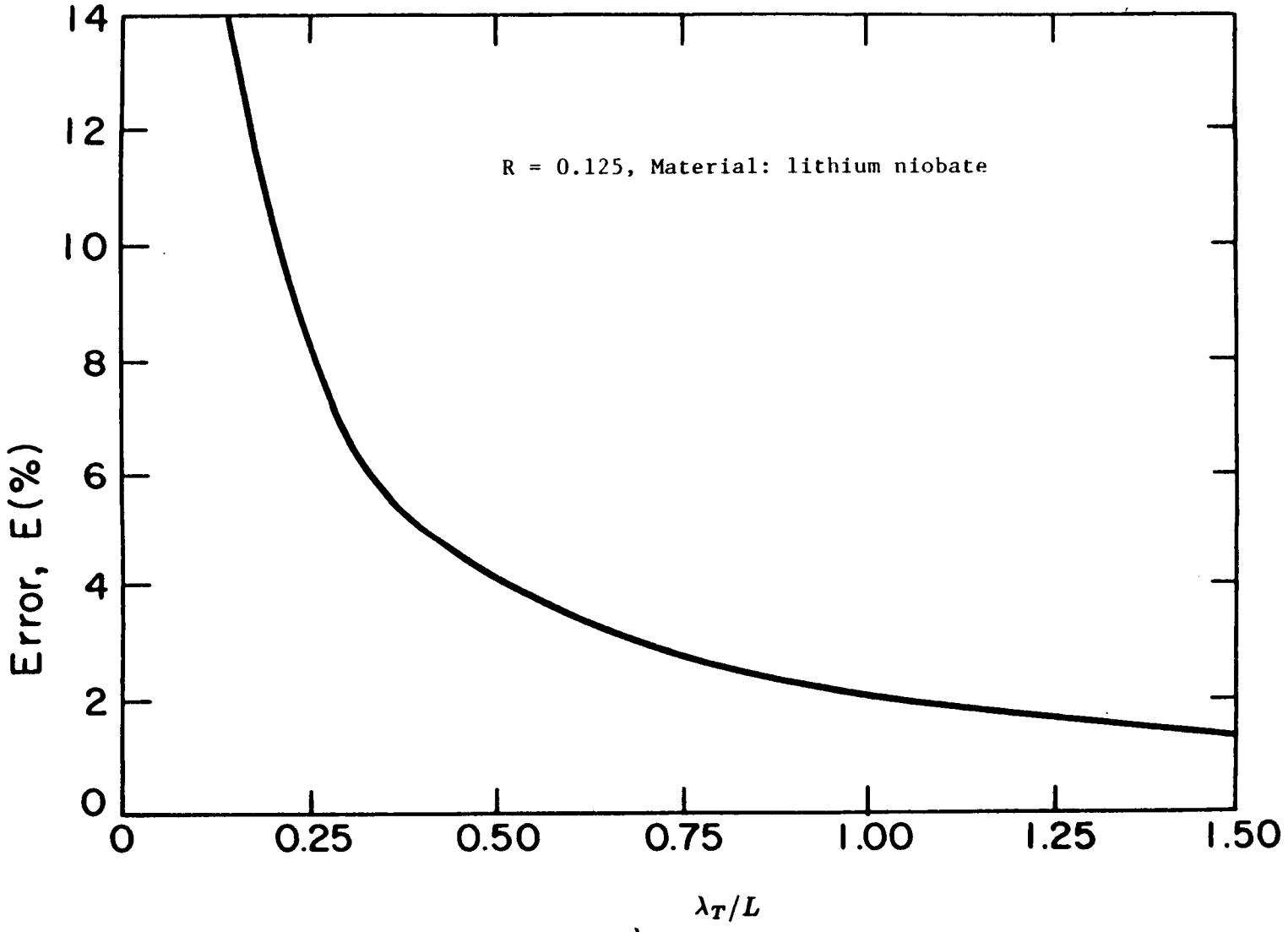

Fig. 14a Error versus $\frac{\lambda_T}{L}$ for lithium niobate rod with R = 0.125.

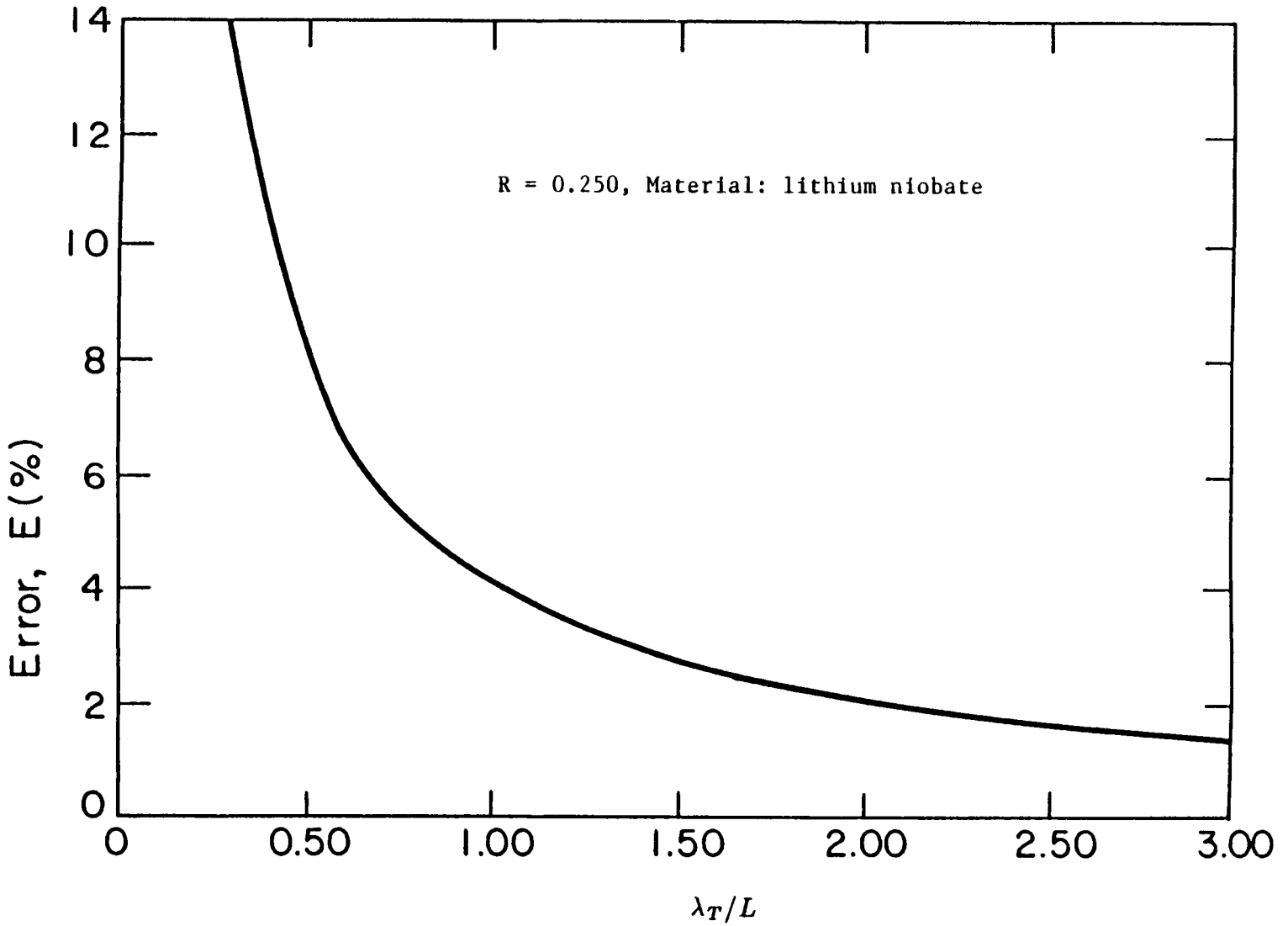

Fig. 14b Error versus $\frac{\lambda_T}{L}$ for lithium niobate rod with R = 0.250.

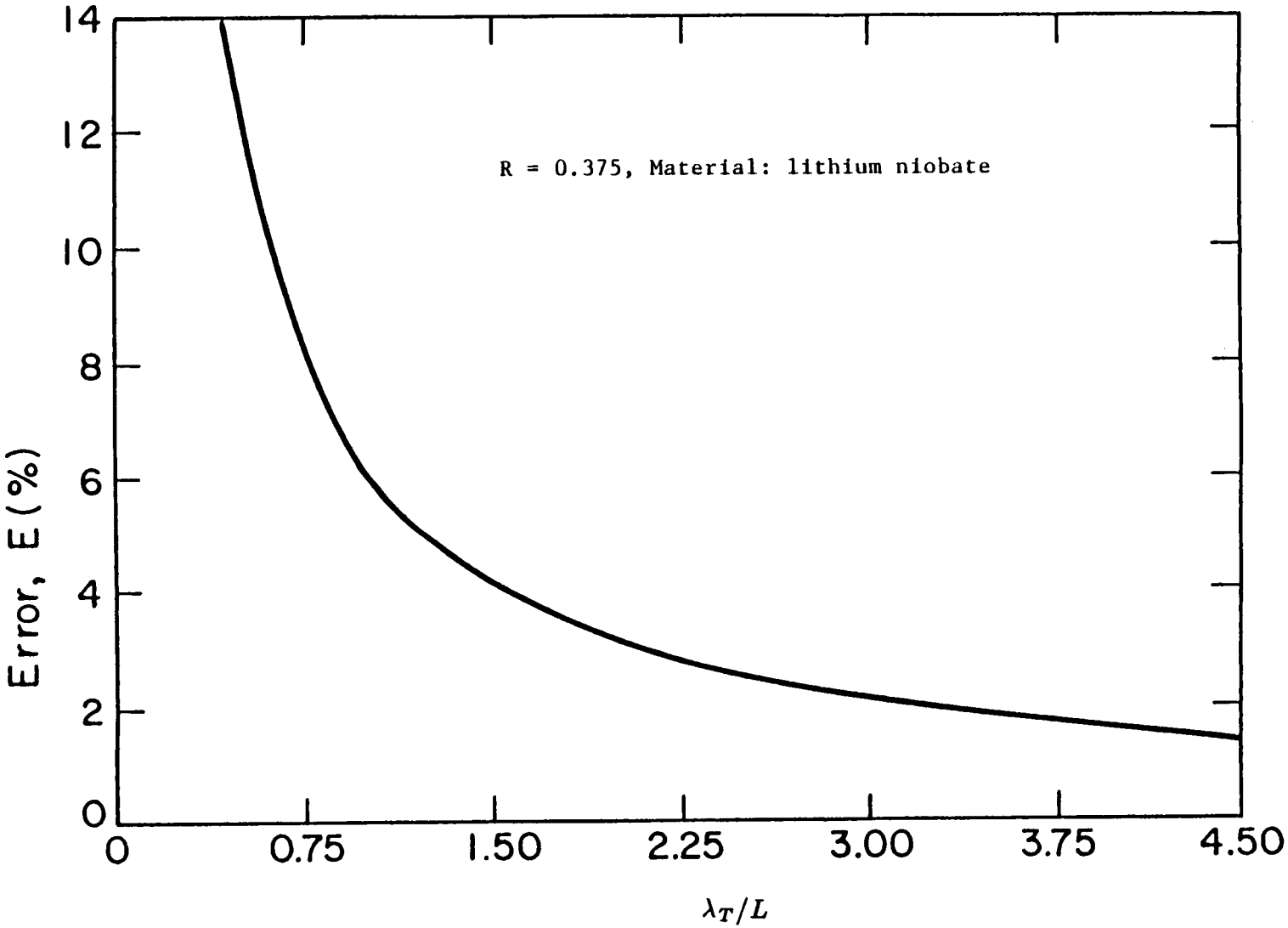

Fig 14c. Error versus $\frac{\lambda_T}{L}$ for lithium niobate rod with R = 0.375.

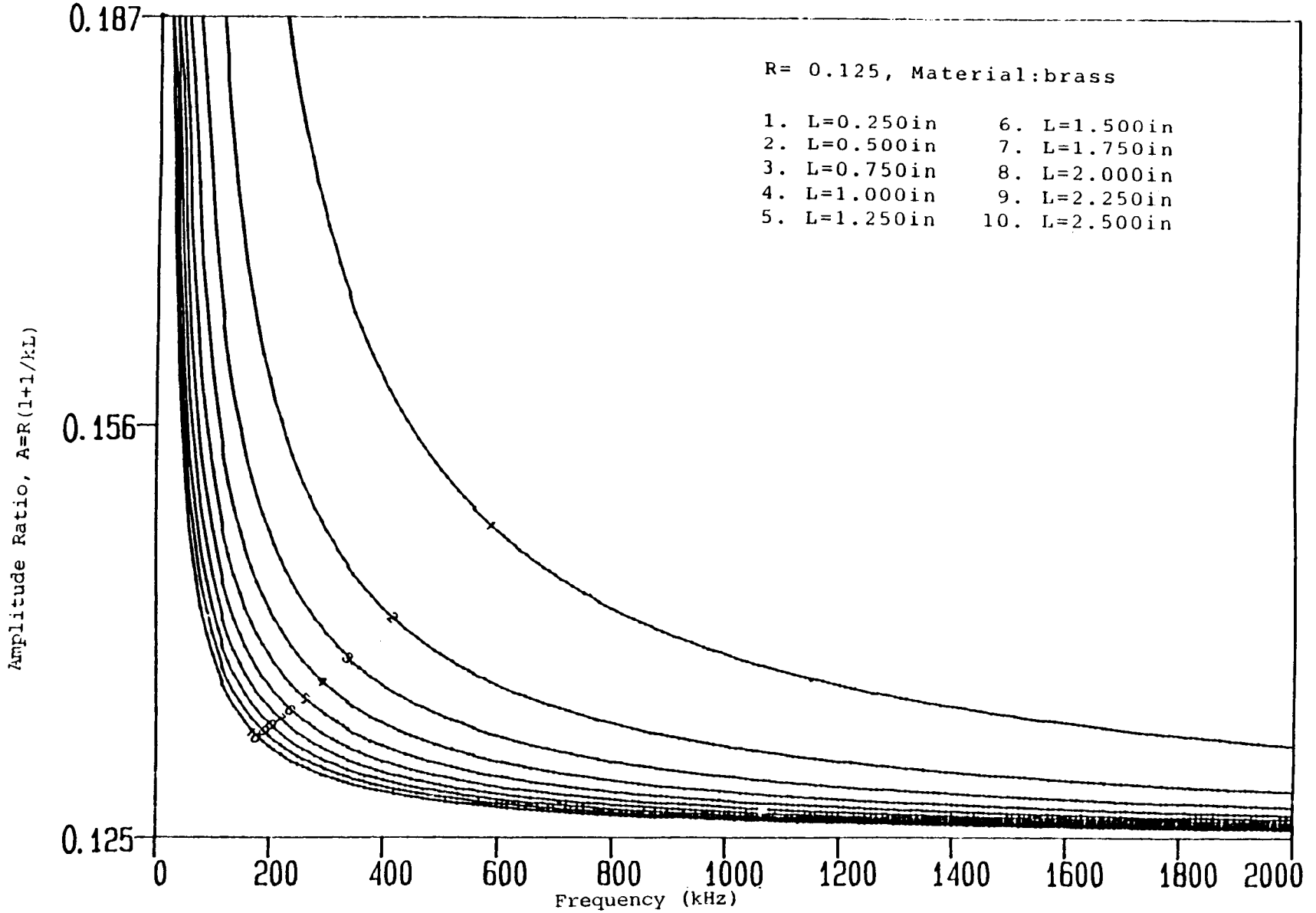

Fig. 15a Amplitude ratio versus frequency for brass rod with R = 0.125.

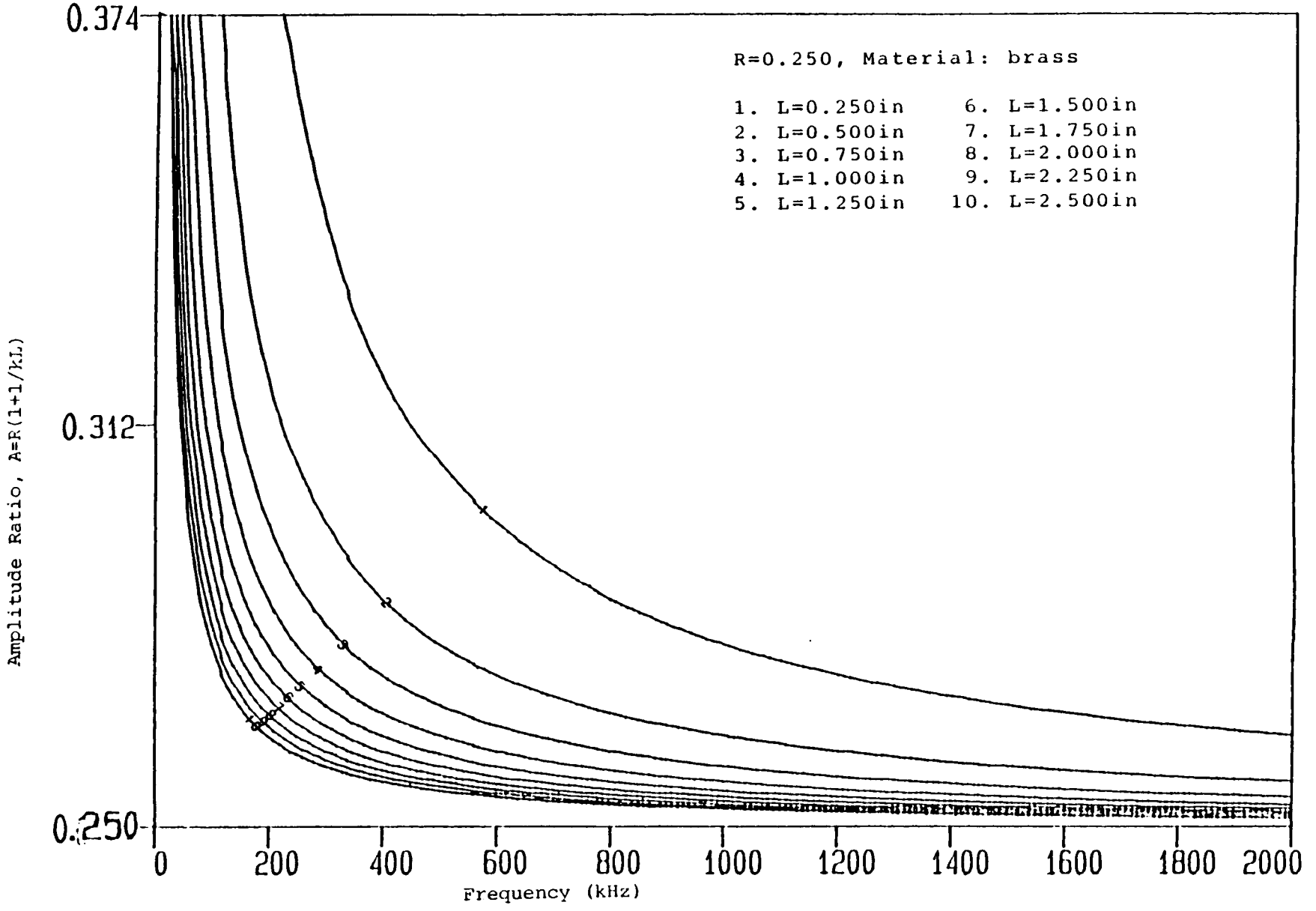

Fig. 15b Amplitude ratio versus frequency for brass rod with R = 0.250.

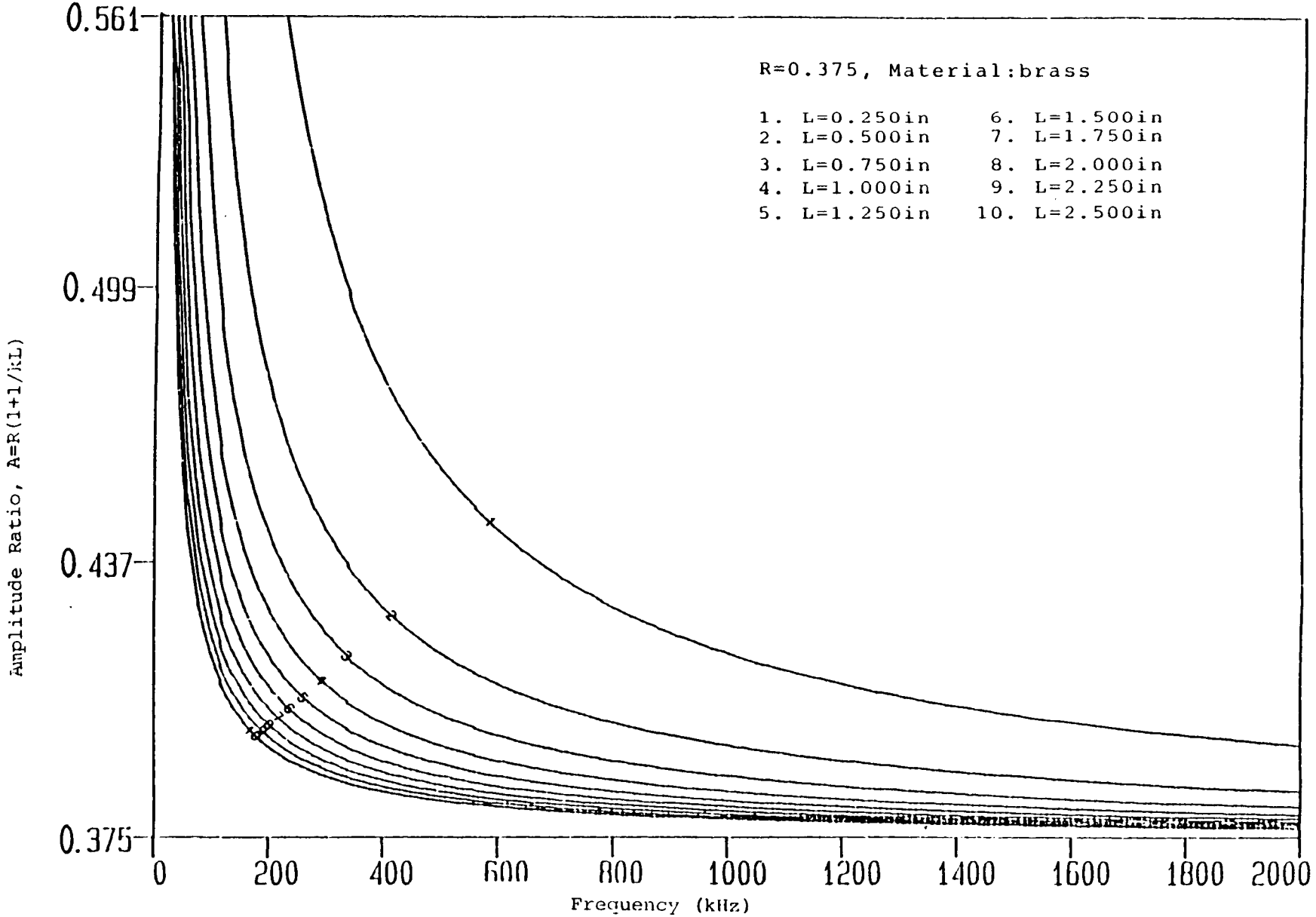

Fig. 15c Amplitude ratio versus frequency for brass rod with R = 0.375.

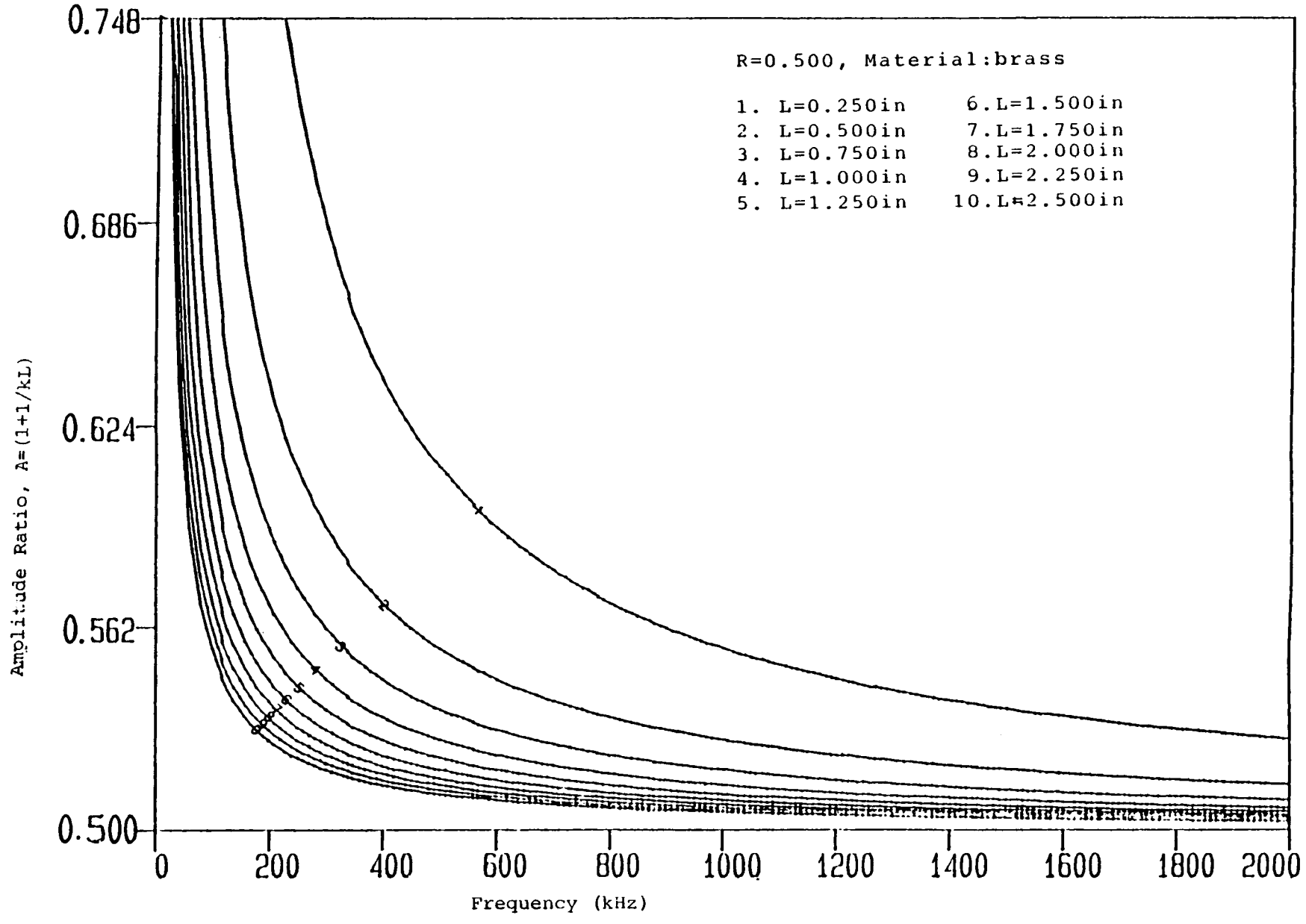

Fig. 15d Amplitude ratio versus frequency for brass rod with R = 0.500.

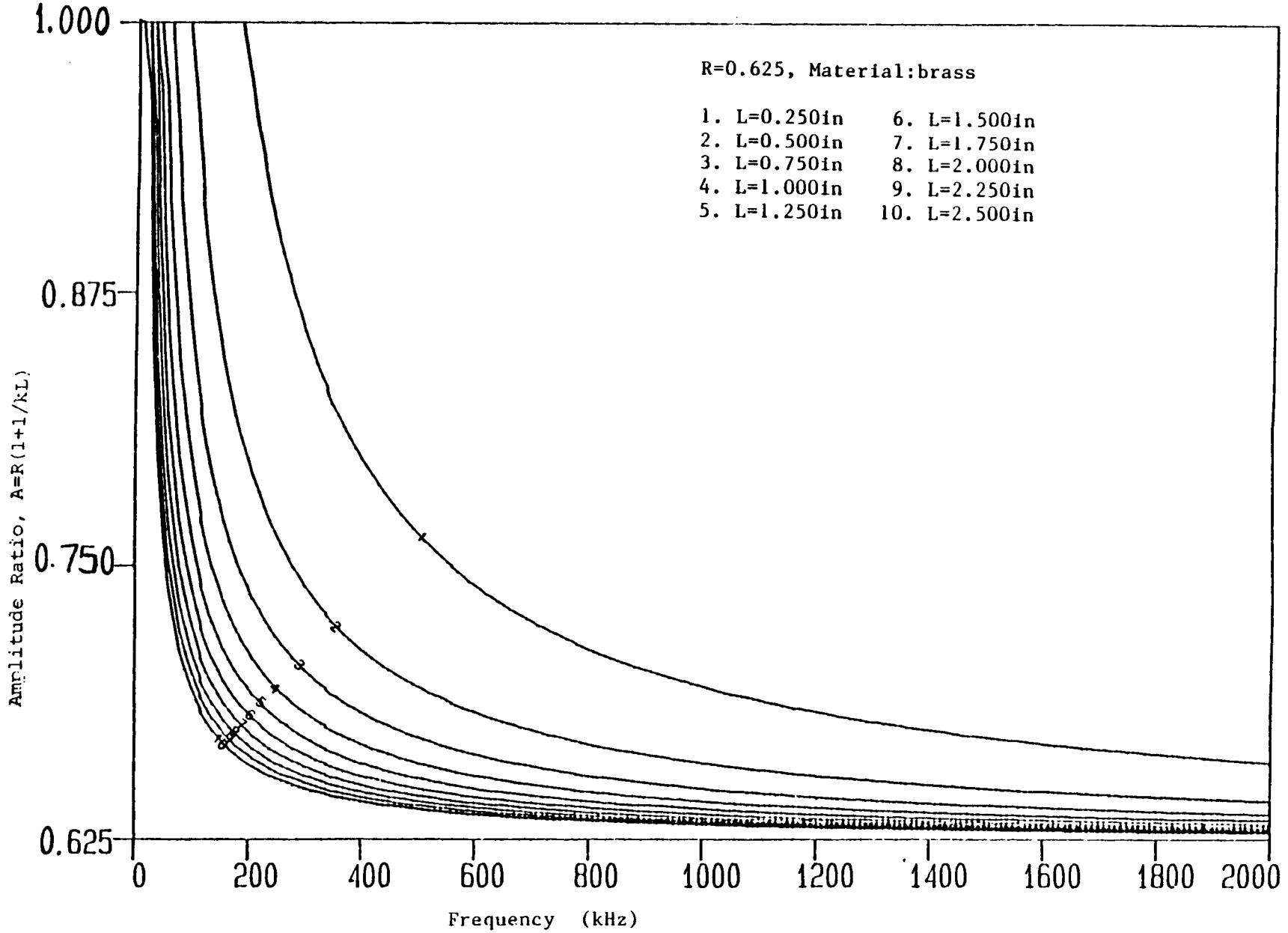

Fig. 15e Amplitude ratio versus frequency for brass rod with R = 0.625.

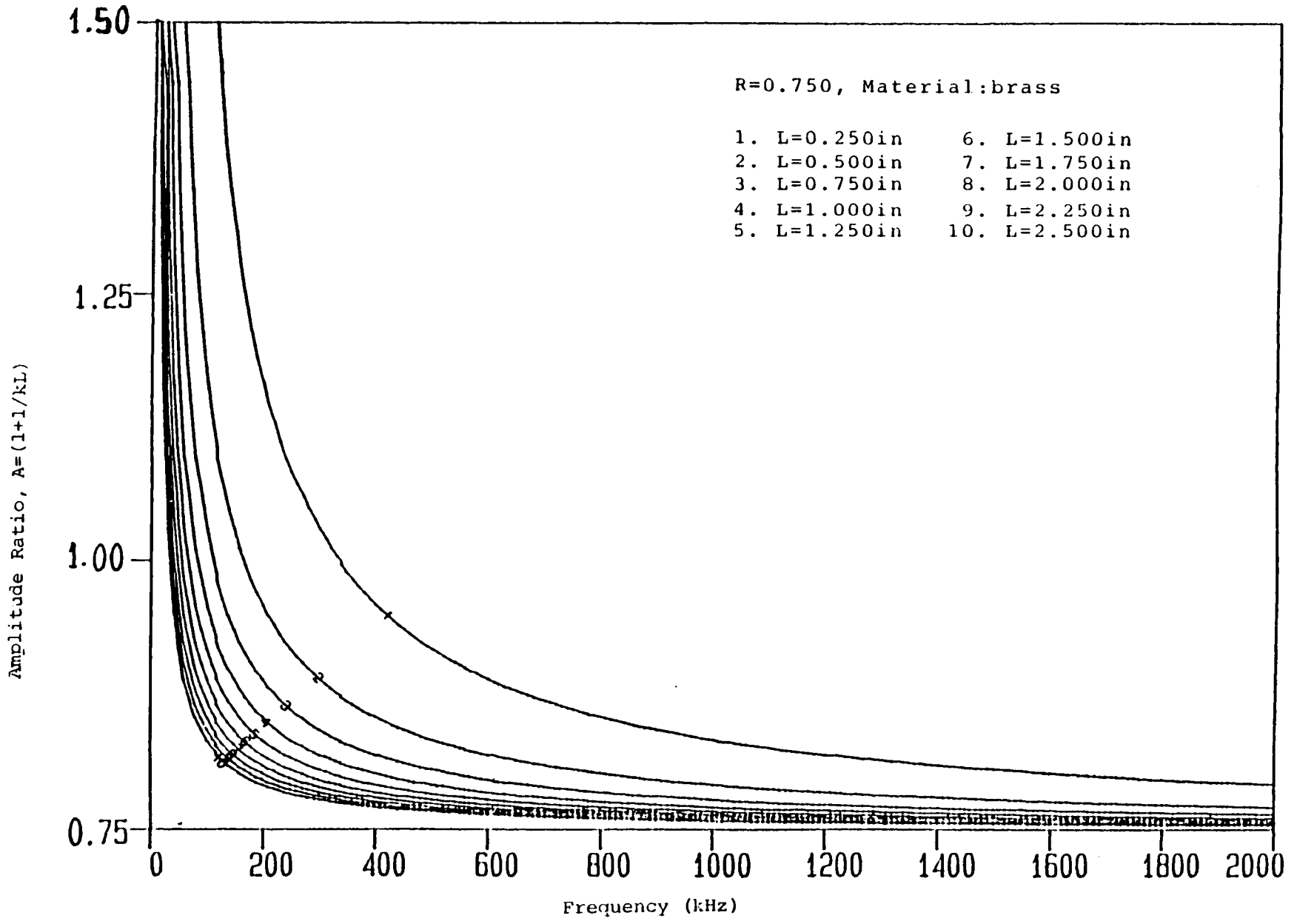

Fig. 15f Amplitude ratio versus frequency for brass rod with R = 0.750.

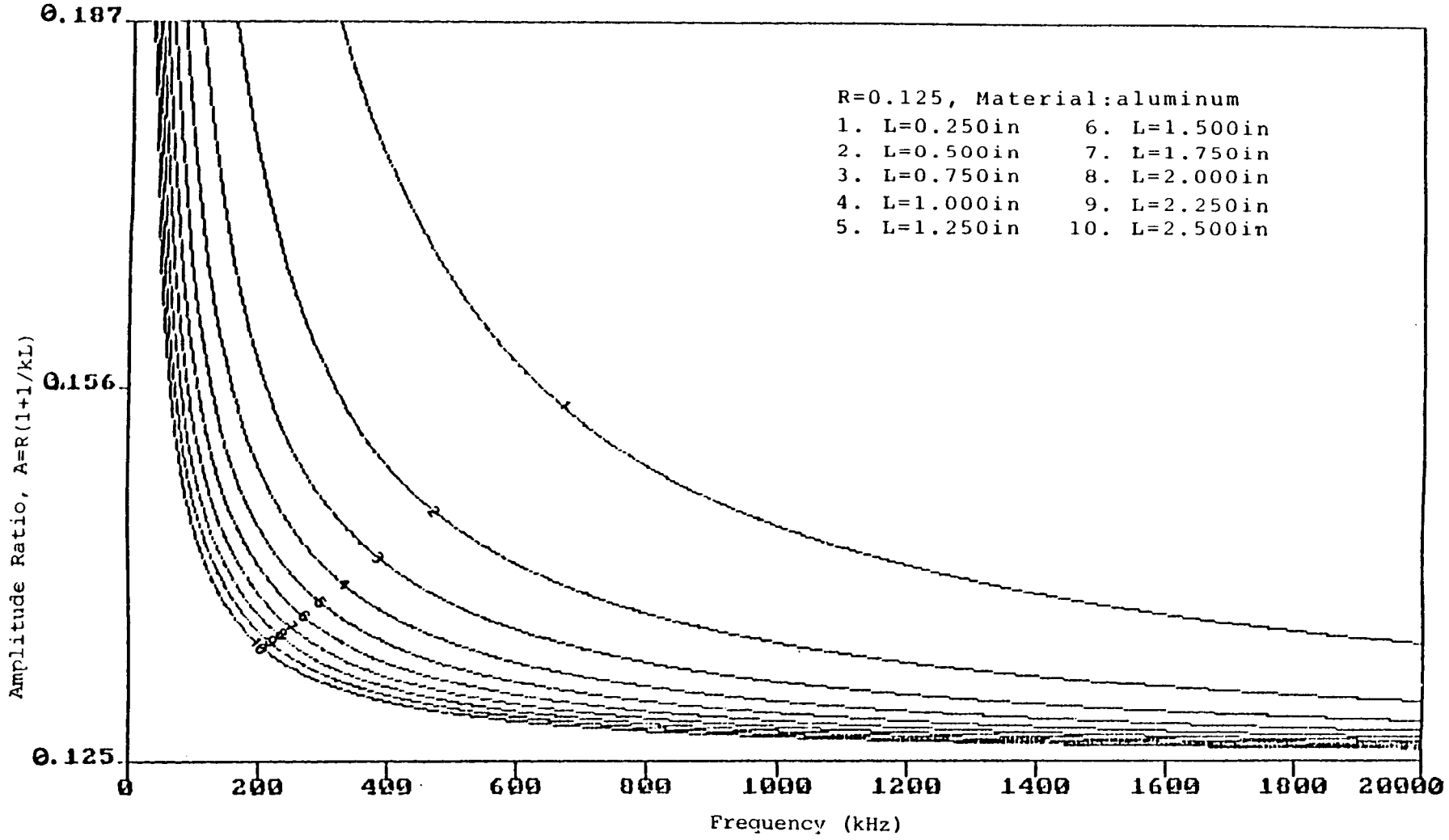

Fig. 16a Amplitude ratio versus frequency for aluminum rod with R = 0.125.

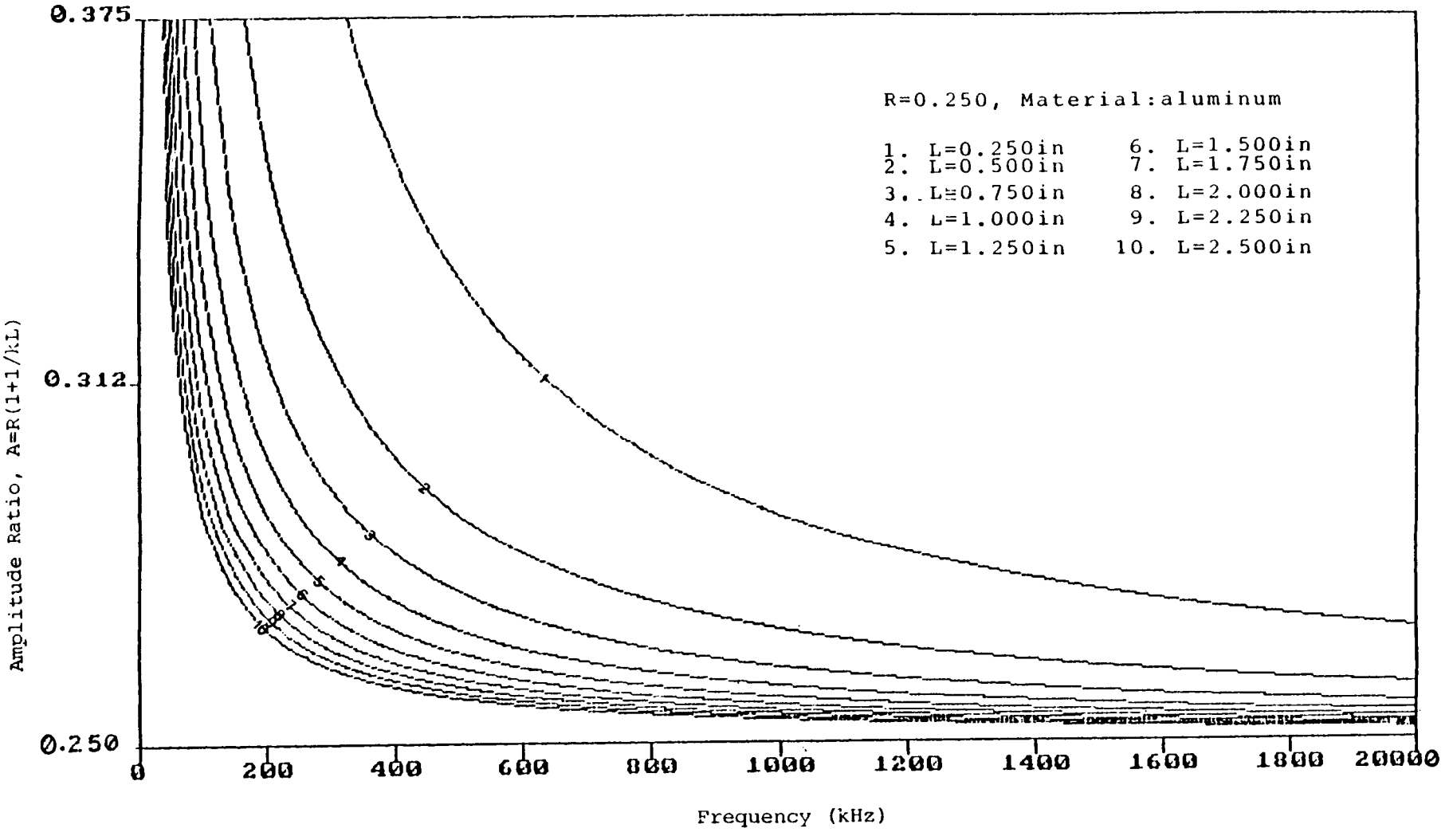

Fig. 16b Amplitude ratio versus frequency for aluminum rod with R = 0.250.

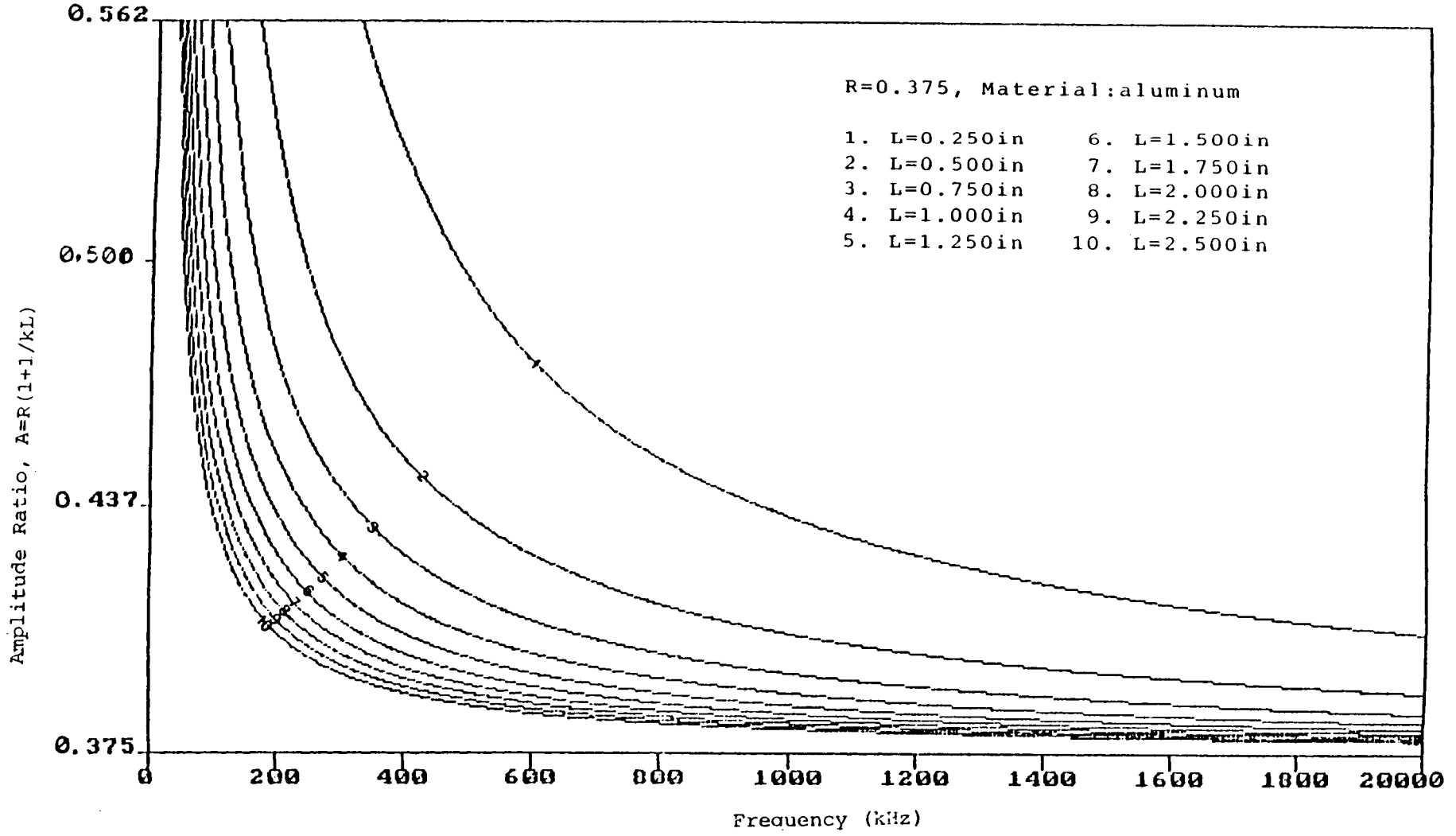

Fig. 16c Amplitude ratio versus frequency for aluminum rod with R = 0.375.

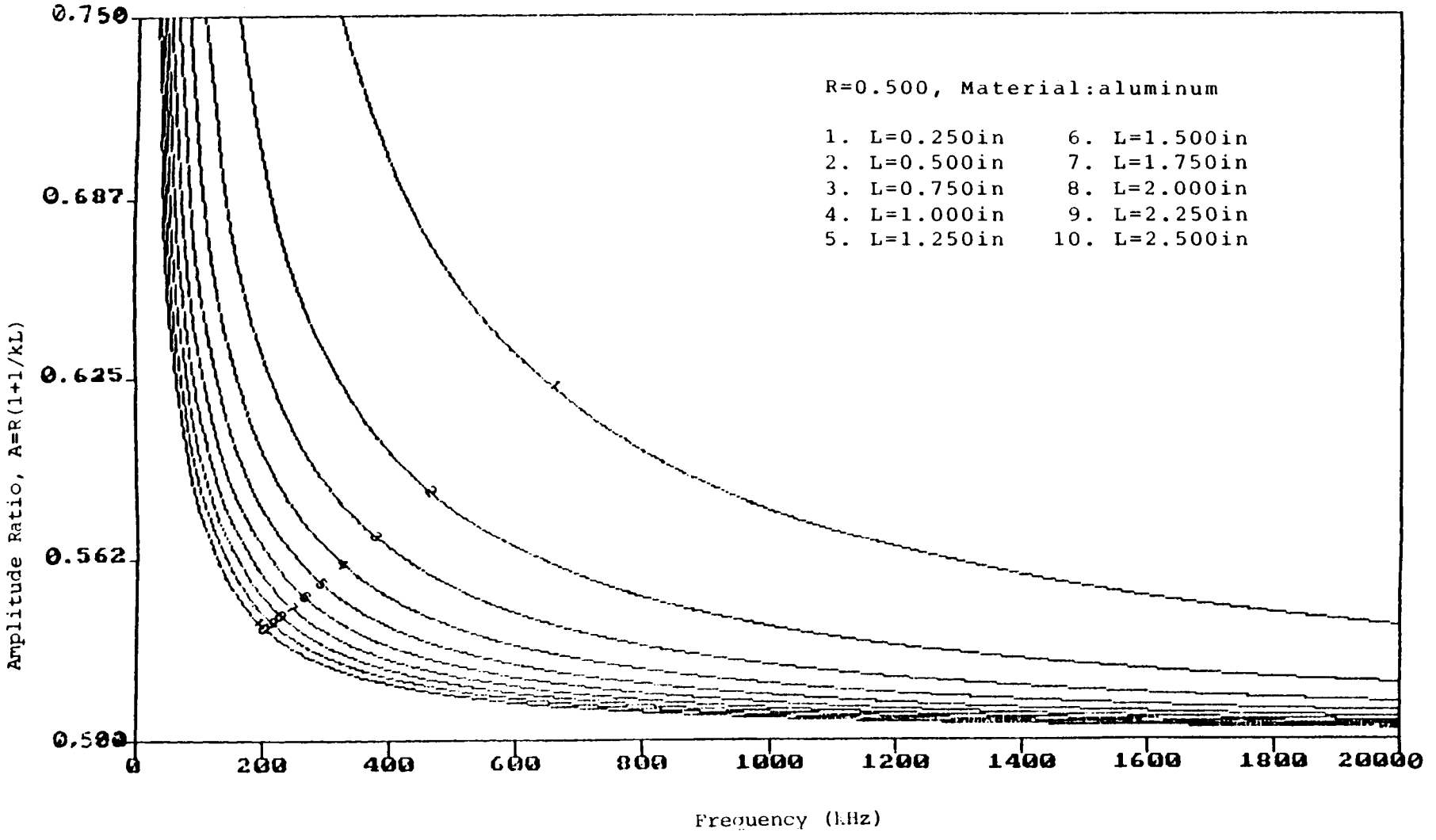

Fig. 16d Amplitude ratio versus frequency for aluminum rod with R = 0.500.

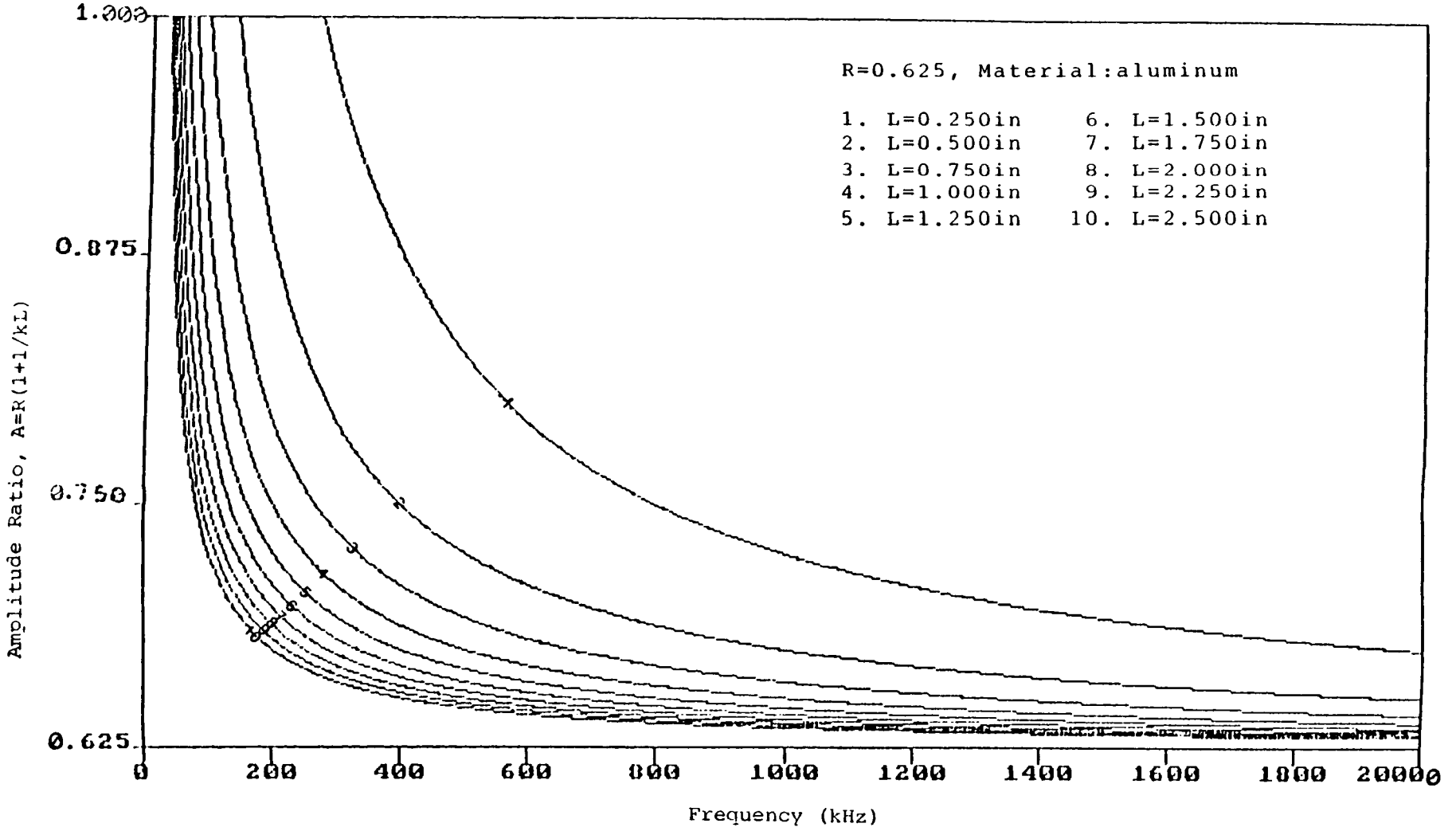

Fig. 16e Amplitude ratio versus frequency for aluminum rod with R = 0.625.

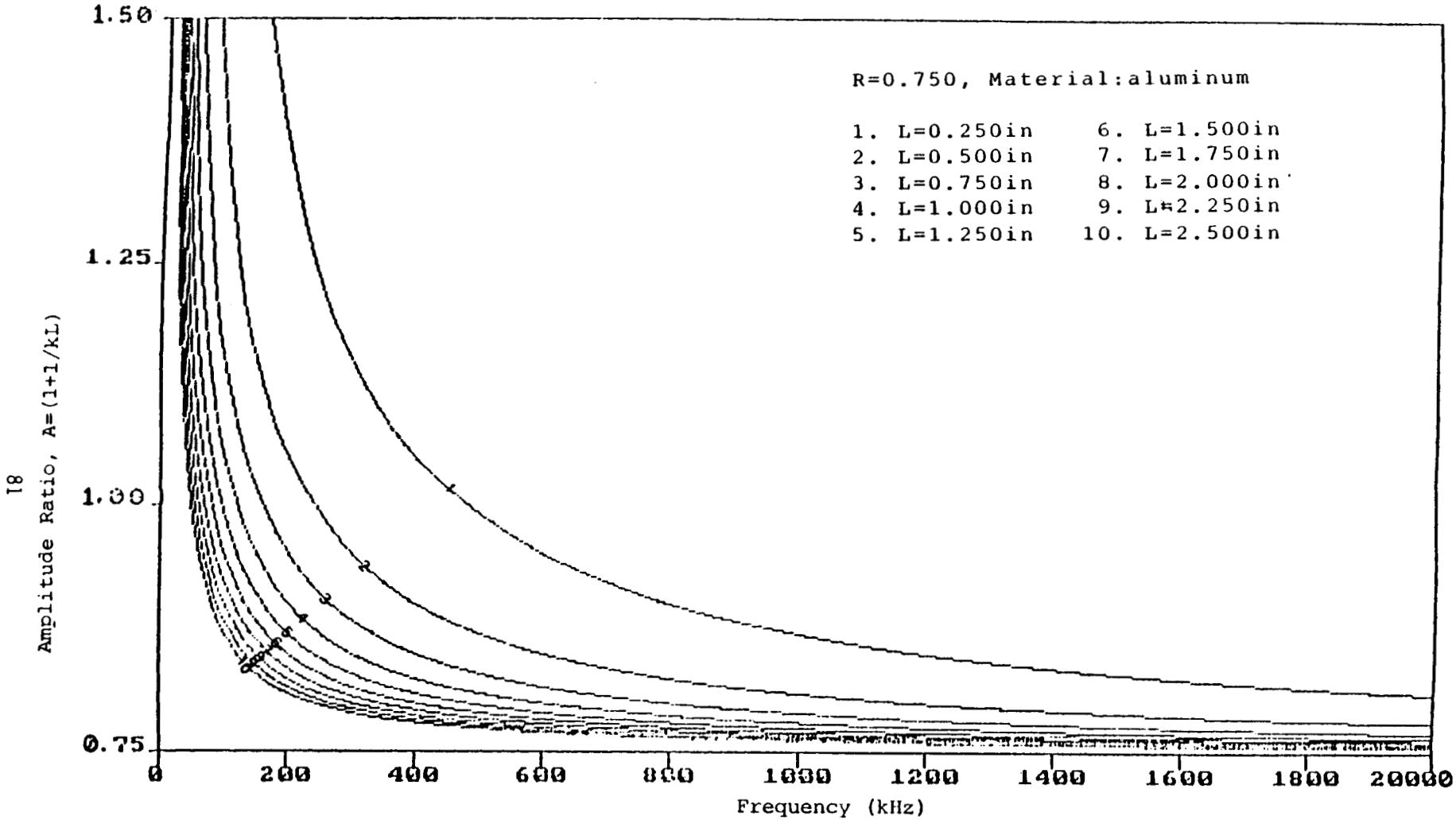

Fig. 16f Amplitude ratio versus frequency for aluminum rod with R =0.750.

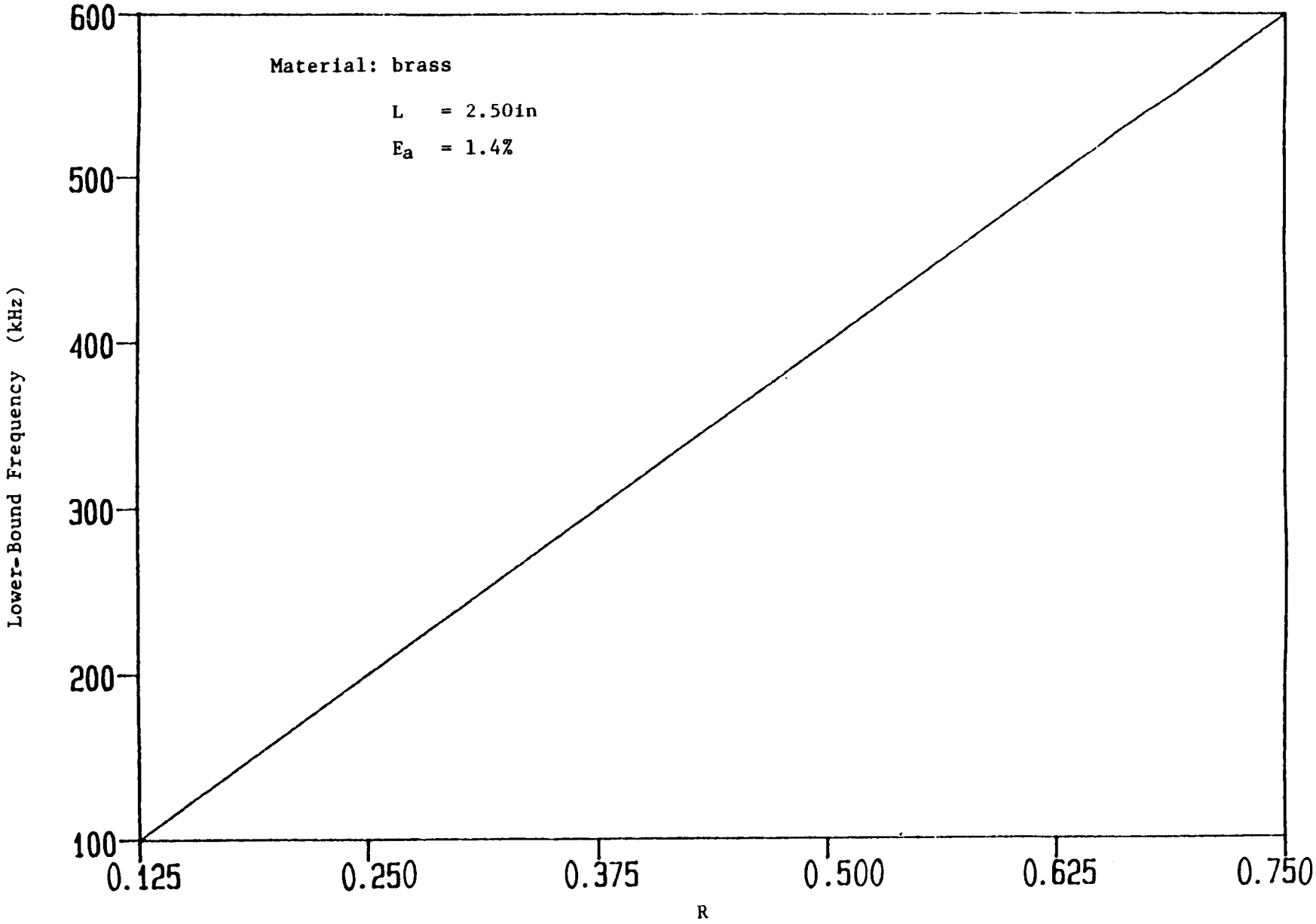

Fig. 17 Lower-bound frequency versus R for brass.

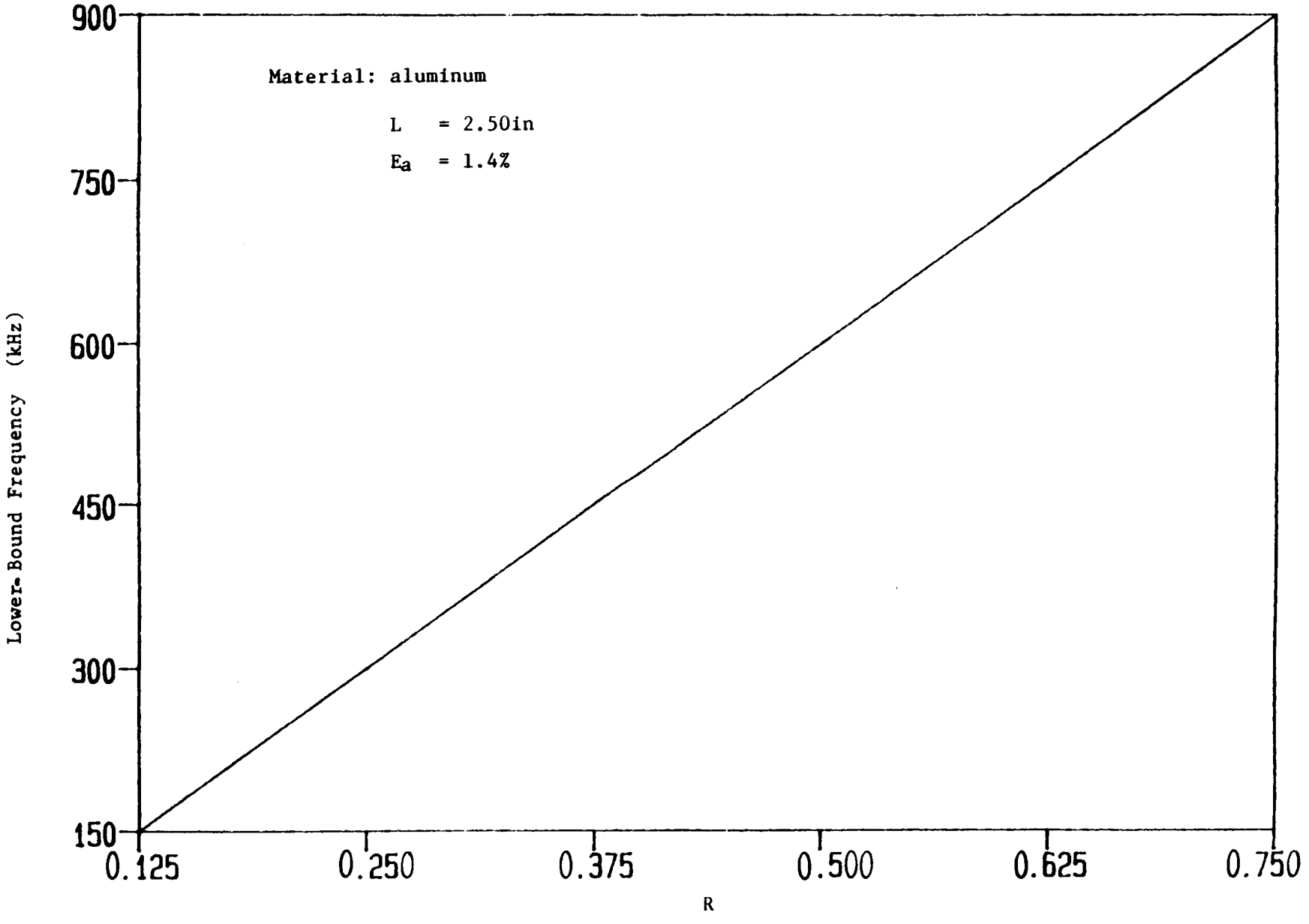

Fig. 18 Lower bound frequency versus R for aluminum.

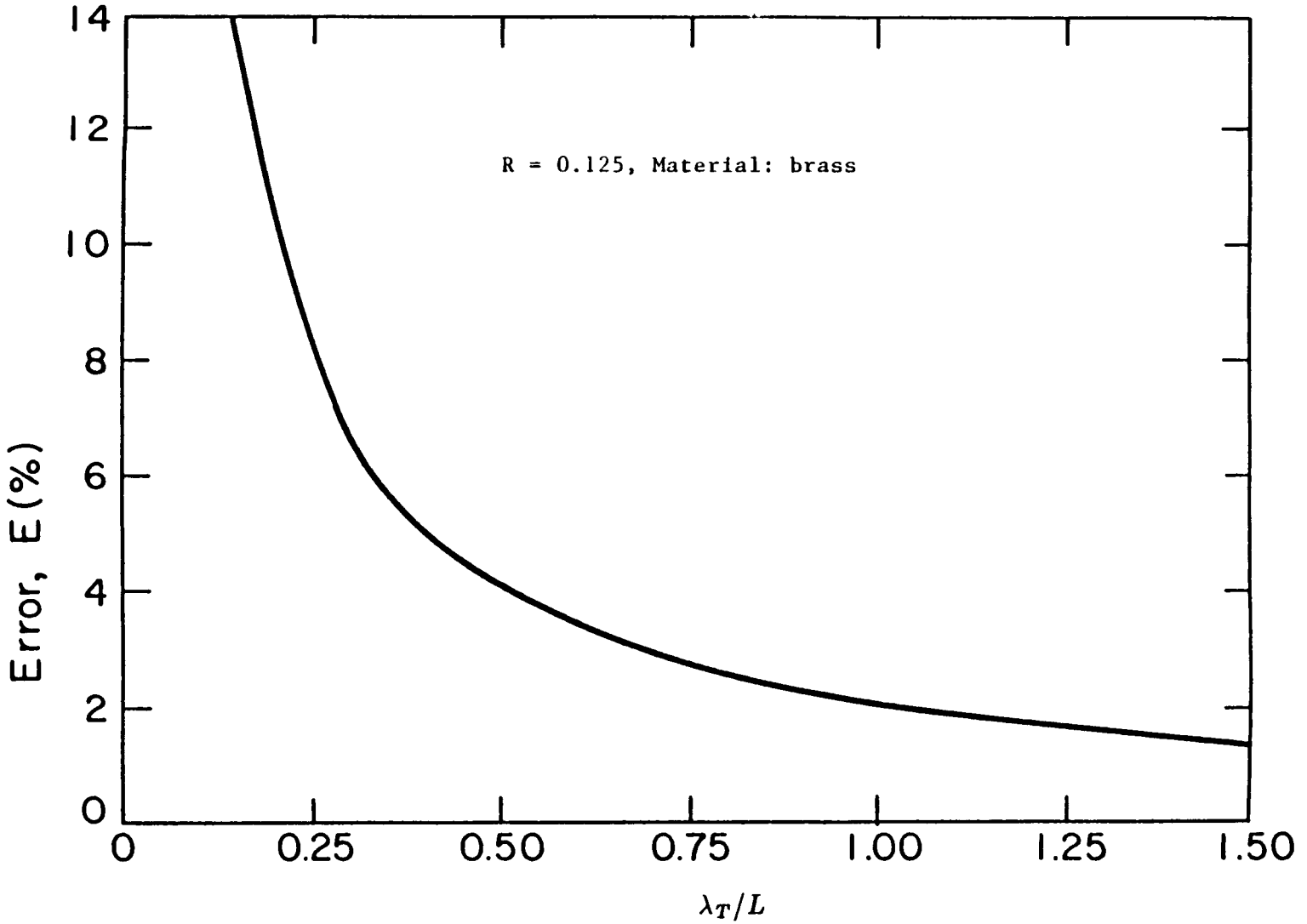

Fig. 19a Error versus $\frac{\lambda_T}{L}$ for brass rod with R = 0.125.

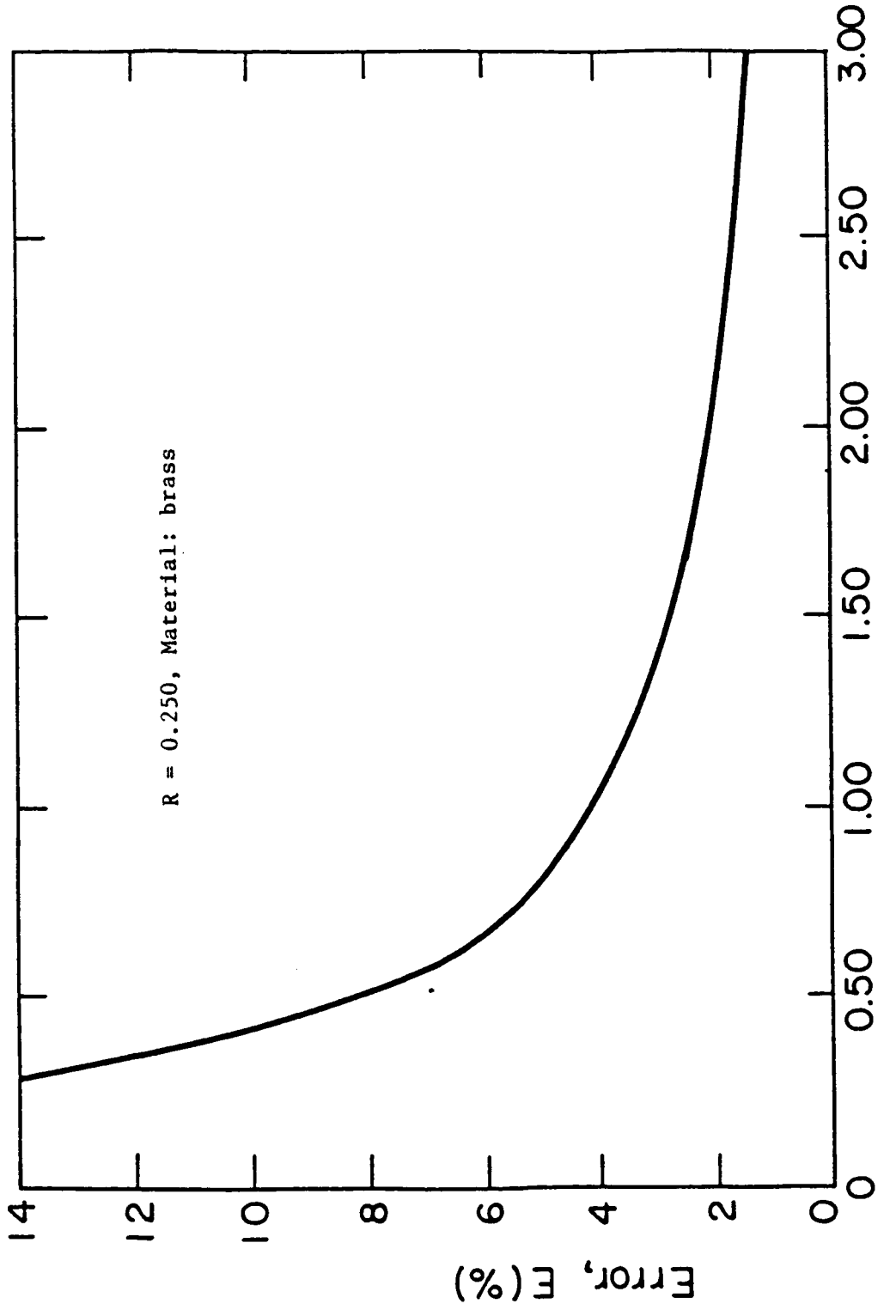

Fig. 19b Error versus $\frac{\lambda_T}{L}$ for a brass rod with R = 0.250.

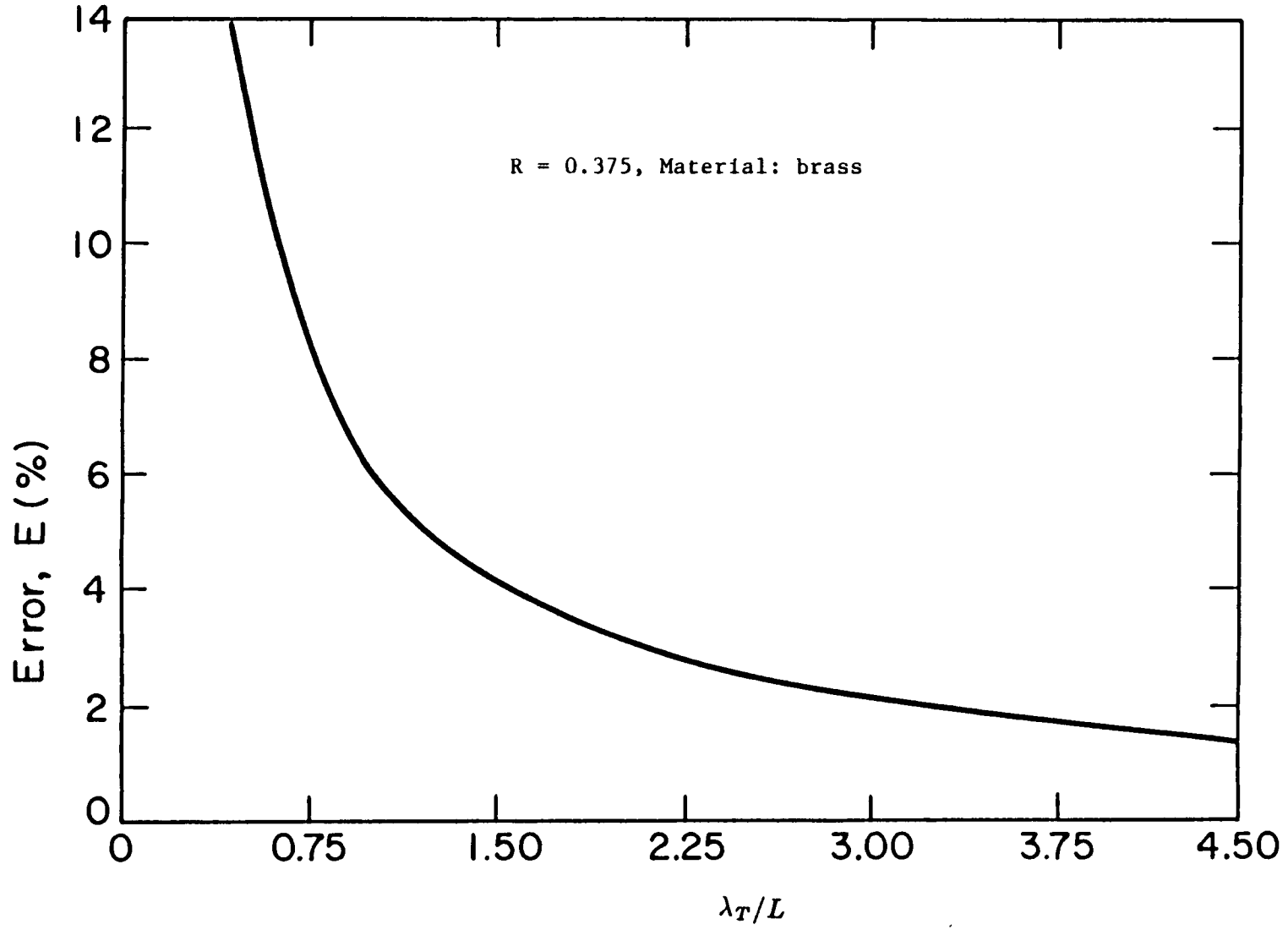

Fig. 19c Error versus $\frac{\lambda_T}{L}$ for a brass rod with R = 0.375.

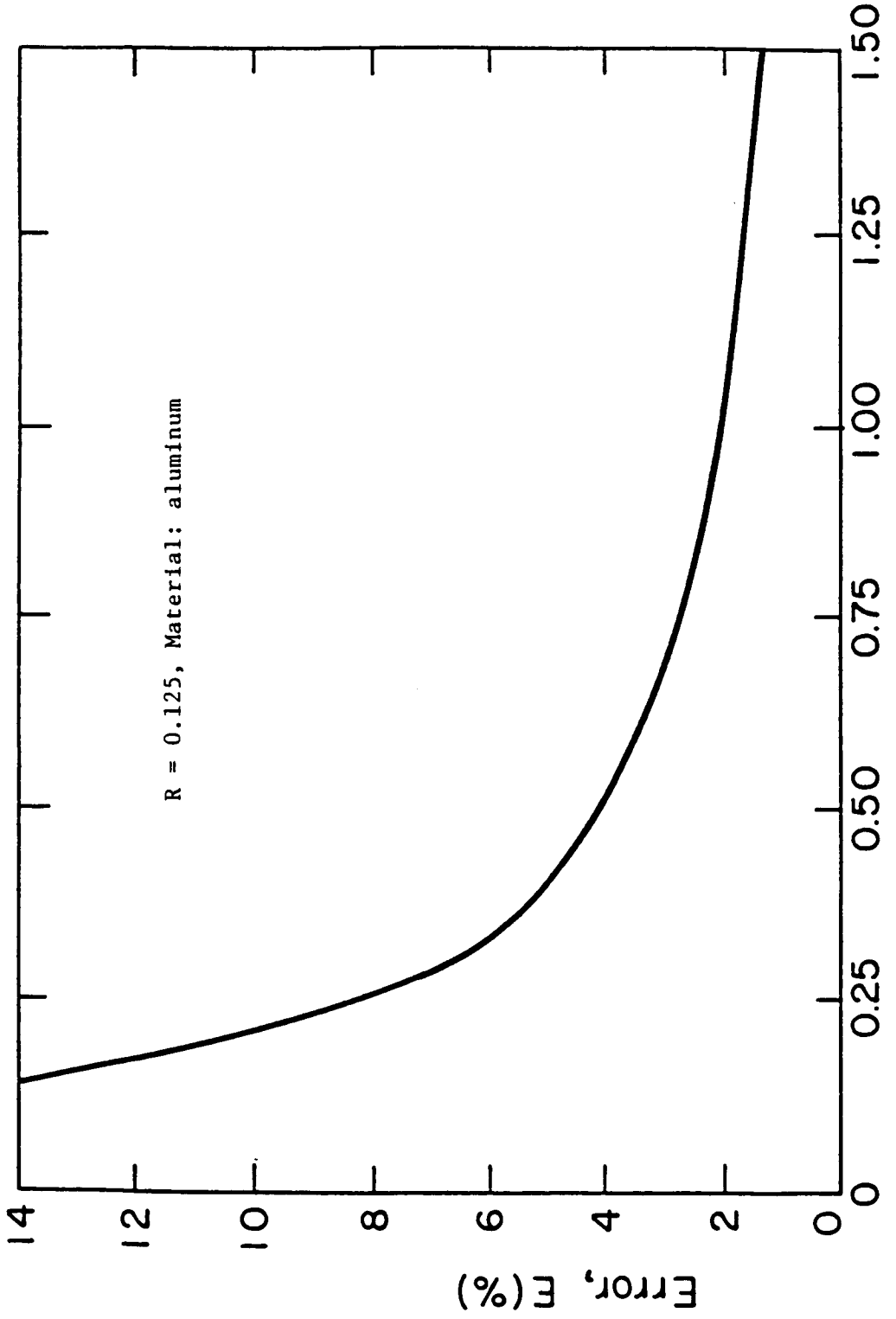

Fig. 20a. Error versus $\frac{\lambda_T}{L}$ for aluminum rod with R = 0.125.

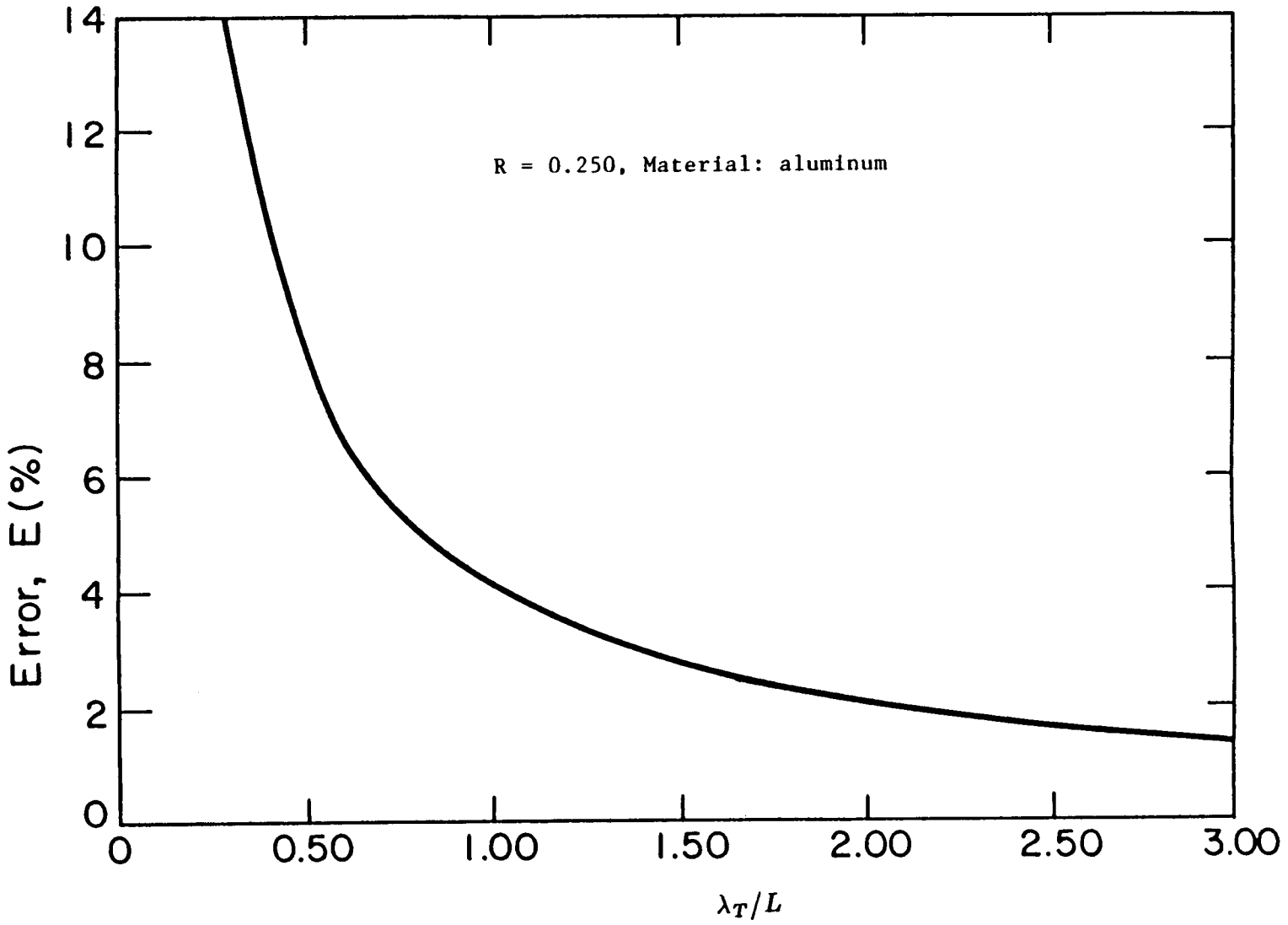

Fig. 20b Error versus $\frac{\lambda_T}{L}$ for aluminum rod with R = 0.250.

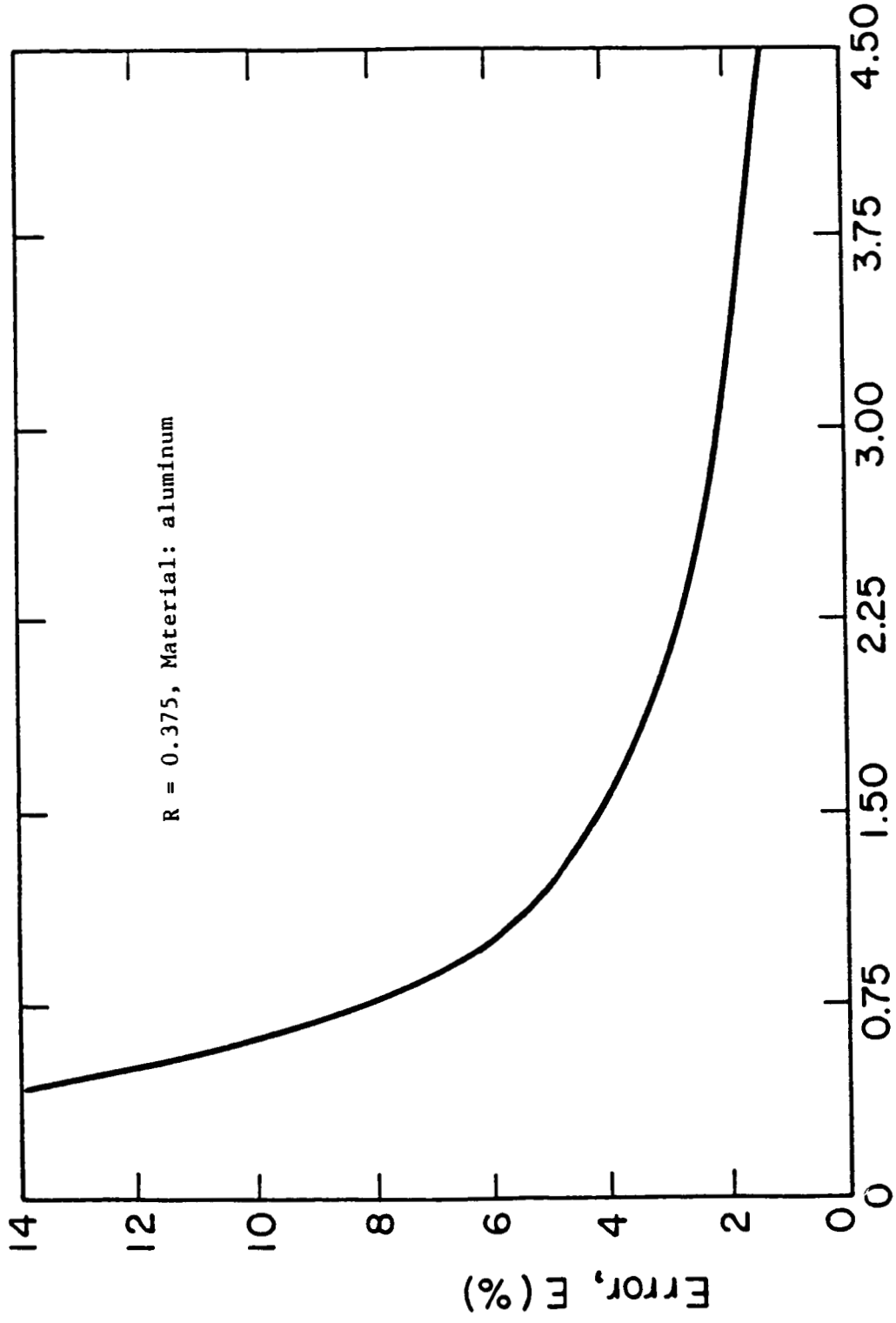

Fig. 20c Error versus $\frac{\lambda_T}{L}$ for aluminum rod with R = 0.375.

NASA
National Aeronautics and Space Administration

Report Documentation Page

1. Report No.	2. Government Accession No.	3. Recipient's Catalog No.
NASA CR-4086		

4. Title and Subtitle
One-Dimensional Wave Propagation in Rods of Variable Cross Section: A WKBJ Solution

5. Report Date
July 1987

6. Performing Organization Code

7. Author(s)
Simeon C. U. Ochi and James H. Williams, Jr.

8. Performing Organization Report No.
None (E-3651)

10. Work Unit No.
506-43-11

9. Performing Organization Name and Address
Massachusetts Institute of Technology
Department of Mechanical Engineering
Cambridge, Massachusetts

11. Contract or Grant No.
NAG3-328

13. Type of Report and Period Covered
Contractor Report
Final

12. Sponsoring Agency Name and Address
National Aeronautics and Space Administration
Lewis Research Center
Cleveland, Ohio 44135

14. Sponsoring Agency Code

15. Supplementary Notes
Project Manager, Alex Vary, Structures Division, NASA Lewis Research Center.

16. Abstract
As an important step in the characterization of a particular dynamic surface displacement transducer (IQI Model 501), this report presents one-dimensional wave propagation in isotropic nonpiezoelectric and piezoelectric rods of variable cross section. With the use of the Wentzel-Kramers-Brillouin-Jeffreys (WKBJ) approximate solution technique, an approximate formula, which relates the ratio of the amplitudes of a propagating wave observed at any two locations along the rod to the ratio of the cross sectional radii at these respective locations, is derived. The domains of frequency for which the approximate solution is valid are discussed for piezoelectric and nonpiezoelectric materials.

17. Key Words (Suggested by Author(s))	18. Distribution Statement
Ultrasonics; Acoustic waves; Nondestructive testing; Piezotransducers; Longitudinal waves	Unclassified - unlimited STAR Category 38

19. Security Classif. (of this report)	20. Security Classif. (of this page)	21. No of pages	22. Price*
Unclassified	Unclassified	90	A05

NASA FORM 1626 OCT 86

*For sale by the National Technical Information Service, Springfield, Virginia 22161

NASA-Langley, 1987